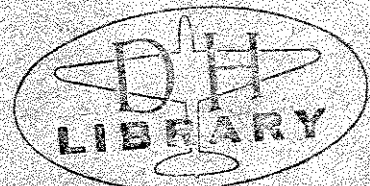


NACA Rpt 1192

NATIONAL ADVISORY COMMITTEE  
FOR AERONAUTICS



REPORT 1192

THEORETICAL AND EXPERIMENTAL INVESTIGATION  
OF MUFFLERS WITH COMMENTS ON ENGINE-  
EXHAUST MUFFLER DESIGN

By DON D. DAVIS, Jr., GEORGE M. STOKES, DEWEY MOORE,  
and GEORGE L. STEVENS, Jr.



1954

For sale by the Superintendent of Documents, U. S. Government Printing Office, Washington 25, D. C. Yearly subscription, \$10; foreign, \$11.25;  
single copy price varies according to size - - - - - Price 40 cents

---

---

## REPORT 1192

---

### THEORETICAL AND EXPERIMENTAL INVESTIGATION OF MUFFLERS WITH COMMENTS ON ENGINE- EXHAUST MUFFLER DESIGN

By DON D. DAVIS, Jr., GEORGE M. STOKES, DEWEY MOORE,  
and GEORGE L. STEVENS, Jr.

Langley Aeronautical Laboratory  
Langley Field, Va.

---

---

## CONTENTS

	Page
SUMMARY .....	1
INTRODUCTION .....	1
SYMBOLS .....	2
<b>I. INFINITE TAILPIPE</b>	
THEORY .....	3
MUFFLERS .....	4
APPARATUS .....	4
METHODS AND TESTS .....	7
RESULTS AND DISCUSSION .....	8
Single Expansion Chamber .....	8
Effect of expansion ratio .....	8
Effect of length .....	9
Effect of shape .....	10
Multiple Expansion Chamber .....	11
Effect of number of chambers .....	11
Effect of connecting-tube length with an external connecting tube .....	11
Effect of connecting-tube length with an internal connecting tube .....	12
Effect of having the internal-connecting-tube length equal to the chamber length .....	12
Principles of Single-Chamber Resonators .....	13
Branch Resonators .....	13
Effect of varying resonator volume .....	13
Effect of varying $c_0$ and $V$ with the ratio $\sqrt{c_0/V}$ constant .....	13
Effect of varying cross-sectional area of the connecting tube .....	14
Effect of varying length of connecting tube .....	14
Effect of changing connecting-tube configuration with $c_0$ held constant .....	14
Concentric Resonators .....	15
Effect of varying $\sqrt{c_0V/2S}$ with the resonance parameter constant .....	15
Effect of varying the chamber length and connector location with the chamber volume constant .....	16
Venturi-shaped central tube .....	17
Multiple Resonators .....	18
Effect of number of chambers .....	18
Effect of diameter with resonance parameter constant .....	19
Effect of length .....	19
Effect of conductivity .....	20
Elimination of the first upper pass band .....	20
Conductivity Prediction .....	21
Tuned Tubes .....	22
Side-branch tubes .....	22
Quincke tubes .....	22
Combinations .....	22
Mufflers for a 12-Inch Exhaust Pipe .....	23
<b>II. FINITE TAILPIPE</b>	
THEORY .....	23
MUFFLERS .....	25
APPARATUS AND TESTS .....	25
RESULTS .....	26
<b>III. APPLICATION TO MUFFLER DESIGN</b>	
VARIABLES DEPENDENT ON OPERATING CONDITIONS .....	
Temperature .....	26
Exhaust-Gas Velocity .....	27
Increased Sound Pressure .....	27
RELATIVE MERITS OF MUFFLER TYPES INVESTIGATED .....	27
MUFFLER-DESIGN PROCEDURE .....	28
Required Attenuation Spectrum .....	28
Muffler Selection .....	28
DESIGN CURVES .....	28
Single Expansion Chamber .....	28
Single-Chamber Resonator .....	29
Multiple-Chamber Resonator .....	30

## IV. ENGINE TESTS

	Page
BASIC DATA.....	32
MUFFLERS AND DESIGN.....	32
APPARATUS.....	34
TESTS.....	35
RESULTS AND DISCUSSION.....	35
Muffler-Engine Tests.....	35
Frequency analysis.....	35
Band-pass analysis.....	36
Tailpipe characteristics.....	36
Internal sound pressures of the exhaust system.....	36
Possible Reasons for Discrepancies Between Cold Tests and Engine Tests.....	37
Differences in operating conditions.....	37
Extraneous noise.....	37
Significance of Measured Noise Reduction.....	37
CONCLUDING REMARKS.....	38
APPENDIX A—ATTENUATION OF EXPANSION-CHAMBER MUFFLERS.....	39
Assumptions and General Method.....	39
Single Expansion Chamber.....	39
Double Expansion Chamber With External Connecting Tube.....	40
Double Expansion Chamber With Internal Connecting Tube.....	41
Cutoff Frequency.....	41
APPENDIX B—ATTENUATION OF RESONATOR MUFFLERS.....	42
Single Resonators.....	42
Multiple Resonators.....	43
APPENDIX C—COMBINATIONS.....	44
Two Resonators Tuned at Different Frequencies.....	44
A Resonator and an Expansion Chamber.....	45
APPENDIX D—ATTENUATION OF MUFFLERS WITH FINITE TAILPIPS.....	46
Single Expansion Chamber.....	46
Single Resonator.....	46
REFERENCES.....	47

## REPORT 1192

### THEORETICAL AND EXPERIMENTAL INVESTIGATION OF MUFFLERS WITH COMMENTS ON ENGINE-EXHAUST MUFFLER DESIGN<sup>1</sup>

By DON D. DAVIS, JR., GEORGE M. STOKES, DEWEY MOORE, and GEORGE L. STEVENS, JR.

#### SUMMARY

*Equations are presented for the attenuation characteristics of single-chamber and multiple-chamber mufflers of both the expansion-chamber and resonator types, for tuned side-branch tubes, and for the combination of an expansion chamber with a resonator. Experimental curves of attenuation plotted against frequency are presented for 77 different mufflers with a reflection-free tailpipe termination, and the results are compared with the theory. The experiments were made at room temperature without flow; the sound source was a loud-speaker.*

*A method is given for including the tailpipe reflections in the calculations. Experimental attenuation curves are presented for four different muffler-tailpipe combinations, and the results are compared with the theory.*

*The application of the theory to the design of engine-exhaust mufflers is discussed, and charts are included for the assistance of the designer.*

*Noise spectrums are presented for a helicopter with each of the four muffler-tailpipe combinations installed. These spectrums are compared with the noise spectrum of the unmuffled helicopter. The results show that the overall noise level of the helicopter was reduced significantly by even the smallest of the four mufflers tested.*

#### INTRODUCTION

A theoretical and experimental investigation of the methods of muffler design has been conducted at the Langley full-scale tunnel of the National Advisory Committee for Aeronautics as part of a general research program directed toward the reduction of airplane noise. The acoustic theory and muffler literature were studied with the aim of obtaining a method of predicting muffler characteristics. The theory of acoustic filters is discussed in reference 1. Sections of particular interest in connection with muffler design are the chapters on change in area of wave front, transmission through a conduit with an attached branch, and the filtration of sound, as well as the appendix which gives the branch-transmission theory of acoustic filtration. Experimental checks have been found in the literature which demonstrate that the theory of reference 1 is reasonably accurate for small

filters with stationary air at room temperature as the sound-conducting medium. When the derivation of the equations of the acoustic-filter theory is studied, however, certain assumptions are found which limit the maximum filter dimensions and also the maximum sound pressures for which these equations are applicable. Only limited data are available regarding the accuracy of the theory when applied to filters as large as engine-exhaust mufflers.

The British have studied the problem of aircraft mufflers with limited model experiments and with engine tests (refs. 2, 3, and 4). The model experiments show fair agreement with theory as to attenuation for a particular multiple resonator low-pass filter of the type described in reference 1 and for a multiple-expansion-chamber silencer. The experiments also showed a definite tendency for increasing flow velocity to increase the attenuation at low frequencies of expansion-chamber silencers. Air flow had little effect on the attenuation of the multiple resonator. In both cases, however, the flow velocities investigated were much lower than those which are found in engine-exhaust pipes. Muffler design has also been studied by the Germans with particular emphasis on mufflers for single-cylinder engines (refs. 5, 6, and 7). Ground tests of a large number of different mufflers on an actual engine are reported in references 8 and 9. The experimental results of reference 8 showed that, for the particular muffler discussed, both the low-frequency cutoff and the first high-frequency cutoff were near the calculated frequencies, which was encouraging. Unfortunately, however, the data of references 8 and 9 were not suitable for detailed verification of the theory because of interfering engine noise from sources other than the exhaust.

Although the literature indicated that certain acoustic theories could be useful in the design of engine-exhaust mufflers, neither the range of validity of the various theories with respect to muffler size nor the accuracy of the theories in predicting the attenuation of mufflers installed on actual engines could be deduced from the available data. It became apparent that, before more detailed information regarding the validity of the equations could be obtained, a test method was needed which would allow conditions to be

<sup>1</sup>Supersedes NACA TN 2893, "Theoretical and Measured Attenuation of Mufflers at Room Temperature Without Flow, With Comments on Engine-Exhaust Muffler Design" by Don D. Davis, Jr., George L. Stevens, Jr., Dewey Moore, and George M. Stokes, 1953 and NACA TN 2943, "The Attenuation Characteristics of Four Specially Designed Mufflers Tested on a Practical Engine Setup" by George M. Stokes and Don D. Davis, Jr., 1953.

closely controlled and which would reduce the number of variables involved. A relatively simple and fundamental approach seemed to be to develop a suitable apparatus and then to measure the attenuation characteristics of various types of mufflers in still air at room temperature. In order to eliminate the effects of tailpipe resonance, a termination with the characteristics of an infinite pipe was indicated. Such an attenuation-measuring apparatus was developed for the first part of this investigation.

The objective of this part of the investigation was to obtain from theoretical considerations equations for the attenuation of various types of mufflers and then to investigate the validity of these equations experimentally throughout a rather large range of muffler size in order to determine the limitations of the various equations with respect to muffler types, muffler dimensions, and sound frequencies. Because it is important in airplane-engine muffling to avoid excessive back pressures, only those types of mufflers which permit the exhaust gas to flow through the muffler without turning have been considered in this investigation.

Of course engine mufflers must be terminated with a tailpipe of finite length in actual practice. The influence of the finite tailpipe was studied in the second part of this investigation. A method for including the effect of the tailpipe in the muffler calculations was proposed, and an experiment was then conducted to investigate the validity of this method.

The problem of practical muffler design is discussed in Part III, and families of calculated attenuation curves for three types of mufflers are presented therein for the assistance of the designer.

The final part of this report describes an application of the theory to the design of four mufflers for a particular aircraft engine and the tests of these mufflers installed on the engine. The purpose of this part of the investigation was to study the practicality of the design methods and equations which had been developed and, also, to obtain some idea of the size of muffler which is required in practice to provide a significant noise reduction. Of particular interest was the question whether certain factors which had not been studied in the previous parts of the investigation would affect seriously the performance of the mufflers. Factors of primary concern were the very large sound pressures in the engine exhaust pipe and the flow velocity of the exhaust gas. In order to make possible a comparison of experimental data, the same mufflers were used for the finite tailpipe study and for the engine tests.

For an investigation of this nature, it is desirable to have an engine dynamometer stand; however, in this case, a helicopter was used for the engine tests because it was readily available. This was believed permissible because the helicopter rotor noise was expected to be lower than the engine noise, at least for the unmuffled engine.

#### SYMBOLS

$a$  radius of connector between exhaust pipe and branch chamber  
 $A$  displacement amplitude of an incident wave

$B$	displacement amplitude of a reflected wave
$c$	velocity of sound
$c_0$	conductivity of connector between exhaust pipe and branch chamber, $\frac{\pi a^2}{l_c + \beta a}$
$d$	diameter of expansion chamber
$f$	frequency
$f_c$	cutoff frequency
$I$	sound current
$k$	wave-length constant, $2\pi f/c$
$l'$	length of conical connector, measured along surface
$l_1$	length of pipe between connectors of two successive branches in a multiple resonator or length of pipe between two chambers of a combination muffler
$l_2$	length of resonant chamber
$l_c$	one-half of effective length of connector between two expansion chambers or length of connector between exhaust pipe and branch chamber
$l_e$	length of expansion chamber
$l_t$	effective length of tailpipe
$m$	expansion ratio; ratio of chamber cross-sectional area to exhaust-pipe cross-sectional area
$M$	number of chambers in multiple-resonator muffler
$n$	number of orifices or tubes which form connector between exhaust pipe and branch chamber
$p$	sound pressure
$R$	resistive component of impedance
$S$	cross-sectional area
$t$	time
$V$	volume of resonant chamber
$x$	distance coordinate measured along pipe
$X$	reactive component of impedance
$Z$	impedance
$Z_0$	characteristic impedance, acoustic resistance to transmission of a plane wave in a pipe, $\rho c/S$
$\beta$	constant in conductivity equation
$\lambda$	wave length, $c/f$
$\mu$	coefficient of viscosity of sound-conducting medium
$\rho$	average density of sound-conducting medium
$\sigma = 4\pi \frac{l'}{\lambda}$	
$\xi$	instantaneous displacement of a particle of the medium in which a plane acoustic wave is transmitted
$\dot{\xi}$	instantaneous velocity of a particle of the medium in which a plane acoustic wave is transmitted
$\omega$	circular frequency, $2\pi f$
Subscripts:	
$b$	branch
$c$	connector
$i$	incident wave
$r$	resonant
$re$	reflected wave
$t$	tailpipe
$tr$	transmitted wave

Note: Bars || are used to denote the absolute value (modulus) of a complex number.

## I. INFINITE TAILPIPE

### THEORY

The equations that have been used in the calculation of attenuation for the mufflers discussed in this report are derived and presented in the appendixes. Mufflers of the expansion-chamber type are treated in appendix A. The method used throughout the derivation of attenuation equations for single expansion chambers, double expansion chambers with external connecting tubes, and double expansion chambers with internal connecting tubes is that of plane-wave theory. In this theory the sound is assumed to be transmitted in a tube in the form of one-dimensional or plane waves. At any juncture where the tube area changes, part of the sound incident on the juncture is transmitted down the tube and part of it is reflected back toward the source. An expansion-chamber muffler consists of one or more chambers of larger cross-sectional area than the exhaust pipe, which are in series with the exhaust pipe. This type of muffler provides attenuation by taking advantage of the reflections from the junctures at which the cross-sectional area changes. A three-dimensional sketch of a typical double expansion chamber with an internal connecting tube is shown in figure 1 (a). The theory shows that below a certain frequency, which is called the cutoff frequency, the muffler is relatively ineffective. An approximate equation for determining this cutoff frequency has been derived and is presented in appendix A.

Mufflers of the resonator type are treated in appendix B. A typical single-chamber resonator is shown in figure 1 (b). This type of muffler consists of a resonant chamber which is connected in parallel with the exhaust pipe by one or more tubes or orifices. In certain frequency ranges the impedance at the connector is much lower than the tailpipe impedance. The resonant chamber then acts as an effective short circuit which reflects most of the incident sound back toward the source; thus, the amount of sound energy that is permitted to go beyond the muffler into the tailpipe is reduced. The attenuation equation for the single-chamber resonator is first derived by the method of lumped impedances; that is, phase differences between the two ends of the connector and between different points in the chamber are considered negligible. For this case, attenuation equations are developed first by considering the resistance in the connector and then by omitting this resistance; then, two additional equations, both of which omit the resistance, are developed. The first equation considers the effect of phase differences in the connector, whereas the second equation considers the effect of phase differences inside the chamber.

A typical multiple-chamber resonator is shown in figure 1 (c). For mufflers of this type, the equation given in reference 8 is used. In the derivation of this equation resistance is neglected, the connector and chamber are considered as lumped impedances, and the central tube between the resonators is treated as a distributed impedance. The sound in this central tube is considered to be transmitted in the form of plane waves. The multiple resonators, like the multiple expansion chambers, have a cutoff frequency. An

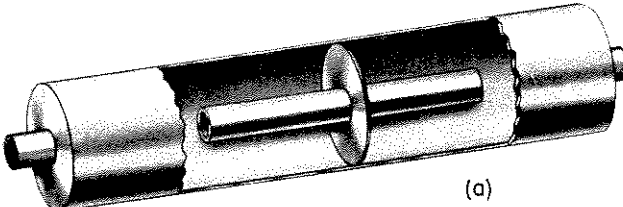
approximate equation for this cutoff frequency is also given in appendix B.

The conductivity  $c_0$  is a very important physical quantity which enters into the determination of both the resonant frequency and the amount of attenuation for resonator-type mufflers. The quantity  $\rho/c_0$  is, as is explained in reference 1, the acoustic inertance that is associated with a physical restriction in an acoustic conduit. Because this quantity is determined by the acoustic kinetic energy that is associated with the presence of the restriction and because this energy is a function of the conduit configuration on either side of the restriction as well as of the physical dimensions of the restriction itself, the conductivity is physically a rather elusive quantity which is predictable in only certain special cases, such as that of a circular orifice in an infinite plane. In most practical cases, it is therefore necessary to base an estimate of  $c_0$  on past experimental evidence.

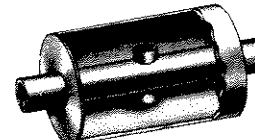
The prediction of  $c_0$  is discussed in reference 1. In the case of a single connector, with diameter not too large in comparison with the exhaust-pipe diameter, the equation given is

$$c_0 = \frac{\pi a^2}{l_c + \beta a}$$

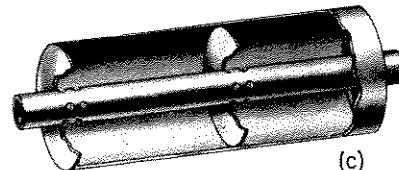
where  $\beta$  is an empirical constant, which has been found to be usually between  $\pi/2$  and  $\pi/4$ . If the connector is composed



(a)



(b)



(c)

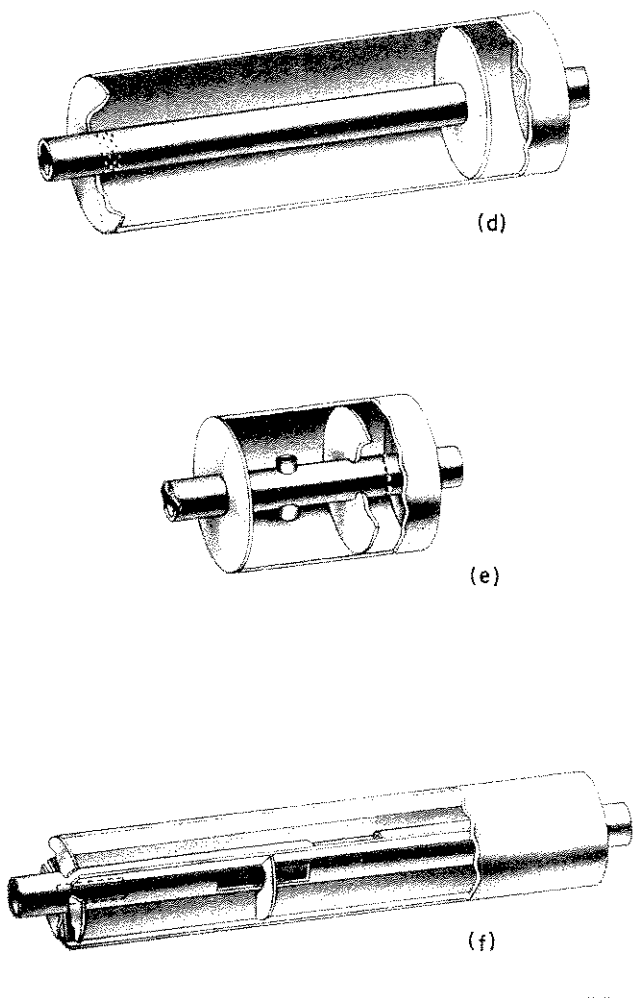
L-77028

- (a) Double expansion chamber with internal connecting tube (muffler 19).
- (b) A typical single-chamber resonator.
- (c) Double-chamber resonator (muffler 54).

FIGURE 1.—Sketches showing internal details of several mufflers.

of several orifices, a further uncertainty is introduced since the interference effects among the orifices are not known. In this report, the calculated curves will be based on the experimentally measured conductivity in those cases where the calculated and experimental conductivities show significant differences. In a section immediately following the presentation of the single-resonator and multiple-resonator results, the problem of conductivity prediction is discussed with the assistance of the experimental results.

Equations are derived in appendix C for two types of combination mufflers. The first is a combination of two resonators tuned at different frequencies and the second is a combination of an expansion chamber and a resonator. Combinations of these types are shown in figures 1(d) and 1(e).



(d) Combination of a resonator and an expansion chamber (muffler 71).  
 (e) Two resonators tuned to different frequencies (muffler 73).  
 (f) Combination of several quarter-wave resonators (muffler 74).

FIGURE 1.—Concluded.

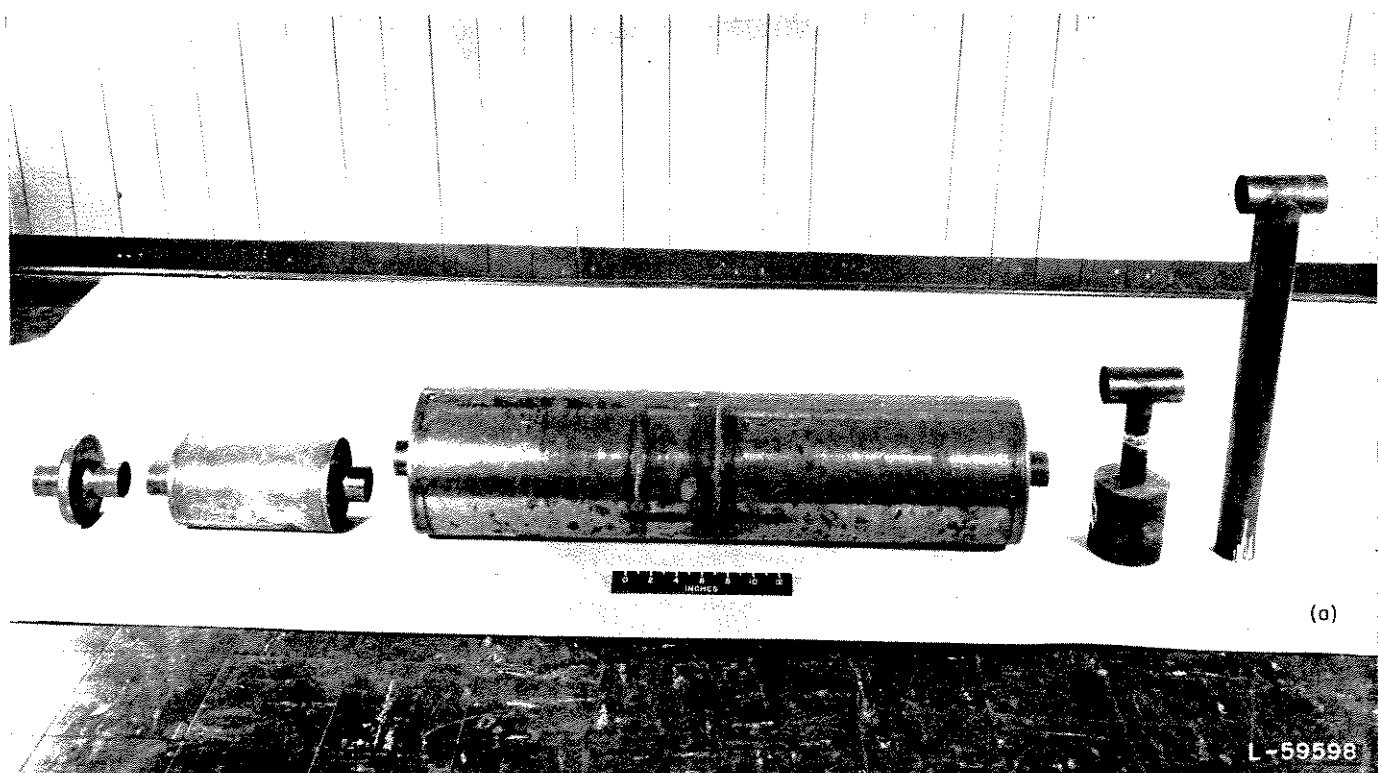
## MUFFLERS

The mufflers used in the "infinite" tailpipe part of the experimental investigation were constructed of 18-gage sheet steel (0.049-in. thickness) and unless otherwise specified were of circular cross section. Seam welds were used throughout to prevent leakage between the adjacent chambers of the mufflers. In all cases, the exhaust-gas flow is from left to right. Three-dimensional sketches showing internal details of several of the mufflers are given as figure 1. Photographs of some of the mufflers are shown as figure 2. Results are presented for 74 mufflers that were built to fit a 3-inch-diameter exhaust pipe. These mufflers varied in diameter from 4 inches to 24 inches and in length from 1 inch to 96 inches. In addition, results are presented for three mufflers that were built to fit a 12-inch-diameter exhaust pipe.

The types of mufflers on which the most extensive tests were made are the single expansion chamber, the multiple expansion chamber, the single resonator, and the multiple resonator. The single-expansion-chamber mufflers were empty cylindrical tanks with inlet and outlet tubes centrally located at the two ends. Multiple expansion chambers were constructed by placing two or more expansion chambers in series and connecting them with either internal or external tubes. These connecting tubes varied in length from 0.05 inch (the thickness of the central baffle in the muffler) to 42 inches and had a diameter of 3 inches. Each of the single-resonator mufflers consisted of an enclosed volume connected to the exhaust pipe by either tubes or circular orifices. The resonant chamber was located either as a branch projecting from the side of the exhaust pipe or as an annular chamber concentric with the exhaust pipe. In this type of muffler and in others in which the muffling element is located in "parallel" with the exhaust pipe, the exhaust gas, as a whole, is not required to flow through the volume chamber as it is in the expansion-chamber type of muffler. The multiple-resonator mufflers consist of two or more identical resonators spaced at equal intervals along the exhaust pipe. A few mufflers were constructed of combinations of the above types. In addition, side-branch tubes with one end closed were investigated.

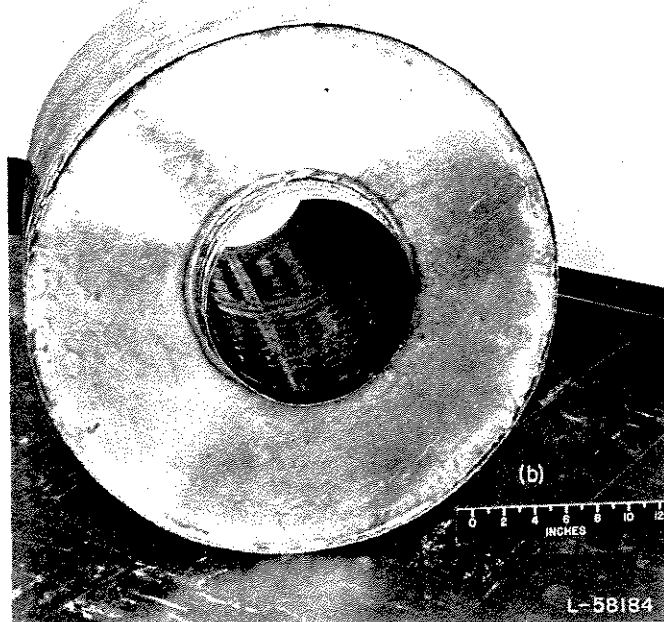
## APPARATUS

The test apparatus used in this investigation is shown schematically in figure 3 and a photograph of the equipment used for testing the mufflers with 3-inch inlet diameter is shown as figure 4. The sound was generated by the 15-inch coaxial loud-speaker shown at the left and was conducted through a 3-inch tube to the muffler, which was attached to the tube by rubber couplings. The sound which passed through the muffler continued down a 3-inch tube to the termination, which consisted of several feet of loosely packed cotton. The section of the tube between the loud-speaker and the muffler is called the exhaust pipe in this report, and the section of the tube beyond the muffler is called the tailpipe.



(a) Mufflers for 3-inch-diameter exhaust pipe.

FIGURE 2.—A group of mufflers investigated.



(b) Central-tube diameter, 12 inches; muffler 74.

FIGURE 2.—Concluded.

Measuring stations at which microphones could be inserted were installed in the exhaust pipe and the tailpipe. These measuring stations had the same cross-sectional area as the tube and were so designed that the microphone, when inserted, produced only a slight restriction in the acoustic tube. Because of the interaction between the incident sound wave traveling toward the muffler and the wave reflected by the muffler traveling back to the loud-speaker, the sound pressure varied with distance along the exhaust pipe. A sliding measuring station was, therefore, installed in the exhaust pipe. Three stationary measuring stations, unevenly spaced, were inserted in the tailpipe between the muffler and the cotton termination. With a 3-inch pipe in the muffler position instead of a muffler, the cotton was adjusted until the reflections from the termination were minimized. Reflections were detected by differences in the sound pressures at the various tailpipe measuring stations. With the termination used in this investigation, the pressures at these three stations varied by a maximum of about  $\pm \frac{3}{4}$  decibel for frequencies between 120 and 700 cycles per second and about  $\pm 1\frac{1}{2}$  decibels for frequencies between 40 and 120 cycles per second.

A General Radio Company type 759-B sound-level meter was used to determine the sound-pressure levels at the measuring stations. The crystal microphone of this meter

produced an electrical signal proportional to the sound pressure when it was inserted at the measuring stations. The meter indicated the sound-pressure level in decibels, defined as  $20 \log_{10} \frac{p}{p_0}$  where  $p_0$  is the standard base-pressure level of 0.0002 dyne per square centimeter. An oscilloscope and a sound analyzer were used as auxiliary equipment to make periodic checks of the wave form (freedom from harmonics) of the sound at the measuring stations.

The power supply for the loud-speaker consisted of the output of an audio oscillator feeding into a 50-watt amplifier. No harmonics were detectable within 40 decibels of the fundamental level in the input to the loud-speaker at the operating conditions used in this investigation. An electronic voltmeter was used to determine the input voltage supplied to the loud-speaker.

Part of the investigation involved the testing of three large mufflers in a 12-inch-diameter tube. A photograph of the apparatus used is shown in figure 5. In general, the

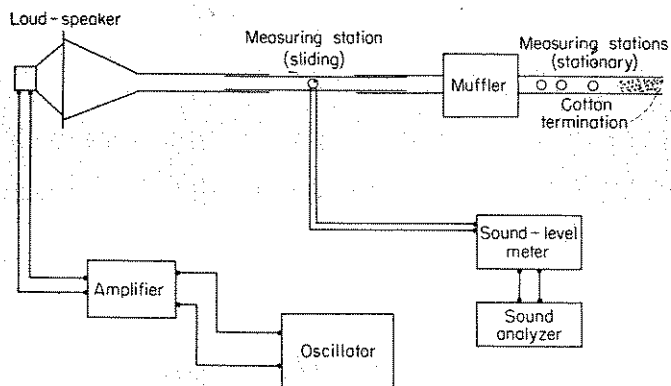


FIGURE 3.—Schematic diagram of experimental apparatus for infinite tailpipe investigation.

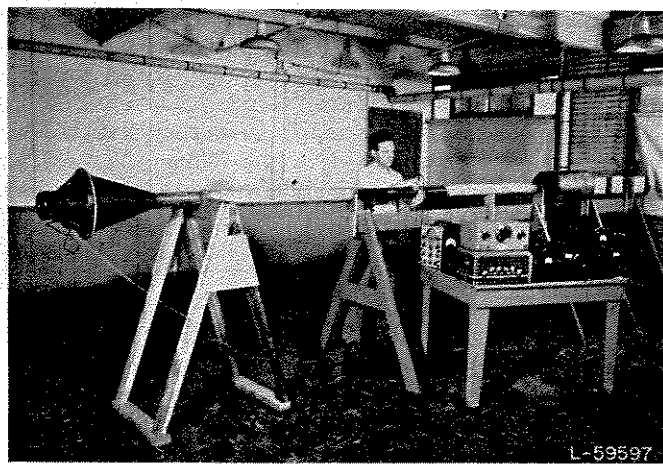


FIGURE 4.—Apparatus used for testing mufflers designed for a 3-inch exhaust pipe.

apparatus was similar in principle to the 3-inch apparatus. Traversing microphones operated by a pulley and cable arrangement were used in both the exhaust pipe and the tailpipe. In order to simplify the apparatus, the microphones were placed inside the 12-inch pipes, as shown in figure 6, where they imposed less than a 4-percent maximum area restriction. A cotton termination was again used, although it was not quite as effective as was the termination of the 3-inch apparatus.

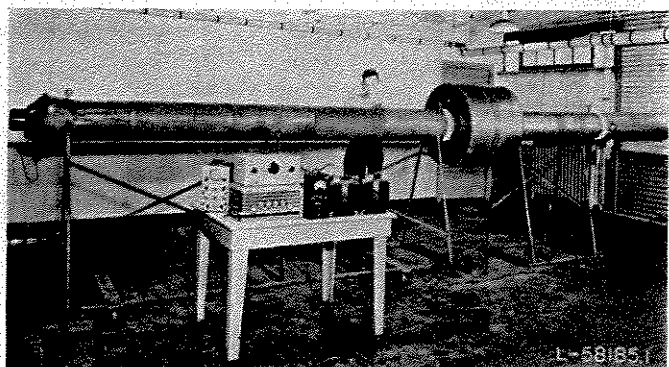


FIGURE 5.—Apparatus used for testing mufflers designed for a 12-inch exhaust pipe.

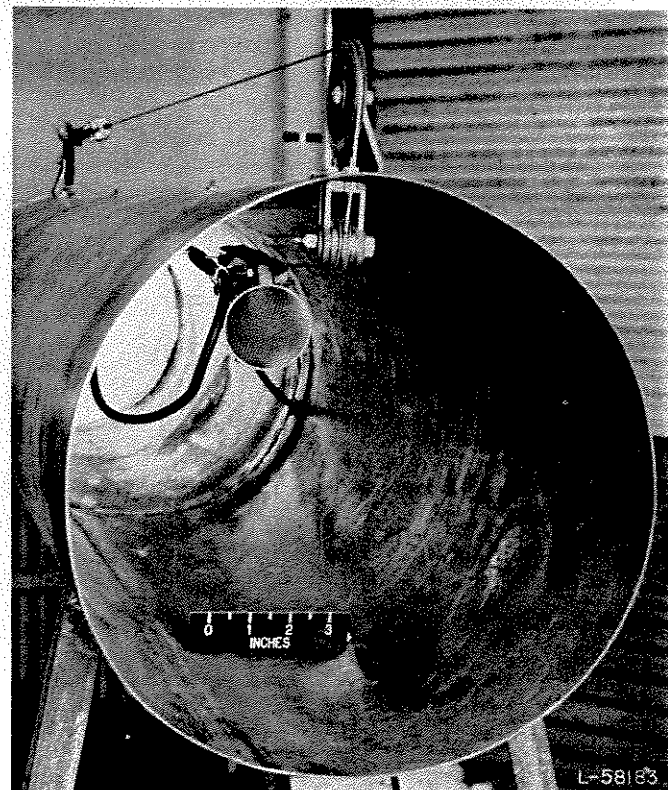


FIGURE 6.—Movable-microphone arrangement in the 12-inch tailpipe.

## METHODS AND TESTS

In the tests of each of the muffler configurations, the maximum sound-pressure level obtainable at the sliding measuring station in the exhaust pipe and the sound-pressure levels at the three stationary measuring stations in the tailpipe were recorded. The data from the three tailpipe stations provided a running check on the absence of reflections in the tailpipe. The attenuation is defined as  $20 \log_{10} \frac{p_i}{p_{tr}}$ , where  $p_i$  is the incident-wave pressure in the exhaust pipe and  $p_{tr}$  is the transmitted-wave pressure in the tailpipe. The tailpipe data obtained in these tests give the true transmitted sound-pressure levels in the tailpipe, but the exhaust-pipe readings do not give the incident-wave sound-pressure levels in the exhaust pipe; instead, they give the maximum sound-pressure levels in the exhaust pipe. This maximum pressure is due to the superposition of the incident wave and the wave which is reflected from the muffler. In some cases, it is possible to calculate precisely the difference between the true attenuation and the quantity measured in these tests. This measured quantity is the maximum drop in sound-pressure level between the exhaust pipe and the tailpipe. The calculated difference can be applied as a correction to the experimental data. The corrected experimental data can then be compared with the calculated attenuation curves. Although this method provides an exact correction for the experimental data, it has certain disadvantages. It becomes quite tedious because separate correction calculations must be made for each separate muffler. Also, each time the muffler type is altered slightly, new equations must be derived. This process would become quite difficult and time-consuming for some of the more complicated muffler types. For these reasons a much simpler method of correction was devised, although at some sacrifice in terms of accuracy. This approximate correction was obtained as follows:

Assume that all sound reflection takes place from a single point and that the incident sound pressure is unity. If five percent of the incident wave is reflected, the maximum pressure in the exhaust pipe, which occurs at that point where the incident and reflected waves are exactly in phase, is 1.05. Then the sound-pressure level in the exhaust pipe will be  $20 \log_{10} \frac{1.05}{1.00}$  or 0.42 decibel higher than the incident-wave sound-pressure level. Ninety-five percent of the incident pressure will be transmitted, so that the true attenuation will be  $20 \log_{10} \frac{1.00}{0.95}$  or 0.45 decibel. The maximum drop which would be measured experimentally would be  $0.42 + 0.45$  or 0.87 decibel. By this procedure, table I was compiled, from which the approximate correction curve shown in figure 7 was plotted. This correction has been applied to all experimental data presented in Part I of this report. Some idea of the magnitude of the error introduced by using this approximate correction instead of the exact correction

may be obtained from figure 8, which was calculated for an expansion-chamber muffler. The top curve is the calculated difference between the maximum sound-pressure level in the exhaust pipe (at the point where the incident and reflected waves are in phase) and the sound-pressure level in the tailpipe (see eq. (A13)). The top curve is labeled "measured" because this is the quantity which, in the tests, was determined directly from experimental measurements. The lower curve shows the true attenuation of the muffler, based on the difference between the incident-wave pressures in the exhaust and tailpipes (eq. (A10)). The middle curve was obtained by applying the approximate corrections (fig. 7) to the measured attenuation curve. Note that the difference between the exact and approximately corrected attenuation curves is quite small at the higher values of attenuation.

Insofar as was practicable, the attenuation was calculated for each muffler tested by the theory of the appendixes, and the calculated attenuation curves and corrected experimental attenuation data were plotted. A maximum frequency of 700 cycles per second was chosen for the experiments because most of the exhaust noise energy is contained in the range below this frequency (ref. 9).

TABLE I.—CALCULATED CORRECTIONS TO MEASURED ATTENUATION VALUES (PART I)

Percent reflection	Rise in exhaust pipe = Correction, db	True attenuation, db	True attenuation + Rise = Measured attenuation, db
5	0.42	0.45	0.87
10	.83	.92	1.74
20	1.58	1.94	3.52
30	2.28	3.10	5.38
40	2.92	4.24	7.16
50	3.52	6.02	9.54
60	4.08	7.96	12.04
70	4.61	10.46	15.07
80	5.11	13.98	19.09
85	5.34	16.48	21.82
90	5.58	20.00	25.58
95	5.80	26.03	31.83
97	5.90	30.46	36.35
99	5.98	40.00	45.98
99.5	6.00	46.02	52.02
99.9	6.02	60.00	66.02
100	6.02	$\infty$	$\infty$

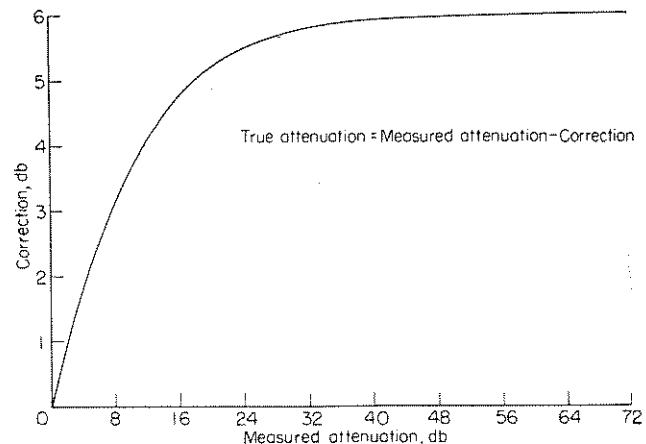


FIGURE 7.—Corrections to measured attenuation (Part I).

The leakage of room noise into the microphone at the tailpipe measuring stations limited the minimum measurable noise level. Consequently, the maximum measured attenuation for any muffler tested was limited to about 50 decibels and at the higher frequencies was somewhat less. If the tailpipe measuring stations and the microphone had been better isolated from external noise and if the muffler walls had been rigid and nonconducting to sound, higher values of attenuation could have been measured. No attempt was made to obtain such measurements because values of attenuation higher than 50 decibels did not seem important to this investigation. In practice, noise transmission through the muffler walls prevents the attainment of even a 40-decibel attenuation with the usual thin-wall sheet-metal construction. Furthermore, other noise sources on an airplane are normally loud enough so that an exhaust noise reduction of the order of 50 decibels is not warranted.

#### RESULTS AND DISCUSSION

The results of this part of the investigation are presented in the form of curves of attenuation in decibels plotted against frequency in cycles per second. The curves have been calculated by the theory of the appendixes and they are accompanied by experimental points. The validity of the theory is examined by comparing the theoretical and experimental results. A sketch of each muffler is shown beside the corresponding attenuation curve. The unit of length for the dimensions or constants given below the individual sketches

is 1 foot. The results for the various types of mufflers are presented in the following order:

Expansion chamber (figs. 9 to 11)

Resonator (figs. 12 to 14)

Side-branch tube (fig. 15)

Combinations (fig. 16)

Large-diameter mufflers (fig. 17)

The speed of sound was about 1,140 feet per second and this number has been used to determine the wave lengths corresponding to the frequencies presented  $(\lambda = \frac{c}{f})$ .

#### SINGLE EXPANSION CHAMBER

The attenuation in decibels of a muffler which consists of a single expansion chamber is given by the following formula (appendix A, eq. (A10)):

$$\text{Attenuation} = 10 \log_{10} \left[ 1 + \frac{1}{4} \left( m - \frac{1}{m} \right)^2 \sin^2 kl_e \right]$$

This equation indicates that the attenuation increases as the ratio  $m$  of the chamber area to the exhaust-pipe area increases and that the attenuation curve is cyclic, repeating itself at frequency intervals determined by the length of the muffler  $l_e$  and the velocity of sound inside the muffler  $c$   $(k = \frac{2\pi f}{c})$ .

**Effect of expansion ratio.**—The effect of varying the expansion ratio is shown in figure 9 (a) where  $m$  is varied from

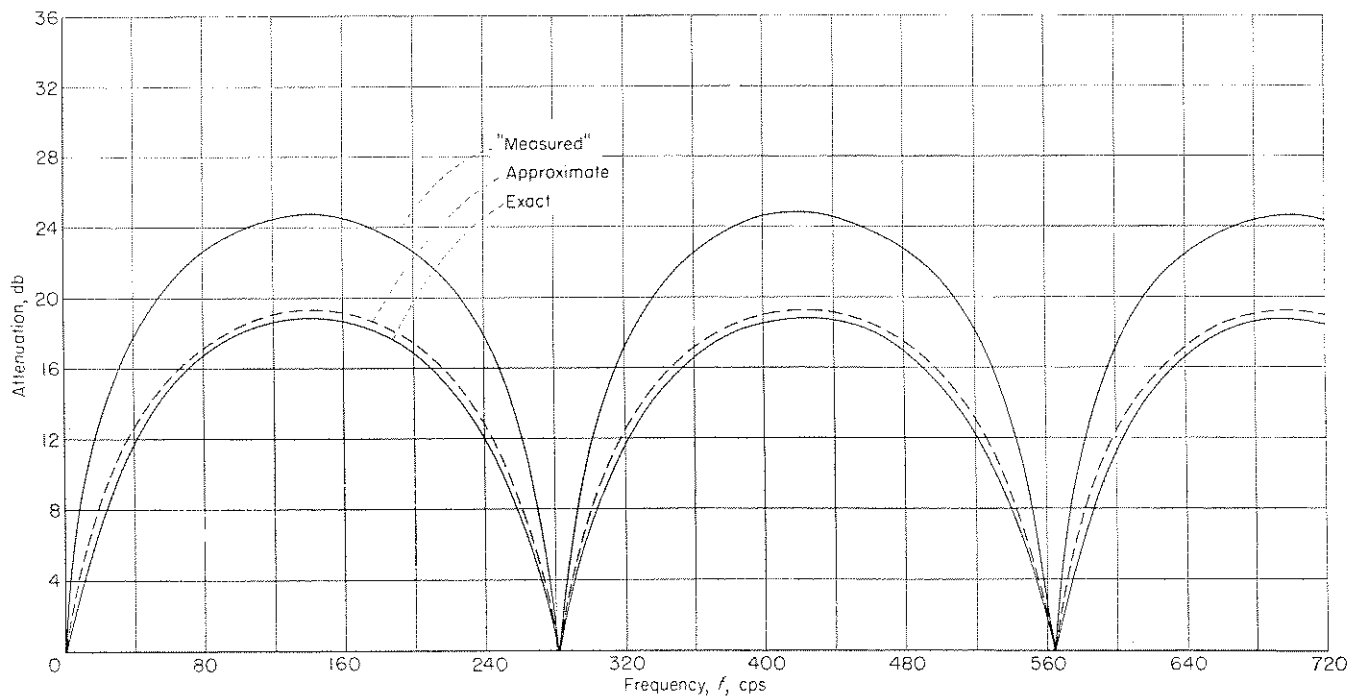


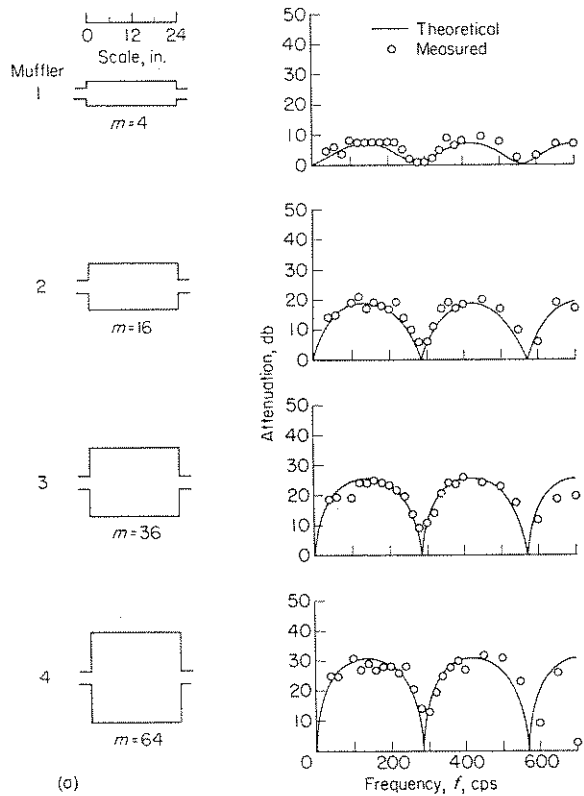
FIGURE 8.—Computed comparison of exact and approximately corrected attenuation curves for a single expansion chamber.

4 to 64. This figure shows clearly that the requirement for high attenuation is that the muffler have a large expansion ratio. Although the experimental points show some scatter, it appears that the theory is valid for muffler diameters as large as the wave length of the sound. This region of validity includes the region of practical interest in airplane-muffler design. The failure of the theory to predict the large loss of attenuation for muffler 4 at 700 cycles per second is believed to be due to the fact that the theoretical assumption of plane sound waves is no longer valid.

The complete solution for the velocity potential inside a circular tube shows that there are an infinite number of possible vibrational modes for the transfer of sound energy. Equation (A10) is based on the plane-wave mode, which may exist at any frequency. Other modes, which contain angular and radial nodes, are also possible at sufficiently high frequencies. Because the tubes and chambers which make up these mufflers are concentric, no vibrational modes which involve angular nodes would be expected. If these modes are eliminated, the lowest frequency at which any mode other than the plane wave can be transmitted without attenu-

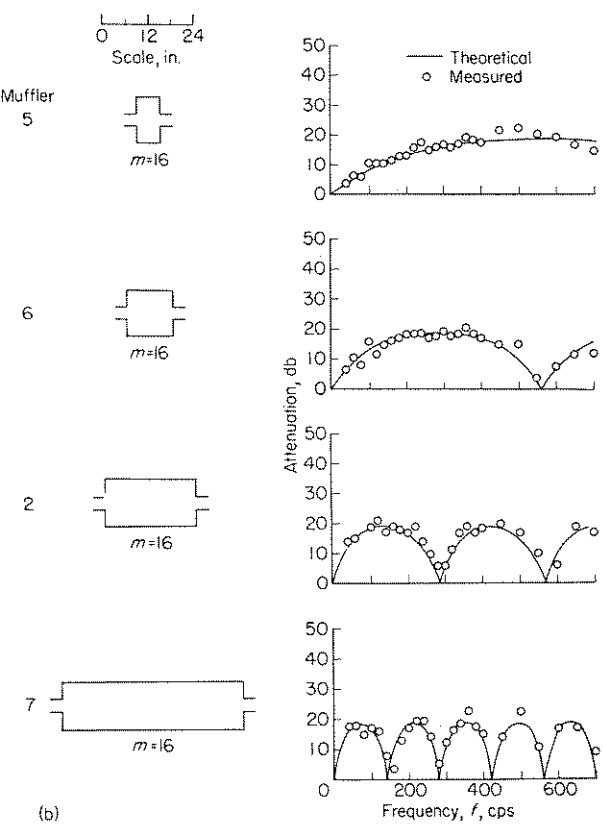
ation is given by  $f = 1.22 \frac{c}{d}$ . (The basic limiting condition is that  $J_1\left(k \frac{d}{2}\right) = 0$ , where  $J_1$  is the Bessel function of the first kind of order 1, which has  $\frac{2\pi f}{c} \frac{d}{2} = 3.83$  for its lowest root.) In terms of the wave length, this expression can be rewritten as  $\lambda = 0.82d$ . Thus, the assumption of plane waves is valid for wave lengths down to somewhat less than the chamber diameter. For muffler 4 the critical frequency given by this formula is 694 cycles per second. The experimental results show a sudden loss of attenuation between 650 and 700 cycles per second, which indicates that the appearance of this undamped higher vibrational mode has reduced seriously the muffler effectiveness.

**Effect of length.**—The effect of varying the length of the muffler is shown in figure 9 (b). The peak attenuation, about 20 decibels, is essentially unaffected by the length change and is a function only of the expansion ratio. The frequency at which this peak occurs is reduced, however, as the length of the muffler is increased. The frequency at which the peak attenuation occurs is inversely proportional to the muffler length. The cyclic nature of the attenuation



(a) Effect of expansion ratio  $m$ .

FIGURE 9.—Comparison of theoretical and experimental attenuation characteristics for single-expansion-chamber mufflers. Equation (A10).

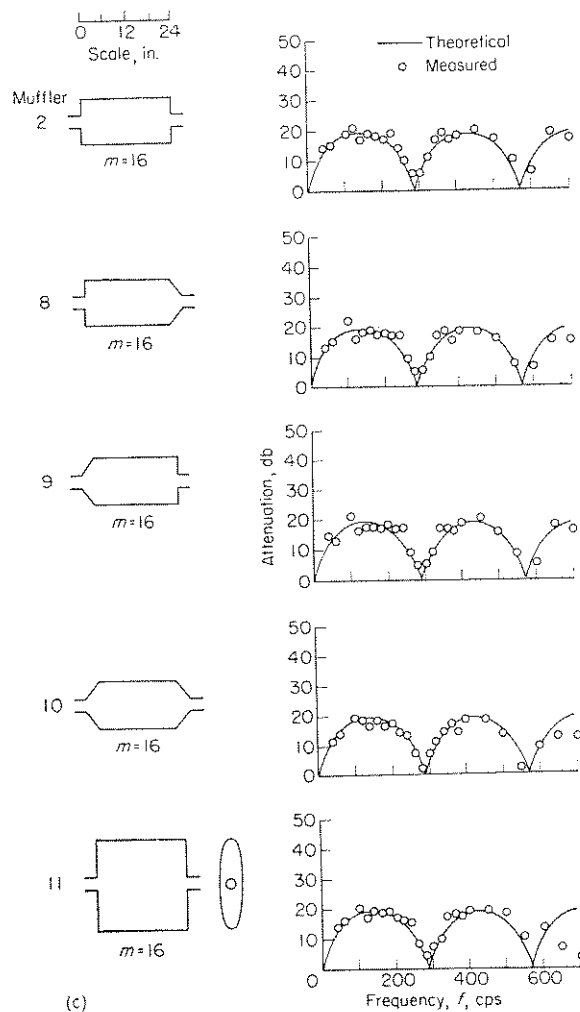


(b) Effect of length.

FIGURE 9.—Continued.

curve is evident with the attenuation dropping to zero for frequencies at which the muffler length equals an integral multiple of one-half the wave length  $\lambda/2$  ( $f = \frac{nc}{2l_e}$ , where  $n$  is any integer). The experiment and theory agree throughout the range tested which includes wave lengths as short as 0.4 of the muffler length in the case of the longest muffler. The theory contains no assumptions which directly limit this length. From the scale sketch of muffler 5, however, which has a diameter twice its length, it might appear that the sound waves inside the chamber would hardly be plane waves. Nevertheless, the experimental points are in good agreement with the plane-wave theory. Inasmuch as agreement is shown throughout the frequency range investigated ( $\lambda = 0.4l_e$  to  $57l_e$ ), there appears to be no practical length limitation on the plane-wave theory for expansion chambers.

**Effect of shape.**—The effect of shape variations is shown in figure 9 (c). Tapering either or both ends of the chamber



(c) Effect of shape.

FIGURE 9.—Concluded.

has little effect on the muffler performance except for some loss of attenuation near 700 cycles per second. The acoustical length of these mufflers was measured from the longitudinal center of the tapered sections. Although the mufflers are relatively insensitive to the steep tapers tested, it is probable that long slender tapers would act as horns and would tend to reduce the muffler effectiveness severely at the high frequencies. This effect is demonstrated in figure 10, which shows the attenuation for conical connectors as a function of the wave length, taper length, and expansion ratio. The curves of figure 10 were calculated from the equation

$$\text{Attenuation} = 10 \log_{10} \left\{ \left[ 1 + \frac{(\sqrt{m}-1)^2}{\sqrt{m}} \left( \frac{1-\cos \sigma}{\sigma^2} \right) \right]^2 + \left[ \frac{(\sqrt{m}-1)^2}{\sqrt{m}} \left( \frac{\sigma-\sin \sigma}{\sigma^2} \right) \right]^2 \right\}$$

where  $m = \frac{S_2}{S_1}$  and  $\sigma = 4\pi \frac{l'}{\lambda}$ . This equation was derived from equation (3.97) on page 86 of reference 1.

Changing from a circular to approximately elliptical cross section with the cross-sectional area held constant resulted in a loss of attenuation above 600 cycles per second (muffler 11, fig. 9 (c)). At this frequency the wave length is slightly less than the length of the major axis of the ellipse. The loss of attenuation is probably due to the appearance of a higher-order vibrational mode as was found in the case of muffler 4. The solution of the wave equation in elliptic coordinates (ref. 10) shows that the critical frequency for the mode which was found to limit the circular muffler 4 (the  $H_0$  mode in electrical terminology) is actually increased as the chamber becomes elliptic, whereas the measured critical frequency for muffler 11 is much lower than for a circular muffler of the same perimeter. Thus, some other vibrational mode, with a lower critical frequency, must be responsible for the loss of attenuation of muffler 11 above 600 cycles per second. The lack of circular symmetry in

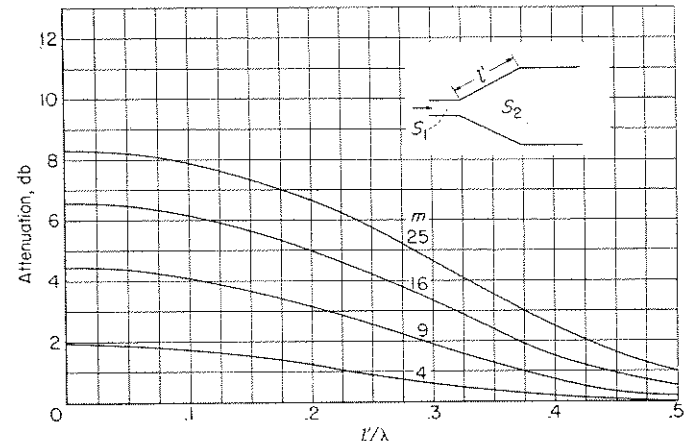


FIGURE 10.—Acoustical characteristics of truncated cone. (See ref. 1, p. 86.)

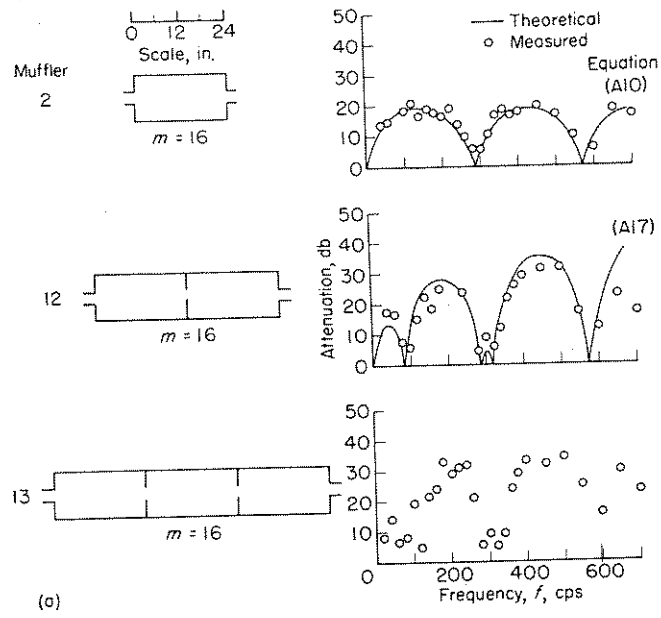
the elliptic case suggests consideration of the elliptical modes comparable to the unsymmetrical circular modes. Reference 10 describes two such modes oriented at right angles to each other. The mode which most closely matches the measured critical frequency is the odd  $H_1$  mode.

In connection with the effect of changes of shape, reference 9 shows that large flat walls should be avoided wherever possible because of their tendency to vibrate and thus transmit exhaust noise energy to the atmosphere.

#### MULTIPLE EXPANSION CHAMBER

Equations are developed in appendix A for the attenuation of double expansion chambers with external connecting tubes and with internal connecting tubes. The method used in appendix A may also be used to develop equations for three or more expansion chambers connected in series. The data to be presented include calculated attenuation curves for the double expansion chambers.

**Effect of number of chambers.**—The effect of increasing the number of expansion chambers in a muffler is shown in figure 11 (a) where data are presented for mufflers of one, two, and three chambers. The maximum attenuation is shown to increase as the number of chambers is increased, although the addition of the third expansion chamber results in only a small increase in the measured attenuation. Because the attenuation of the three-chamber muffler was found to be quite similar to that of the two-chamber muffler, it appears that the addition of a third chamber will result in little increased attenuation for mufflers of practical construction. For this reason and because of the increased complexity of the calculations, the theoretical attenuation of muffler 13 was not calculated. A region of low attenuation is encountered at the lower frequencies with the multiple

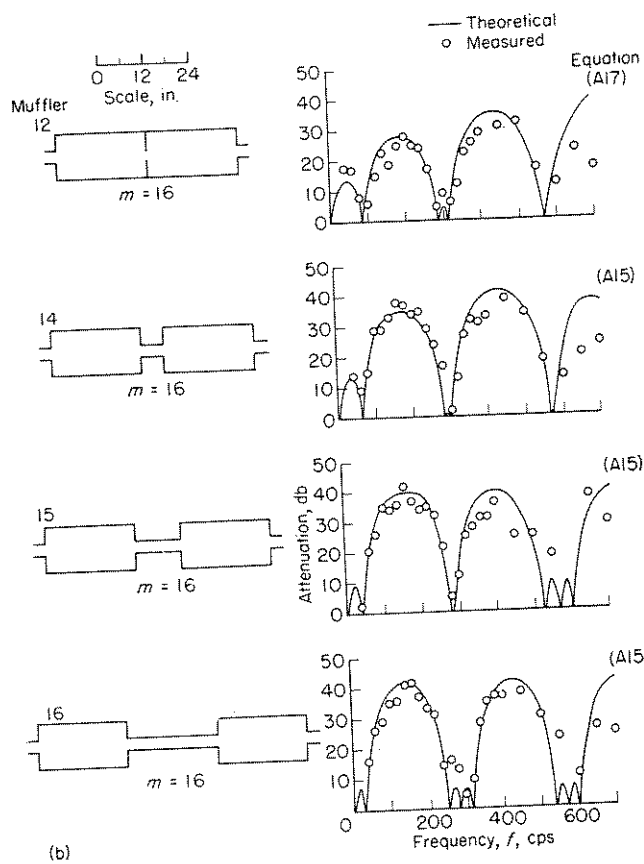


(a) Effect of number of chambers.

FIGURE 11.—Multiple-expansion-chamber mufflers.

expansion chambers. This region is predicted theoretically and will be discussed further. In the case of muffler 12, the calculated values agree fairly well with experiment down to a wave length about equal to the length of one of the chambers.

**Effect of connecting-tube length with an external connecting tube.**—Figure 11 (b) shows the effect of changing the length of the tube connecting the expansion chambers when this connecting tube is external to the chambers. The frequency at which the low-frequency pass region (region of relatively low attenuation) occurs is shown to decrease as the length of the connecting tube is increased. An approximate formula for the upper-frequency limit, which is called herein the cutoff frequency, of this low-frequency pass region has been developed and is included as equation (A18) in appendix A. Cutoff frequencies determined from this equation are compared with those determined from the more exact equation (A17) in table II. The maximum attenuation in the first attenuating band above the low-frequency pass region is shown to increase as the connecting-tube length is increased. With the longer connecting tubes, regions of low attenuation, with a width of 50 cycles per second or more, occur between the large loops of the attenuation curves. These pass bands would be objectionable in a muffler if a significant amount of exhaust



(b) Effect of connecting-tube length with an external connecting tube.

FIGURE 11.—Continued.

TABLE II.—CUTOFF FREQUENCY FOR DOUBLE EXPANSION CHAMBERS

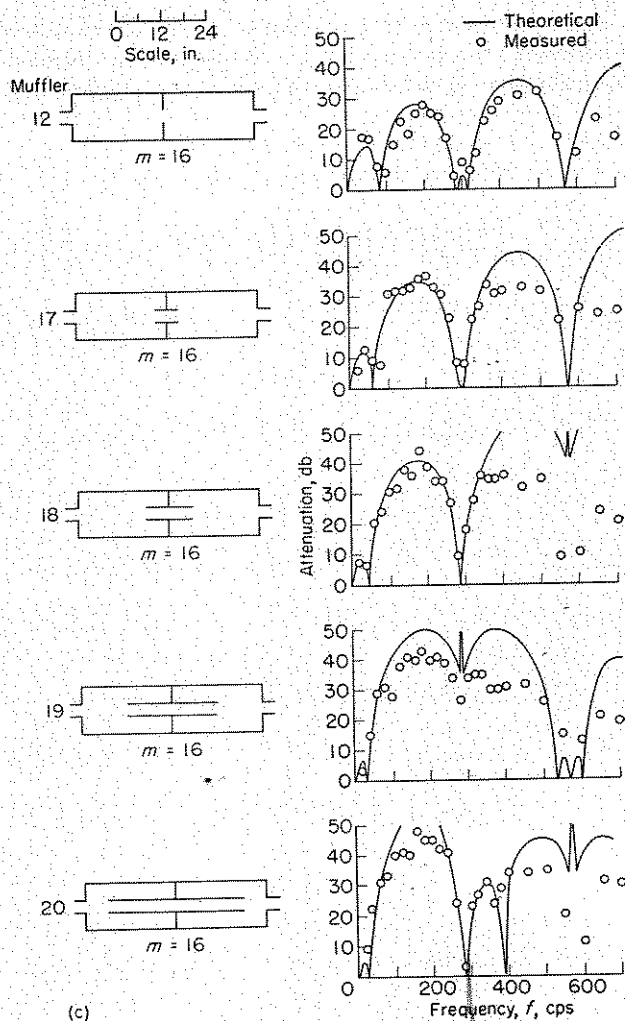
[ $c = 1140$  fps]

Muffler	$m$	$l_s$ , ft	$l_c$ , ft	$f_c$ , cps	
				Approximate (eq. (A18))	Exact (eq. (A17))
12	16	2	0.10	85.8	86.1
14	16	2	0.25	59.9	59.1
15	16	2	0.50	44.0	43.3
16	16	2	1.00	31.7	30.6
17	16	2	2.50	59.9	60.6
18	16	2	5.00	44.0	43.8
19	16	2	1.00	31.7	31.7
20	16	2	1.50	26.1	25.9
21	4	1	0.50	123.2	122.4
22	9	1	0.50	84.0	83.9
23	16	3	1.50	21.2	21.2

noise was present within these bands. The calculations and experiment are in agreement down to a wave length about equal to the length of one of the chambers.

**Effect of connecting-tube length with an internal connecting tube.**—Figure 11 (c) shows the effect of connecting-tube length when the connecting tube is symmetrically located inside the expansion chambers. The low-frequency pass region is again present and the frequency at which it occurs is again lowered as the connecting-tube length is increased. The cutoff frequency may be found approximately by using the same formula as in the case of the external connecting tubes (appendix A). The maximum attenuation in the first attenuating band above the low-frequency pass region is again increased as the connecting-tube length is increased. Also, pass regions are again encountered at the higher frequencies. The calculations again seem valid throughout most of the range investigated. When extremely high values of attenuation are calculated, the measurements are not accurate because of limitations of the apparatus. (See section entitled "Methods and Tests.") Very interesting results were obtained with muffler 19, for which the connecting-tube length was the same as the chamber length. The pass frequency at about 280 cycles per second, which is due to half-wave resonance of the expansion chambers, was eliminated. Although the attenuation did decrease in this region, the minimum attenuation measured was 27 decibels. The elimination of this pass region could prove quite useful in the design of a muffler which is required to attenuate over a wide frequency band. Further calculations and experiments have been made to investigate this phenomenon.

**Effect of having the internal-connecting-tube length equal to the chamber length.**—Results are shown in figure 11 (d) for four mufflers of different expansion ratios and lengths which had the common feature of an internal connecting tube of the same length as one of the expansion chambers. The results show, in all cases, that the pass region which normally occurs when the length of the expansion chamber is one-half the wave length is eliminated. This region is replaced by a region of reduced attenuation. The calculations for muffler 23 show that this phenomenon again occurs when the muffler length is  $3/2$  times the wave length. The pass region which occurs when the muffler length is equal to the wave length is not affected. The calculations show

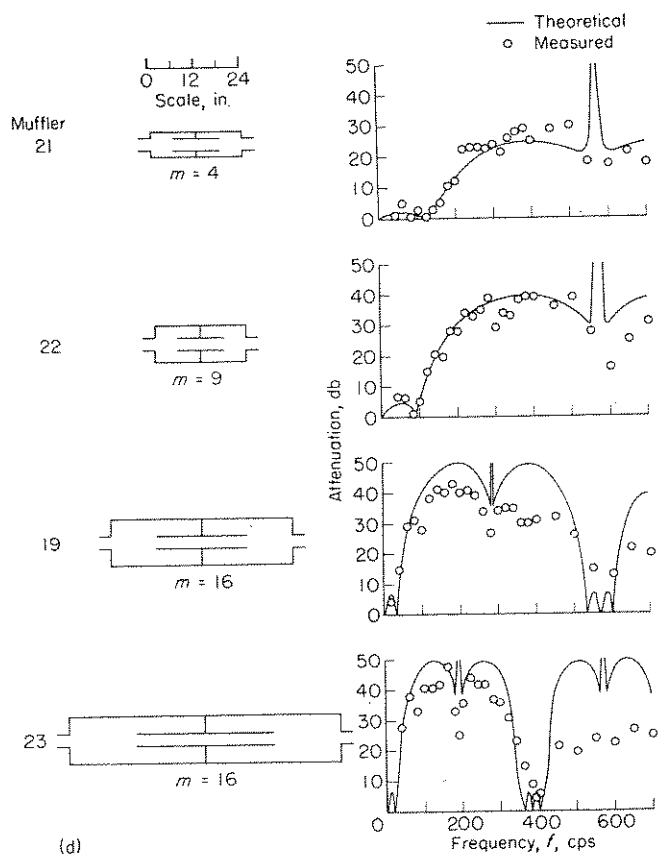


(c) Effect of connecting-tube length with an internal connecting tube. Equation (A17).

FIGURE 11.—Continued.

regions where the attenuation increases rapidly to infinity. Except for some discrepancy shown by the lower attenuation points in these regions, the calculations agree moderately well with the measurements down to a wave length about equal to the length of one of the chambers. The experiments, which were performed in advance of the detailed attenuation calculations, do not show points of extraordinarily high attenuation in these regions. A careful experimental survey which has since been made on another muffler of this general type, however, revealed in each such region a point of very high attenuation which was so sharply tuned that it appears to have no practical value.

Figure 9 (b) shows that, if a broad attenuation band is desired with a single expansion chamber, the chamber length should be reduced, but this reduction lowers the attenuation at low frequencies. If a longer double expansion chamber of the type shown in figure 11 (d) can be used, a broad attenuation band may be obtained without the loss of low-frequency attenuation, if the cutoff frequency is not too high. (Compare mufflers 6 and 19.)



(d) Mufflers with internal connecting tubes equal in length to the individual chamber lengths. Equation (A17).

FIGURE 11.—Concluded.

#### PRINCIPLES OF SINGLE-CHAMBER RESONATORS

Figure 1 (b) is a sketch of a typical resonator-type muffler which consists of an enclosed volume surrounding the exhaust pipe, the volume being connected to the exhaust pipe through two short tubes. The pressure fluctuations in the exhaust pipe are transmitted to the volume chamber through the two small connecting tubes. Since these tubes are short compared to the wave length of the sound, the phase differences between the two ends of the tubes can be neglected. Thus, the gas in the tubes can be considered to move as a solid piston of a certain mass upon which the tube walls exert a certain viscous or friction force. As this effective piston of gas moves in and out, the gas inside the volume chamber undergoes alternate compression and expansion. The attenuation of such a resonator can be computed by substituting equations (B7) and (B8) into equation (B4) of appendix B. In a large number of practical cases, the friction force between the air and the walls of the connecting tube is sufficiently small that it can be neglected in comparison with the mass forces acting on the air in the connecting tube and the compression forces within the volume chamber. Because of this fact, the equation for the attenuation of a frictionless resonator is also presented in appendix B (eq. (B10)).

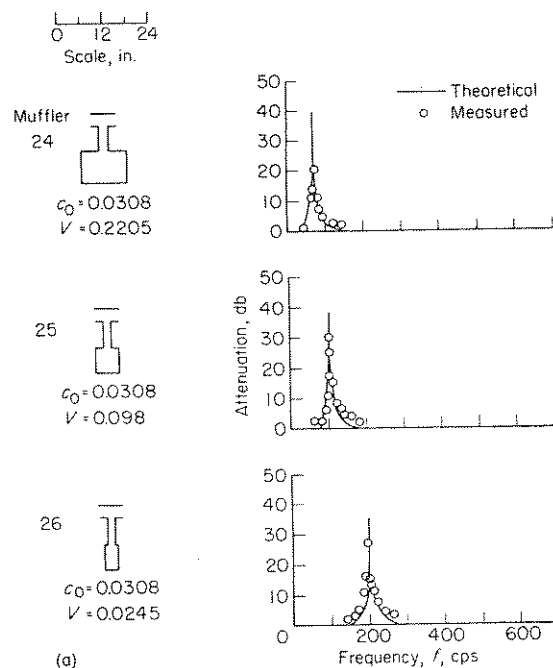
Single resonators of two very different physical configura-

tions were investigated. The first configuration consisted of a resonant chamber located as a branch from the exhaust pipe. These resonators were, in general, relatively small and the calculations included viscous forces in the connecting tubes. In the second configuration, the resonator was an annular chamber surrounding the exhaust pipe (fig. 1 (b)). The resonators of this configuration were generally somewhat larger than those of the first configuration and viscous forces were omitted from the calculations.

#### BRANCH RESONATORS

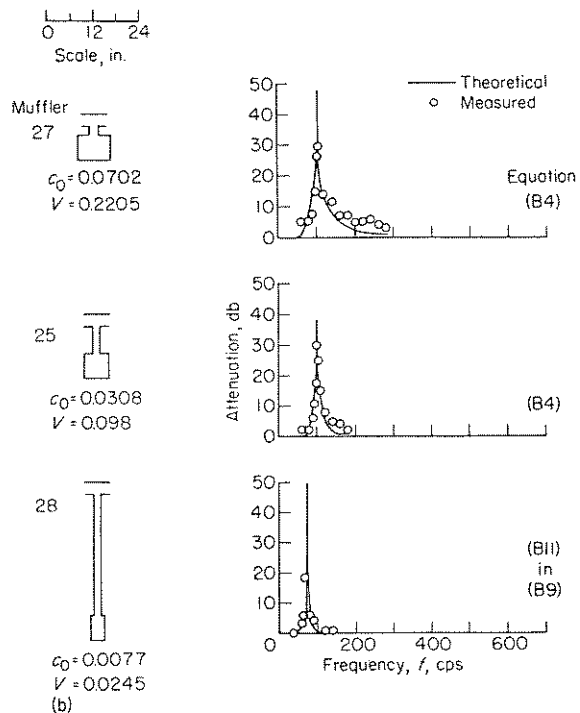
**Effect of varying resonator volume.**—The effect of varying the chamber volume of a resonator is shown in figure 12(a). The calculated and experimental curves are in general agreement although there is here, as in the succeeding data of figure 12, a general tendency for the muffler to give a higher than calculated attenuation at frequencies above resonance and a lower than calculated attenuation at the resonant frequency. As the calculations indicate, decreasing the volume  $V$  raises the resonant frequency. These resonators are quite effective at the resonant frequency but the attenuation falls off rapidly at lower or higher frequencies.

**Effect of varying  $c_0$  and  $V$  with the ratio  $\sqrt{c_0/V}$  constant.**—Figure 12(b) shows the effect of varying  $c_0$  and  $V$  together while keeping their ratio constant. The resonator equation states that the resonant frequency of a group of mufflers should be constant if the ratio  $\sqrt{c_0/V}$  is constant. This ratio will be called the resonance parameter. Mufflers 27 and 25 are found to have the same resonant frequency, but muffler 27 has a broader region of attenuation. This broader attenuation region is predicted by the theory and is due to the



(a) Effect of volume  $V$ . Equation (B4).

FIGURE 12.—Single-chamber resonators with resonator chambers separate from tailpipe.



(b) Effect of varying volume  $V$  and conductivity  $c_0$  together, with  $\sqrt{c_0/V}$  constant.

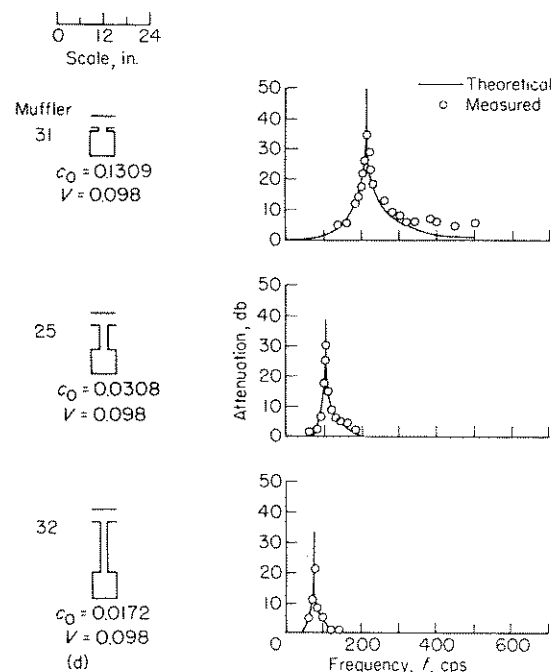
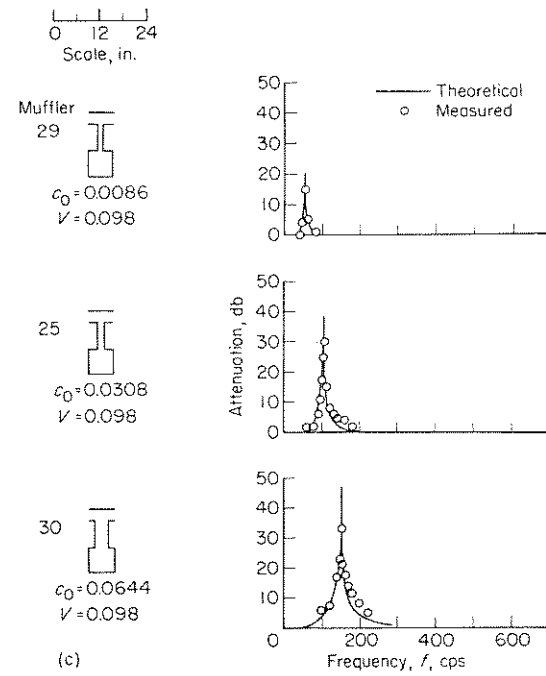
FIGURE 12.—Continued.

larger values of both  $c_0$  and  $V$  for muffler 27. The value of the parameter  $\sqrt{c_0V}/2S$ , which will be called the attenuation parameter, is increased to more than twice that for muffler 25. The data for muffler 28 show a decrease in the resonant frequency. This apparent contradiction of the theory is due to the fact that the connecting tube in muffler 28 is not negligibly short compared to the wave length. The calculated attenuation curve for muffler 28 was obtained by taking into account the wave nature of the sound flow in the connecting tube. (See appendix B, eq. (B11).) At the resonant frequency of this muffler, the length of the connecting tube is of the order of one-fifth of the wave length.

**Effect of varying cross-sectional area of the connecting tube.**—Increasing the connecting-tube area increases  $c_0$ ; thus, the values of both the resonance and attenuation parameters  $\sqrt{c_0/V}$  and  $\sqrt{c_0V}/2S$  are increased. Consequently, the resonant frequency is increased and the attenuation region becomes broader (fig. 12(c)). A comparison of mufflers 29 and 30 shows that, if an attempt is made to obtain low-frequency attenuation simply by decreasing  $c_0$ , the result may be very disappointing. Both the magnitude of the attenuation and the width of the attenuation region decrease as  $c_0$  decreases.

**Effect of varying length of connecting tube.**—Increasing the connecting-tube length decreases  $c_0$  and, therefore, has the opposite effect from an increase of the connecting-tube area. This is shown in figure 12(d). Note again that, when the resonant frequency is decreased without changing the volume, the attenuation region becomes narrower.

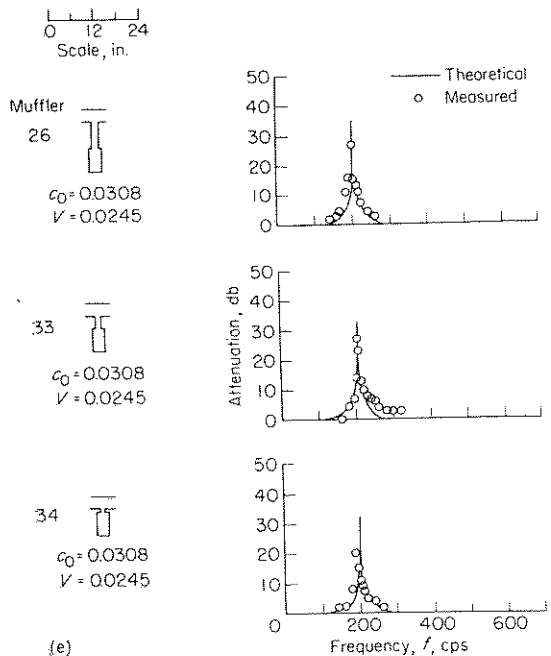
**Effect of changing connecting-tube configuration with  $c_0$  held constant.**—Although the conductivity  $c_0$ , is an important quantity in the attenuation equation, the physical configuration of this conductivity enters into only the viscous resistance term which is very small for most of the



(c) Effect of area of connecting tube  $S_2$ . Equation (B4).  
(d) Effect of length of connecting tube. Equation (B4).

FIGURE 12.—Continued.

resonators tested. Thus, the characteristics of a resonator are theoretically nearly independent of the manner in which the conductivity is obtained. The actual effect of changes in the physical configuration of the conductivity was investigated by testing three mufflers which had different connecting tubes but the same  $c_0$  and  $V$  (fig. 12 (e)). Although mufflers 26 and 33 give about the same results, muffler 34, which has the smallest connecting tube, gives less attenuation than either of the other mufflers. In this connection, a definite, though often unrecognized, limitation of the linearized acoustic theory is of interest. If the three resonators in figure 12(e) are to have the same attenuation, it is necessary that the mass flow in the connecting tubes be the same. But this condition requires a higher velocity as the tube diameter is reduced. Inasmuch as the linearized theory requires that the changes in velocity, pressure, and density be small, it follows that for a given pressure in the exhaust pipe a limiting tube diameter exists below which the velocity is so high that the theory is not valid. This phenomenon has an important bearing on the design of engine-exhaust mufflers. The velocity in a connecting tube of fixed diameter will increase as the sound-pressure level in the exhaust pipe increases. Inasmuch as the sound pressures inside an engine exhaust pipe are extremely high, care must be exercised to avoid a connecting tube which is too small to permit the required flow into and out of the chamber. Apparently this muffler limitation has never been investigated on an actual engine. Muffler configuration 30 of reference 9, however, is interesting in this connection. The performance of this muffler was initially disappointing, but when additional conductivity holes were added (con-



(e) Effect of varying connecting-tube area and length together, with  $c_0$  constant. Equation (B-4).

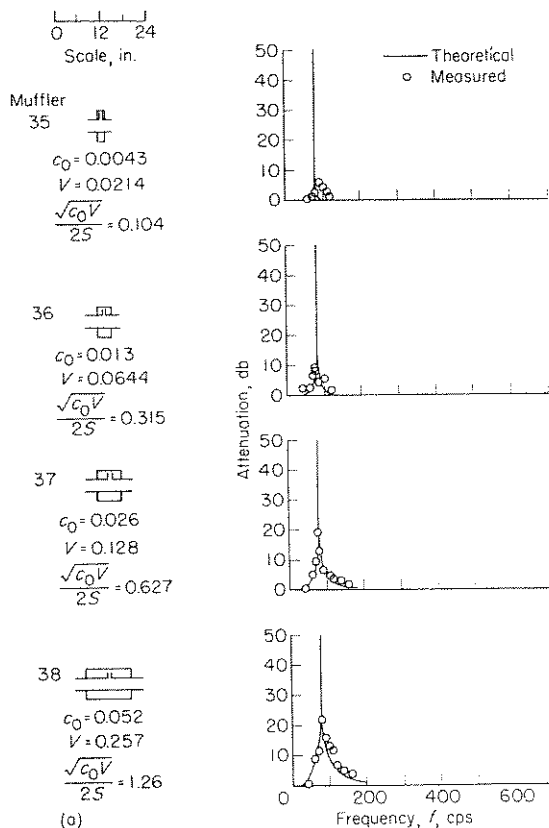
FIGURE 12.—Concluded.

figuration 31, ref. 9) the attenuation was markedly improved, even though the  $c_0$  was much larger than was desired. Perhaps this muffler would have been even better if the  $\frac{1}{4}$ -inch orifices had been replaced by a few tubes of  $\frac{3}{8}$ -inch to 1-inch diameter which had the same  $c_0$  as the  $\frac{1}{4}$ -inch orifices.

#### CONCENTRIC RESONATORS

In general, the resonators so far discussed have had relatively narrow attenuation bands. They would be useful in quieting a fixed-frequency noise source but are inadequate for use on a variable-speed engine or even on a fixed-speed engine with objectionable noise spread over a wide frequency band. For engines of these types a much broader attenuation band is desired. Basically, a broader band requires increased chamber volume and conductivity. Results are presented in figure 13 for single-chamber resonators of larger volume than those presented in figure 12. The mufflers shown in figure 13 are of conventional arrangement with the chamber located concentric with the exhaust pipe.

**Effect of varying  $\sqrt{c_0 V}/2S$  with the resonance parameter constant.**—The data of figure 13(a) show the expected



(a) Effect of varying the attenuation parameter  $\frac{\sqrt{c_0 V}}{2S}$  with the resonance parameter  $\sqrt{\frac{c_0}{V}}$  constant. Equation (B10).

FIGURE 13.—Single-chamber resonators with resonator chambers concentric with tailpipe.

broadening of the attenuation region as the value of the attenuation parameter is increased while the resonance parameter  $\sqrt{c_0/V}$  is kept constant. The resonant frequency was constant as predicted by the theory. Viscous forces were omitted from the calculations for these and all other mufflers shown in figure 13.

A similar investigation was made with the resonators tuned for a higher frequency and with orifices used for the connector instead of tubes (fig. 13 (b)). All four mufflers were designed for a resonant frequency of 280 cycles per second, but mufflers 40 and 41 resonate at higher frequencies. In each of these two mufflers the conductivity was much higher than was expected. This result illustrates a serious problem in muffler design—that of predicting the conductivity of a group of orifices. This problem is considered further after the multiple-resonator data have been discussed. The calculated curves for mufflers 40 and 41 were obtained by using the  $c_0$  as determined from the measured resonant frequency and the chamber volume. No definite resonant frequency was observed for muffler 42.

The measured attenuation of mufflers 41 and 42 falls below the calculated curves in the region near 600 cycles per second. The chamber is about one-half wave length long at this frequency and thus violates the theoretical assumption that the dimensions of the chamber are small compared to the wave length of the sound. Muffler 40, however, does not show this loss of attenuation at 600 cycles per second.

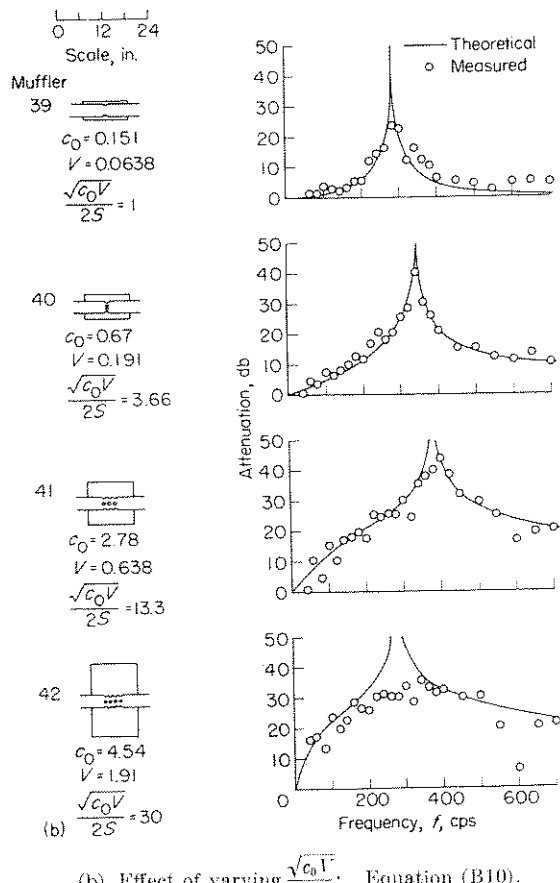


FIGURE 13.—Continued.

**Effect of varying the chamber length and connector location with the chamber volume constant.**—A group of mufflers was investigated in which the length and diameter of the resonator chamber and the location of the connector were varied while holding the chamber volume and the connector configuration constant (fig. 13 (c)). The measured attenuation of muffler 41 agrees with the calculated values except for the previously mentioned dip at 600 cycles per second. The resonator theory gives the same calculated attenuation for all of the mufflers shown in figure 13 (c). Actually no two of the five mufflers have the same measured attenuation. The explanation is found in the length of these mufflers. At the frequency at which muffler 41 resonates, the length of muffler 43 is about two-thirds of the sound wave length; therefore, it seems necessary to consider the wave nature of the sound. With this consideration, it is found that, when the distance from the connector to the end of the chamber is approximately one-fourth wave length, the reflection from the closed end of the chamber is  $180^\circ$  out of phase with the incoming pressure wave at the connector location. This results in high attenuation. For the configuration of muffler 43

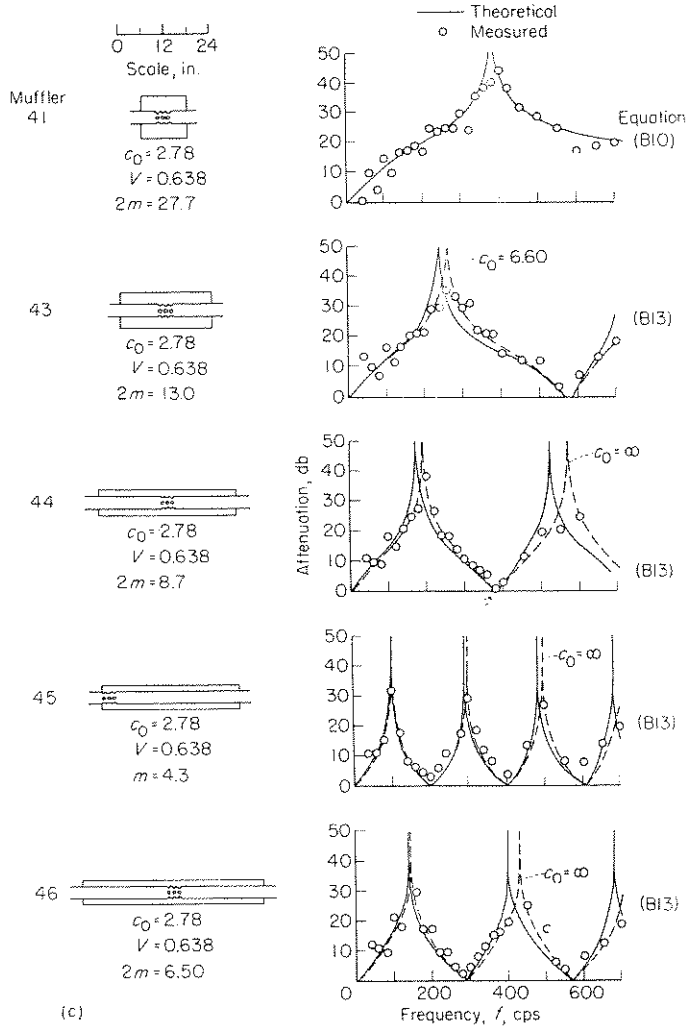


FIGURE 13.—Continued.

(centrally located connector), this condition occurs when the muffler length is one-half the sound wave length. Inasmuch as this condition is satisfied at a frequency lower than the resonant frequency predicted from the values of  $c_0$  and  $V$ , the fact that the resonator calculations fail to predict the characteristics of this muffler is not surprising.

Because the resonator theory was inadequate for mufflers 43 to 46, it was necessary to develop a different theory, based on the distributed impedance of assumed plane waves in the chambers. An equation derived for this case (appendix B, eq. (B13)) was used to calculate the attenuation of mufflers 43 to 46. In applying equation (B13) to the mufflers with the  $c_0$  in the center (mufflers 43, 44, and 46), the chambers were considered to be the equivalent of chambers of twice the cross-sectional area and half the length of the actual chambers. Thus  $m$  was replaced by  $2m$ ,  $S_2$  by  $2S_2$ , and  $l_2$  by  $\frac{1}{2}l_2$  in making the calculations. The value of  $c_0$  for these mufflers was first assumed equal to the measured  $c_0$  value for muffler 41, because the hole configurations were identical. The resulting attenuation curves are shown by the solid lines in figure 13 (c). The calculated curves (solid lines) did not give the correct resonant frequencies. Consideration of the sketches of these mufflers indicated that it was probably incorrect to assume a constant  $c_0$  for this group of mufflers.

A simple consideration can be used to show that the  $c_0$  is a function not only of the connector but also of the objects which it connects. Consider a thin baffle, containing a small orifice, placed in a tube of very large diameter. The  $c_0$  of the orifice then equals the orifice diameter. If, now, the diameter of the large tube be continuously decreased until it reaches the orifice diameter, the same orifice will simply form part of the tube and the  $c_0$  will be infinite. In figure 13 (c), the effective area ratio between the exhaust pipe and the outer chamber varies from 27.7 to 4.3, and it seems reasonable to expect that as this ratio decreases and the pipe and chamber areas become better matched the  $c_0$ , for the same orifices, will increase. As a test of this reasoning, the attenuation was calculated for muffler 43 by using  $c_0=6.60$  and for mufflers 44, 45, and 46 by using the limiting value  $c_0=\infty$ . Comparison of the dashed and solid curves with the experimental data shows that the  $c_0$  must be much higher for these mufflers than for muffler 41.

A comparison of the simple resonator theory with the more exact plane-wave theory will help to define the limitations of the simple theory, which is a "lumped impedance" theory. The impedance of the volume chamber is given as

$$-i \frac{\rho c}{S_2} \cot kl_2$$

by the plane wave or "distributed impedance" theory (note second term of eq. (B12)). If the assumption is made that

$\tan kl_2=kl_2=\frac{\omega}{c}l_2$ , the chamber impedance becomes

$$-i \frac{\rho c^2}{\omega S_2 l_2} = -i \frac{\rho c^2}{\omega V}$$

This is the value used in the lumped-impedance theory, and the difference in chamber impedance is the only difference between the two theories. When  $l_2$  is one-eighth of the

sound wave length, this difference is about 10 percent of the chamber impedance, and the error increases as the ratio  $l_2/\lambda$  increases. Because  $\cot kl_2$  is a cyclic function, the distributed-impedance theory predicts a series of resonant frequencies, whereas only a single resonant frequency is predicted by the lumped-impedance theory. The experimental results show that with the appropriate value for  $c_0$  the distributed-impedance theory is valid throughout the frequency range for mufflers 43 to 46, inclusive.

Comparison of the two theories indicates that the lumped-impedance theory is valid in the region near and below the first resonant frequency if  $l_2$  is less than one-eighth of the wave length at the resonant frequency. In order to compare further the two theories, the attenuation of muffler 41 has been calculated by both methods. The value of  $c_0$ , computed by the distributed-impedance theory from the measured resonant frequency, was found to be almost double the value that was used in the lumped-impedance calculation (fig. 13 (c)). The attenuation calculated with this higher value of  $c_0$  in the distributed-impedance equation (B13), however, differed from that calculated with the lumped-impedance equation by a maximum of only 1.4 decibels at a frequency of 700 cycles per second. Thus, in the case of muffler 41, the lumped-impedance theory has been extended to a case where  $l_2$  is 0.175 times the resonant wave length by the expedient of using a fictitious value of  $c_0$  that is much lower than the actual  $c_0$  as given by the distributed-impedance theory. This fictitious value of  $c_0$  was determined by using the equation

$$k_r = \sqrt{\frac{c_0}{V}}$$

from the lumped-impedance theory and by using the measured resonant frequency to determine  $k_r$ .

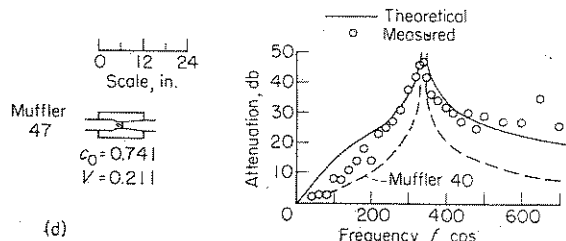
A comparison of the results for mufflers 44 and 45 shows that the attenuation region between two consecutive pass regions is wider when the conductivity is in the center of the muffler than when it is at one end, because of a decrease in the effective chamber length and an increase in the effective area ratio. The effect of the difference in chamber length, which changes the resonant frequency, can be eliminated by dividing the width of the attenuation region for a particular muffler by the resonant frequency of that muffler. A comparison on this basis shows that in the first attenuation band muffler 44 provides 10 decibels or more of attenuation over a frequency range of about 1.2 times the resonant frequency, while muffler 45 provides this attenuation over a range of only 0.8 times the resonant frequency. This difference in relative width of the attenuation bands is due to the difference in the effective area ratios. Mufflers based on this phenomenon of plane-wave resonance of the chambers are discussed further in a subsequent section of this report.

**Venturi-shaped central tube.**—The data that have been presented show that the width of the attenuation band can be increased by increasing the value of the attenuation parameter  $\sqrt{c_0 V}/2S$ . It is obviously possible to increase the value of this parameter without increasing the external size of a muffler if the area  $S$  is reduced. A significant reduction of the exhaust-pipe and tailpipe area is, however, impractical

or most aircraft engines because of the resultant increase in engine back pressure. An idea for avoiding this difficulty has nevertheless been devised. It was believed that a significant decrease in the central-tube area at the connector location might be obtained without excessive back pressure if the central tube of the muffler were built in the shape of a venturi with the connector located at the throat. The acoustics of such a muffler were investigated by designing and testing a muffler with the same external dimensions as muffler 40 but with a venturi-shaped central tube which reduced the area at the connector by a factor of four. The data of figure 13 (d) show that the modified muffler 47 provides much more attenuation than muffler 40. This increase is particularly striking in the region above the resonant frequency. For comparative purposes, a theoretical curve is shown which gives the attenuation of a muffler having the same values of  $c_0$  and  $V$  as muffler 47 but which has an exhaust pipe of constant diameter equal to the minimum diameter (1.5 in.) of the pipe of muffler 47. For frequencies above about 70 percent of the resonant frequency, muffler 47 provides approximately the attenuation of such a muffler. Thus, in cases where some additional back pressure is permissible, the venturi-shaped central tube is a powerful means for increasing the attenuation of a muffler of fixed external dimensions. Design curves based on equation (B10) show that a significant attenuation increase is obtained if the area is reduced by a factor of two.

#### MULTIPLE RESONATORS

If it is desired to increase the amount of attenuation from a resonator-type muffler, one obvious possibility is to combine two or more resonators in a single muffler. A muffler of this type with two consecutive identical resonators is discussed in reference 8. An equation for the attenuation is included along with other approximate equations useful in the preliminary design of such mufflers. The attenuation equation of reference 8 has been modified in appendix B (eq. (B15)) to emphasize the important parameters. In addition to the attenuation parameter  $\sqrt{c_0 V / 2S}$  and the resonance parameter  $\sqrt{c_0 / V}$ , the distance between connectors  $l_1$  is found to be a third important parameter. The attenuation is directly proportional to the number of resonant chambers in the muffler. The validity and range of application of this attenuation equation have been investigated by testing a group of mufflers of the multiple-resonator type (fig. 14).

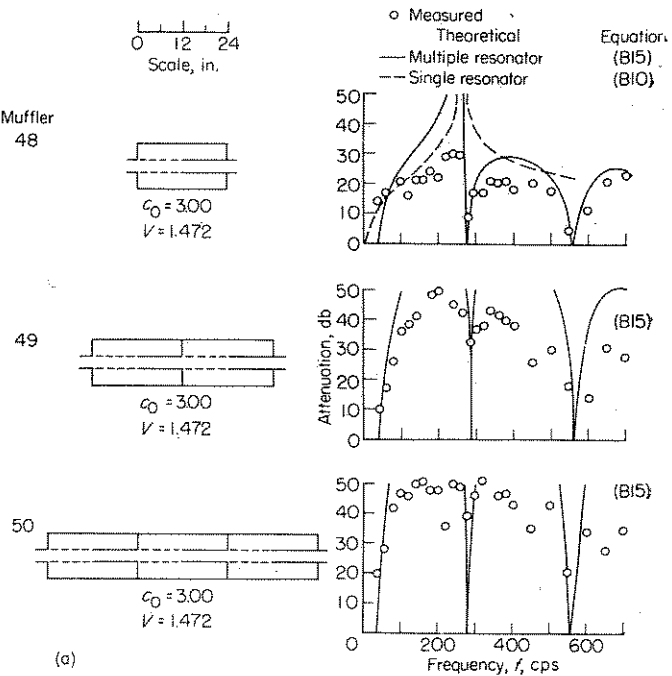


(d) Effect of venturi-shape contraction in central tube.  
Equation (B10).

FIGURE 13.—Concluded.

**Effect of number of chambers.**—The calculated and measured attenuation characteristics of mufflers composed of one, two, and three consecutive resonators are shown in figure 14 (a). For the single-chamber resonator, muffler 48, the attenuation has been calculated by both the multiple-resonator equation and the equation used in the preceding section for single resonators. The single-resonator equation is fairly accurate for wave lengths longer than  $4l_2$  but is considerably in error for shorter wave lengths (higher frequencies). As would be expected, however, it does predict the resonant frequency. The multiple-chamber equation is inaccurate through most of the range but predicts the resonant frequency and the pass frequencies accurately. Inasmuch as the multiple-resonator formula is derived for an infinite filter of identical chambers, the experimental results show that a single resonator produces less attenuation than is predicted for one resonator of an infinite filter.

The data for mufflers 49 and 50 show that the attenuation increases with the number of chambers. Limitations of the apparatus prevented the measurement of the extremely high peak attenuation of these mufflers. General agreement with the theory is found except at the higher frequencies. There is some question as to the cause of the loss of attenuation at high frequencies. Since the attenuation, even though less than predicted, is still quite high, it is not certain that failure of the attenuation equation is responsible. Vibration of the muffler walls may be transmitting high-frequency sound into the tailpipe. Also, the leakage of external noise into the microphone at the measuring stations, which limited the maximum measurable attenuation at lower frequencies to about 50 decibels, may have increased at the higher frequencies, so that the measurable attenuation is limited to somewhat less than 50 decibels.



(a) Effect of number of chambers.

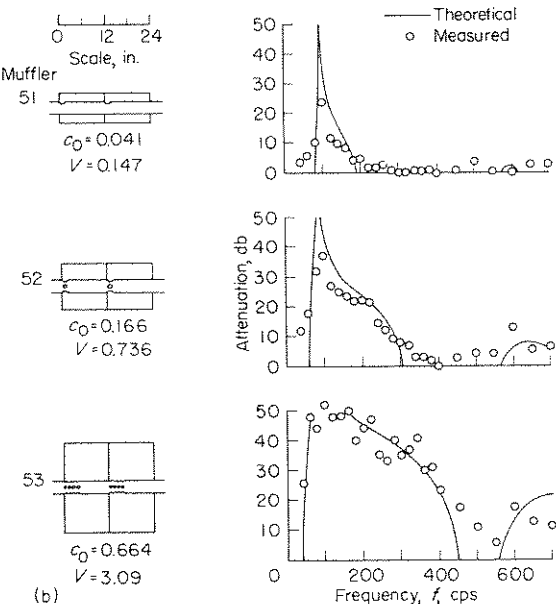
FIGURE 14.—Multiple-chamber resonators.

**Effect of diameter with resonance parameter constant.**—If the diameter of the muffler is increased while the resonance parameter remains constant, the value of the attenuation parameter will increase. The experimental data of figure 14 (b) confirm the theoretical prediction that this increase in the value of the attenuation parameter will result in an increase in both the magnitude of the attenuation and the width of the first attenuation band. The low frequency cutoff occurs at lower frequencies as the diameter is increased. The cutoff frequency for these three mufflers has been computed in three different ways. The results are shown in the following table:

Muffler	Values of $f_c$		
	Exact (eq. (B15))	Approximate (eq. (B16))	Equation (B3) of reference 8
51	87.0	87.3	146.5
52	63.2	63.5	93.8
53	40.1	40.4	45.7

This table shows that for these particular mufflers equation (B16) is sufficiently accurate for preliminary design calculations. The assumption made in obtaining equation (B3) of reference 8, however, is not permissible for these mufflers.

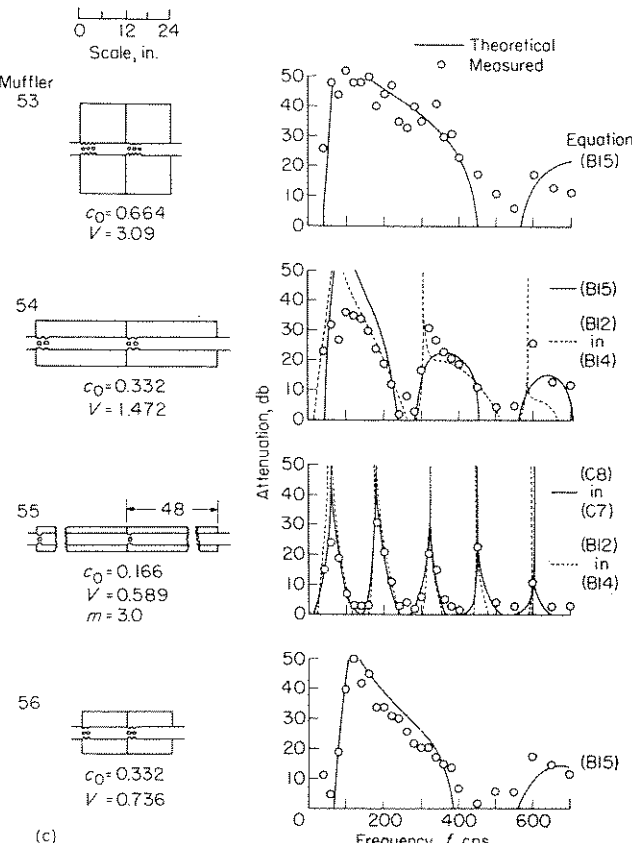
Although both mufflers 51 and 52 show a sharp drop in measured attenuation at the predicted cutoff frequency, the attenuation does not drop to zero until well below the predicted cutoff frequency. This lack of agreement may be due to the fact that the mufflers had only two chambers, whereas the theoretical cutoff frequency was based on an infinite number of chambers. It is known that for a single chamber the cutoff frequency is zero, and it seems plausible that  $f_c$  may approach the predicted value only as the number of chambers becomes large.



(b) Effect of diameter. Equation (B15).

FIGURE 14.—Continued.

**Effect of length.**—Mufflers 53 and 54 differ in both length and volume but the resonance parameter has been kept constant (fig. 14(c)). Comparison of these two mufflers shows that increasing the length decreases the frequency at which the first upper pass band occurs. The attenuation characteristics of muffler 55 are of an altogether different type. It has been pointed out in connection with single resonators that an attenuation curve of this type is characteristic of mufflers in which the plane-wave nature of the sound in the chamber is predominant. Muffler 55 is so long that the plane-wave resonance occurs in the chambers at a lower frequency than the volume resonance. Consequently, it has been necessary to consider the wave nature of the sound field in the chambers in making the calculations. This was accomplished by making use of equation (B12) for the branch impedance. The dashed curve shows the attenuation of two chambers of an infinite filter and was obtained by substituting equation (B12) for  $Z_b$  in equation (B14). The solid curve shows the attenuation of a two-chamber muffler terminated by an infinite tailpipe and was obtained by using equation (C8) in equation (C7). The branch impedance was again obtained from equation (B12). The attenuation of muffler 54 has also been computed by using equation (B12) for the branch impedance. The results, shown by the dashed curve, indicate that the sudden increase in attenuation at frequencies of 320 and 600 cycles per second is due to length resonance in the chambers.

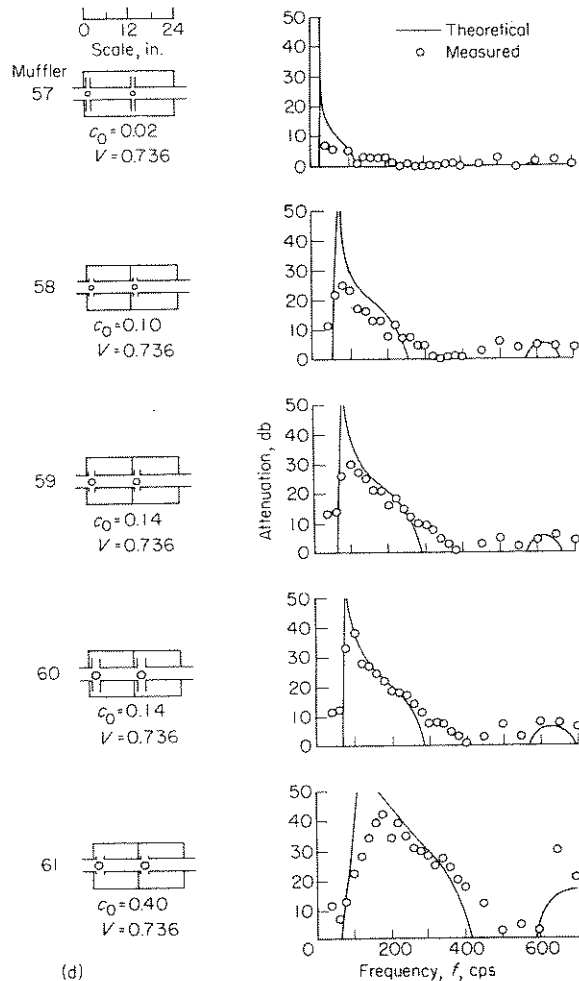


(c) Effect of length.

FIGURE 14.—Continued.

Muffler 56 differs physically from muffler 54 in length alone. This decrease in length, however, affects all three muffler parameters. The result is an increase in the cutoff frequency, an increase in the resonant frequency, an increase in the width of the first attenuation band, and an increase in the width of the first upper pass band.

**Effect of conductivity.**—Figure 14(d) presents results for a group of mufflers identical except for values of  $c_0$ . In all cases, tubes were used to obtain the conductivity. In general, the effects of increasing the conductivity are correctly predicted by the theory. For instance, both the experiment and the theory show that the cutoff and the resonant frequencies are raised, the first attenuation band is widened, and the first upper pass band is narrowed. The attenuation, however, did not drop completely to zero at the calculated cutoff frequency. Muffler 57, which had a very low conductivity, failed to produce the high attenuation predicted near the resonant frequency. This is believed to be due to viscous effects. Another indication of the effect of viscosity is obtained by comparing mufflers 59 and 60. Although both mufflers had the same values of  $c_0$ , muffler 60, which had



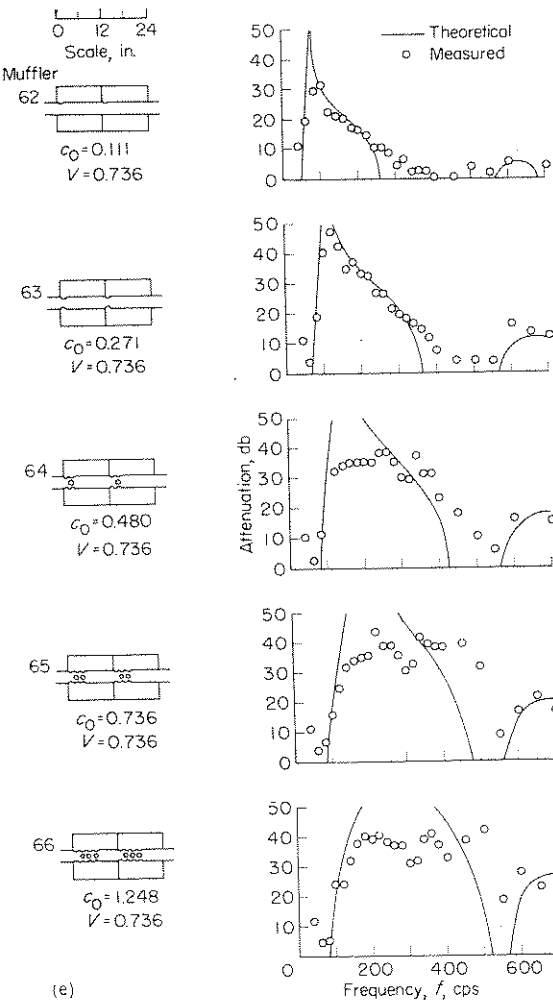
(d) Effect of conductivity  $c_0$  using tubes. Equation (B15).

FIGURE 14.—Continued.

larger diameter tubes, gave more attenuation at frequencies near resonance. The first attenuation band extended to higher frequencies than were predicted for both of these mufflers, although the attenuation was less than 10 decibels at these higher frequencies.

Figure 14(e) shows results from a group of mufflers similar to those shown in figure 14(d). In this case, however, orifices were used to obtain the conductivity. The trends are quite similar to those shown in figure 14(d). Note from the experimental data that, if the value of  $c_0$  is sufficiently high, the first upper pass band is narrowed until it is almost eliminated. At the same time, however, the cutoff frequency is continually increased.

**Elimination of the first upper pass band.**—Consideration of equation (B15) indicates that it might be possible to eliminate the first upper pass band ( $\sin kl_1 = 0$ ) by choosing the resonant frequency such that  $\frac{f}{f_r} = 1$  when  $\sin kl_1 = 0$ . A case of this type is shown in the design curve for  $kl_1 = \pi$ . In



(e) Effect of conductivity  $c_0$  using orifices. Equation (B15).

FIGURE 14.—Continued.

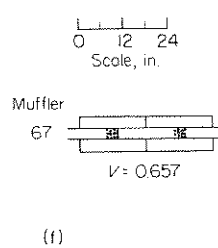
the usual construction of mufflers of this type; however, the chamber length is equal to  $l_1$ . Then when  $k_l l_1 = \pi$ ,  $k_l l_2 = \frac{\pi}{2}$  and the wave length is one-half the chamber length.

Therefore, the chamber cannot properly be considered as a lumped impedance at the resonant frequency. If plane-wave motion is assumed in the chamber,  $k_r$  will approach  $\frac{\pi}{l_1}$  ( $= \frac{\pi}{2l_2}$ )

only as the value of  $c_0$  approaches infinity (see eq. (B12)). In order to determine whether it is possible in practice to eliminate the first upper pass band, muffler 67 was built. This muffler was tested after most of the data presented herein had been analyzed. In order to allow the measurement of higher values of attenuation than those in the previous tests, the experimental apparatus was reassembled in another location with the loud-speaker outside the room in which the measurements were made. The exhaust pipe entered the room through a hole in the wall which was sealed with sponge rubber. The tailpipe extended out the other end of the room through a similar hole. With this arrangement, it was possible to measure an attenuation of 65 decibels.

Two theoretical curves are presented in figure 14(f). The solid curve, which shows the complete elimination of the pass band, was calculated for  $c_0 = \infty$ . The dashed curve, which shows a very narrow pass region, was calculated for  $c_0 = 9.95$ . The experimental points follow the solid curve up to about 340 cycles per second. In the critical first upper pass region, however, the measured attenuation drops from 65 decibels at 340 cycles per second to 29 decibels at 360 cycles per second, then rises sharply to 51 decibels at 380 cycles per second, drops again to 24 decibels at 400 cycles per second, and then begins to rise again. Both the initial drop and the final rise parallel the dashed curve ( $c_0 = 9.95$ ), but the theory gives no explanation for the intermediate peak attenuation of 51 decibels which occurs at the point where the dashed curve goes to zero. Of course the actual behavior of a muffler in this very critical region cannot be accurately predicted without including viscous terms in the impedances. When  $\frac{f}{f_r} = 1$  the branch

reactance is zero, and when  $\sin kl_1 = 0$  the pipe reactance is zero. Since these events both occur at nearly the same



(f) Effect of setting resonant frequency equal to first pass frequency ( $k_r l_1 = \pi$ ). Equation (B12) in (B14).

FIGURE 14.—Concluded.

frequency for muffler 67, only the resistances are left to control the sound flow. Therefore, it is inaccurate to neglect them in this region.

The points at about 360 and 400 cycles per second were determined by careful survey to be points of minimum attenuation. Thus, the experimental results prove that it is possible to obtain significant attenuation in a frequency region which is normally a pass band. The second upper pass band, however, was not eliminated.

#### CONDUCTIVITY PREDICTION

The results that have been presented show that the conductivity is a very important physical quantity which enters into the determination of both the resonant frequency and the amount of attenuation for resonator-type mufflers. It is unfortunate, therefore, that the conductivity should be, as has been mentioned in the section entitled "Theory," a somewhat elusive quantity to predict. In an attempt to eliminate some of the uncertainty regarding the prediction of  $c_0$ , it was computed by the following equation for those volume-controlled resonators which showed a well-defined resonant frequency:

$$c_0 = \frac{\pi a^2}{l_r + \beta a}$$

Two values for  $\beta$ ,  $\pi/2$  and  $\pi/4$ , were used. Where more than one connecting element was used, the calculated conductivity of a single element was multiplied by  $n$ , the number of elements. The results of this calculation are tabulated in table III along with the values of  $c_0$ , that are listed beside the corresponding attenuation curves. In each case, the listed  $c_0$  was used in calculating the theoretical curve.

The data of table III indicate that, within the range of this investigation, when tube connectors are used,  $\beta$  may be

TABLE III.—COMPARISON OF CALCULATED  $c_0$  VALUES WITH  $c_0$  VALUES LISTED IN FIGURES 12 TO 14

Muffler	Number of connectors per chamber	Number of chambers	$l_r$ , in.	$2a$ , in.	Calculated $c_0$ , ft		Listed $c_0$ , ft
					$\beta = \frac{\pi}{4}$	$\beta = \frac{\pi}{2}$	
Tube connector to chamber							
24	1	1	6.8	2.0	0.034	0.031	0.0308
25	1	1	6.8	2.0	0.034	0.031	0.0308
26	1	1	6.8	2.0	0.034	0.031	0.0308
27	1	1	2.16	2.0	0.089	0.070	0.0702
29	1	1	6.8	1.0	0.009	0.009	0.0086
30	1	1	6.8	3.0	0.074	0.064	0.0644
31	1	1	.43	2.0	.215	.131	.1309
32	1	1	13.6	2.0	.018	.017	.0172
33	1	1	3.0	1.4	.036	.031	.0308
34	1	1	1.28	1.0	.039	.032	.0308
37	1	1	1.75	1.0	.031	.026	.026
38	1	1	1.66	1.5	.066	.052	.052
58	4	2	.25	.5	.147	.102	.100
59	4	2	1.00	1.0	.188	.147	.140
60	4	2	3.00	1.5	.164	.141	.140
Orifice connector to chamber							
39	2	1	0.05	1.0	0.296	0.157	0.151
40	5	3	.05	1.0	.887	.470	.470
47	10	1	.05	.50	.684	.369	.341
51	3	2	.05	.50	.066	.037	.041
52	4	2	.05	.50	.265	.148	.166
56	8	2	.05	.50	.529	.296	.322
62	3	2	.05	.50	.198	.111	.111
63	7	2	.05	.60	.463	.259	.271

taken as  $\pi/2$  with sufficient accuracy for design purposes. In the case of orifice connectors, the results are not so conclusive. In general, however, it appears that  $\beta$  can be taken as  $\pi/2$  if only a few orifices are used. The experiments indicate that, as the number of orifices is increased, the conductivity per orifice tends to increase (compare mufflers 39 and 40, or mufflers 51 and 47). The determination of an accurate method of predicting the value of  $c_0$  for a group of orifices would require a study of such parameters as the number, diameter, and spacing of the orifices as well as the diameter of the central tube. Until the results of such research become available, however, the designer should, wherever possible, use only a few tubes or orifices, unless he has available the relatively simple equipment required to determine the resonant frequency experimentally after construction of a sample muffler.

#### TUNED TUBES

Two acoustical circuit configurations have been considered which make use of the velocity at which plane sound waves travel to obtain interference and resulting attenuation.

**Side-branch tubes.**—The first of these configurations consists of a side branch of constant area with the end closed. At a frequency for which such a tube is, for instance, one-quarter wave length long, a wave traveling from the exhaust pipe to the closed end and back to the exhaust pipe will arrive in phase opposition to the incoming wave in the exhaust pipe. The interference between the two waves results in attenuation. Appendix B gives the equation for the attenuation of mufflers of this type (eq. (B13)). The attenuation characteristics of three of these mufflers are presented in figure 15. For each of these mufflers the tube

diameter is equal to the exhaust-pipe diameter so that the area ratio  $m$  is one. Although attenuation above 20 decibels can be obtained, this high attenuation is limited to very narrow frequency bands. Consequently, the mufflers shown in figure 15 would not be suitable for variable-speed engines.

The analysis of the results obtained with resonator-type mufflers has shown that several of these mufflers with high ratios of length to diameter exhibit the characteristic behavior of tuned-tube mufflers (mufflers 43, 44, 45, and 46 of fig. 13 (e) and muffler 55 of fig. 14 (e)). These mufflers had much wider attenuation bands than the tuned tubes of figure 15. The calculations show that this increase in the width of the attenuation band is a direct result of the increased area ratio  $m$ .

**Quincke tubes.**—The second type of tuned-tube muffler is commonly known as the Quincke tube. It consists of two tubes of different lengths connected in parallel, with the combination inserted in series with the exhaust pipe. This arrangement is discussed in reference 1. Because of the characteristics of sharp tuning and narrow attenuation bands, an arrangement of this type seems unsuitable for an engine-exhaust muffler. Consequently, no mufflers of this type were included in this investigation.

#### COMBINATIONS

After investigating several types of mufflers, a few mufflers were tested which either combined two of the types or combined two or more sections of different size but of the same type. Mufflers 71 and 72 combined a resonator with an expansion chamber (fig. 16 and fig. 1 (d)). The results show the importance of the location of the conductivity for, although the mufflers are identical in all other respects, the attenuation of muffler 71 is much higher than that of muffler 72. Apparently the entrances to the two chambers are too close together in the case of muffler 72. The theory (appendix C, eq. (C18)) correctly predicts the better effectiveness of muffler 71.

It appeared probable that the requirement of a very broad attenuation region could best be satisfied by combinations of resonators which were tuned to different frequencies. Consequently an attenuation equation was developed for a combination of two resonators (appendix C, eqs. (C3) to (C7)), and one such combination was investigated experimentally (muffler 73). This muffler is shown in figure 16 and in figure 1 (e). The results show an attenuation of more than 10 decibels over an uninterrupted frequency band of width equal to about six times the lowest frequency of the band, in spite of the fact that this muffler is relatively small (12-inch diameter and 12-inch length). Muffler 73 was also tested in the reverse position (muffler 73R), with the high-frequency chamber to the front. The results show no appreciable difference except in the region below the first resonant frequency.

Muffler 74 is effectively a combination of four tuned tubes. The internal details of this muffler are shown in figure 1 (f). Although some attenuation is obtained over a wide frequency band, the attenuation spectrum consists of a series of very sharp peaks and hollows.

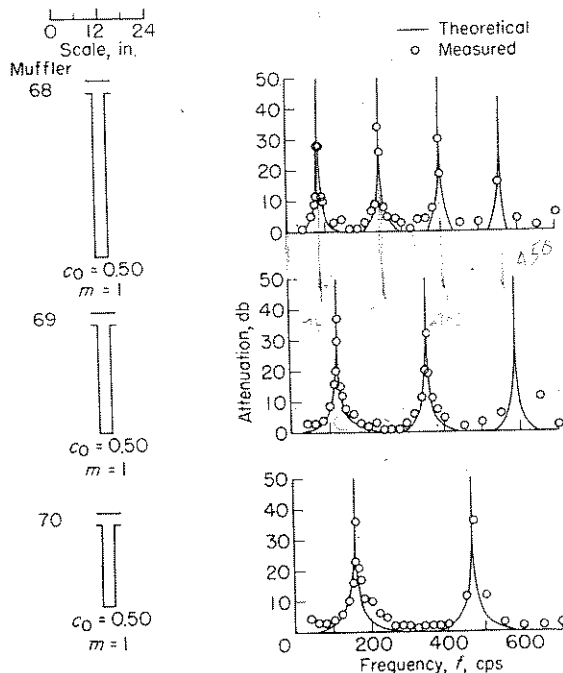


FIGURE 15.—Side-branch tubes with same diameter as exhaust pipe. Equation (B13).

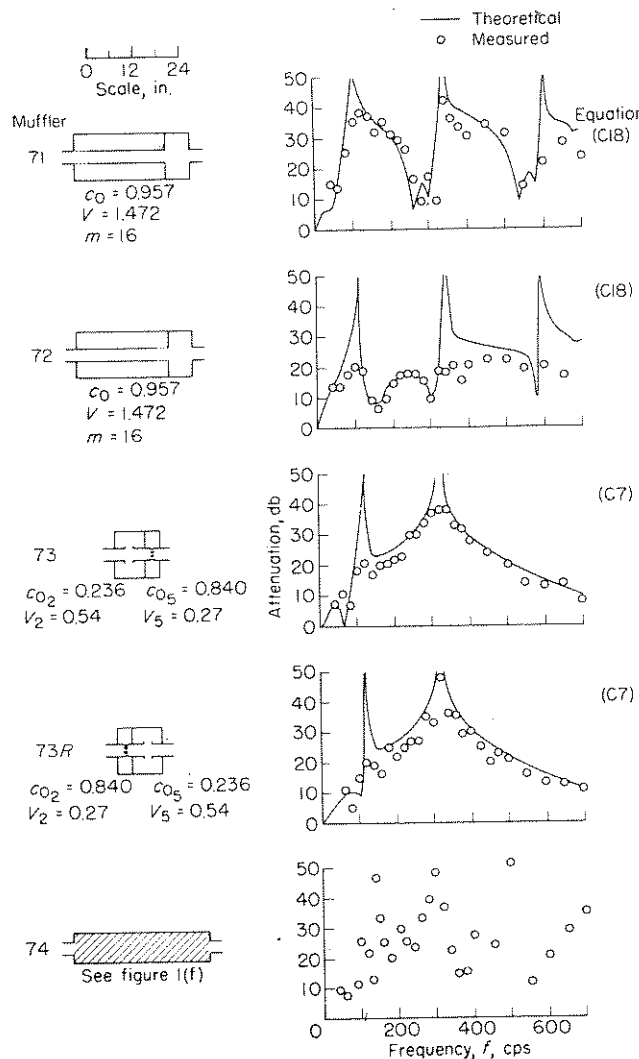


FIGURE 16.—Combination mufflers.

## MUFFLERS FOR A 12-INCH EXHAUST PIPE

All equations which have been presented include, in one manner or another, the assumption that the dimensions of certain elements are small compared to the sound wave length. In order to determine the effect of violating this assumption, three mufflers were designed for installation in a 12-inch-diameter exhaust pipe (fig. 17). Muffler 75 is a large expansion-chamber-type muffler. Inasmuch as the wave motion is accounted for in the expansion-chamber equation, it might seem, at first, that no size assumption has been made. The discussion of expansion chambers, however, showed that the plane-wave assumption carried an implicit assumption regarding the diameter. For muffler 75 the critical frequency for the first radial mode of vibration is 463 cycles per second. The experimental results show a loss of attenuation between 400 and 500 cycles per second. Below 400 cycles the calculations and experiment are in fair agreement, except that the effective length of the chamber seems to be somewhat shorter than the actual length.

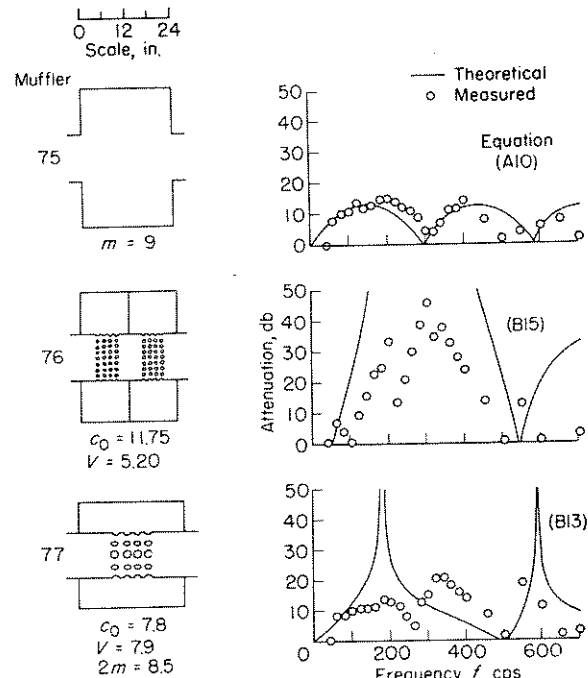


FIGURE 17.—Mufflers for large-diameter (12 in.) exhaust pipes.

Muffler 76 is a double resonator and muffler 77 is a single resonator. For both of these mufflers, the lack of agreement between calculations and experiment is quite pronounced. The results show that it is possible to obtain attenuation in pipes of this size but they also show that, because of the assumptions made, the equations used in this report are not adequate to predict this attenuation. Calculations for such mufflers must include consideration of other vibrational modes in addition to the plane-wave mode.

## II. FINITE TAILPIPE

For the first part of this investigation, a reflection-free muffler termination (an effectively infinite tailpipe) was used in order to reduce the number of variables involved. In some cases a muffler or filter in a long duct or pipe line may have an essentially reflection-free termination. Engine mufflers, however, must be terminated in a tailpipe of finite length in actual practice. In Part II of this report, therefore, a method is presented which permits the tailpipe to be included in the muffler calculations. The validity of this method has been investigated experimentally by testing four muffler-tailpipe combinations. The dimensions of these mufflers are within the limits for which the basic muffler theory has been shown to be valid in Part I. The apparatus used in the tailpipe investigation is described briefly and the results of the tests are discussed.

## THEORY

The problem of radiation from an unflanged circular pipe has been solved for the case where the incident sound is of the plane-wave mode (ref. 11). It is possible by use of this information to compute the tailpipe impedance and, thus, to

introduce the tailpipe into the muffler calculations. A less accurate, but somewhat simpler, method is to add an end correction of 0.61 times the pipe radius to the length of the pipe and to assume that the pipe is terminated in a zero impedance (total reflection) with a phase shift of  $180^\circ$  between the incident and reflected waves. This method is justified at sufficiently low frequencies, because the reflection coefficient approaches unity as the frequency approaches zero. In order to determine the frequency range within which this approximation is applicable, the attenuation of a single-chamber resonator with a tailpipe has been calculated by both methods. The results (table IV) show that the approximation gives results within less than 0.1 decibel for frequencies up to 520 cycles per second. The attenuation curve is plotted in figure 18 (a). Note that the calculations have been made for  $c=2000$  fps. This value is typical of the speed of sound in the hot exhaust gas from an aircraft engine. The attenuation has been based on the ratio of the absolute values of the incident-wave pressure just ahead of the conductivity openings and the incident-wave pressure in the tailpipe. The equation used for the approximate calculation is developed in appendix D (eq. (D10)).

Before proceeding further with the consideration of tailpipe effects, some discussion is necessary concerning this basis for calculating the attenuation. The user of a muffler ordinarily thinks of the attenuation due to a muffler as being the difference, at some point in the open air, between the sound level from an open exhaust pipe and the sound level after a muffler has been installed. The sound pressure in the open air due to an open exhaust pipe or a tailpipe is, at a given frequency, directly proportional to the pressure

TABLE IV.—COMPARISON OF TWO METHODS FOR CALCULATING THE ATTENUATION OF A SINGLE-RESONATOR MUFFLER WITH TAILPIPE

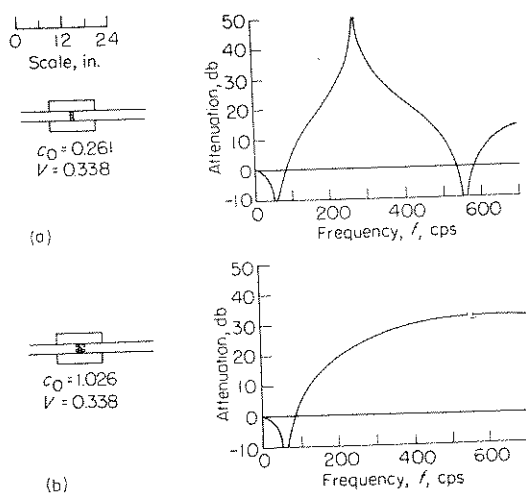
[Muffler constants:  $c_0=0.261$  ft;  $V=0.338$  ft<sup>3</sup>;  $c=2000$  fps; Tailpipe length=20 in.;  $S=0.0247$  sq ft]

Frequency, $f$ , cps	Attenuation, db	
	Calculations using exact tail- pipe impedance	Calculations using approxi- mate tailpipe impedance
20	-0.81	-0.81
40	-4.10	-4.10
60	-9.63	-9.65
80	-2.24	-2.24
100	5.09	5.10
120	9.86	9.87
140	13.67	13.67
160	17.09	17.10
180	20.28	20.29
200	23.37	20.37
220	27.08	27.09
240	31.38	31.39
260	37.35	37.36
280	...	...
300	38.48	38.50
320	33.14	33.16
340	29.35	28.37
360	26.63	26.67
380	24.45	24.48
400	22.39	22.41
420	20.30	20.33
440	18.27	18.30
460	16.00	16.03
480	13.37	13.39
500	10.32	10.34
520	6.34	6.33
540	-1.42	-1.56
560	-14.29	-17.06
580	-7.45	-7.40
600	4.55	4.65

of the incident wave traveling in the pipe. Therefore, the attenuation can also be defined as the difference between the sound-pressure levels of the incident waves inside the open exhaust pipe and the tailpipe. It has been shown that the reflection coefficient from the end of an open exhaust pipe is nearly unity for the frequency range of this investigation. Also, for frequencies at which the attenuation of a muffler is high, there is a very strong reflection from the conductivity location back into the exhaust pipe. (See table I.) Now consider an engine to which are attached alternately an open exhaust pipe and another exhaust pipe of the same length as the open pipe but one that is terminated in a muffler and tailpipe. The reflected waves in the exhaust pipes are very strong in both cases; furthermore, the same sound source is feeding the two exhaust pipes and the pipes have the same length; therefore, it follows that the incident waves will have about the same strength. Thus, it is possible, in approximation, to calculate the attenuation as the difference between the sound-pressure levels of the incident wave entering the muffler in the exhaust pipe and the incident wave leaving the muffler in the tailpipe. This approximation should be valid in the frequency range for which the open-pipe reflection coefficient is near unity and for which the muffler also provides attenuation of the order of 15 decibels or more. Although the exhaust-pipe length has a very definite effect on the sound characteristics of a complete engine-exhaust system, it is possible by this method to separate the effect of the exhaust-pipe length from the rest of the system. Since the open exhaust pipe itself reflects a large part of the sound, it is entirely possible that under certain conditions a muffler could permit more sound to escape than does the open exhaust pipe, with a resultant negative attenuation. A negative attenuation value, under the present definition of attenuation, does not imply that sound energy has been created inside the muffler; it means simply that the percentage of the sound energy which reaches the atmosphere is greater with the muffler installed than it is without the muffler.

Consideration of equation (D10) (appendix D) has led to an idea which may permit the elimination of the first upper tailpipe pass band of a single-chamber-resonator muffler. If the resonator is tuned to the usual pass frequency, then, when  $kl_t = \pi$ , both the tailpipe impedance and the resonator impedance will equal zero. In this event the pass frequency may be eliminated. A calculation has been made for a muffler identical with the muffler of figure 18 (a), except for the large change in conductivity required to tune the resonator to the frequency at which  $kl_t = \pi$ . The results shown in figure 18 (b) indicate that the width of the attenuation band is nearly doubled. At the same time, however, the cutoff frequency is increased slightly and the magnitude of the attenuation is lowered in the low-frequency region. Although no experimental data are available for this muffler, it seems possible, in view of the experimental results for muffler 67 (fig. 14 (f)), that some attenuation may be obtained near the resonant frequency, with the resultant elimination of the first upper tailpipe pass band.

The case of a single expansion chamber with a finite tail-



(a) Single-resonator muffler with tailpipe.  $k_r l_t = 0.48\pi$ . (See also table IV.)  
 (b) Single-resonator muffler with tailpipe.  $k_r l_t = \pi$ .

FIGURE 18.—Theoretical attenuation characteristics of single-chamber resonators with tailpipes.  $c = 2000$  fpm. Equation (D10).

pipe has also been considered, and an equation is presented in appendix D for the attenuation of such a muffler.

### MUFFLERS

Sketches of the muffler-tailpipe combinations that were used in the experimental investigation of the effect of tailpipe length are shown in figure 19. These mufflers were designed for use on a particular aircraft engine. The design of these mufflers will be discussed later in the report in connection with a test of these mufflers on the engine for which they were designed. The mufflers were made from  $\frac{1}{16}$ -inch mild steel.

### APPARATUS AND TESTS

The experimental investigation of the effect of the tailpipe was conducted outdoors in an open area and in calm air. In these tests, as in the previous experiments, the air inside the mufflers was at the ambient temperature and there was no steady air flow. Hence, these tests will be referred to as "cold tests." The apparatus that was used is shown schematically in figure 20. The electronic equipment included an audio oscillator, a power amplifier, a speaker, an oscilloscope for monitoring the wave form, and a sound-level meter.

The cold-test data were obtained by sending sound waves at a single frequency alternately into a muffler and into an open exhaust pipe and by taking the difference between the sound-pressure level observed in the open air at a distance of 20 inches from the outlet of the muffler tailpipe and that observed at a distance of 20 inches from the outlet of the open exhaust pipe. In order to insure that the mufflers were tested for the same wave lengths in the cold test as in the subsequent engine test, the cold-test frequencies were adjusted to produce the wave lengths for which the mufflers were designed. In the presentation of the cold-test results, the experimental frequencies are multiplied by the ratio of

the sonic velocity in the actual exhaust gas to the sonic velocity in the cold test in order to correct for the temperature difference between the two conditions. For the cold test, the frequency range was from 30 cycles per second to 400 cycles per second; for the engine test, the frequency range, having equal wave lengths is 52 to 700 cycles per second. The ambient noise level for the cold tests was about 60 decibels.

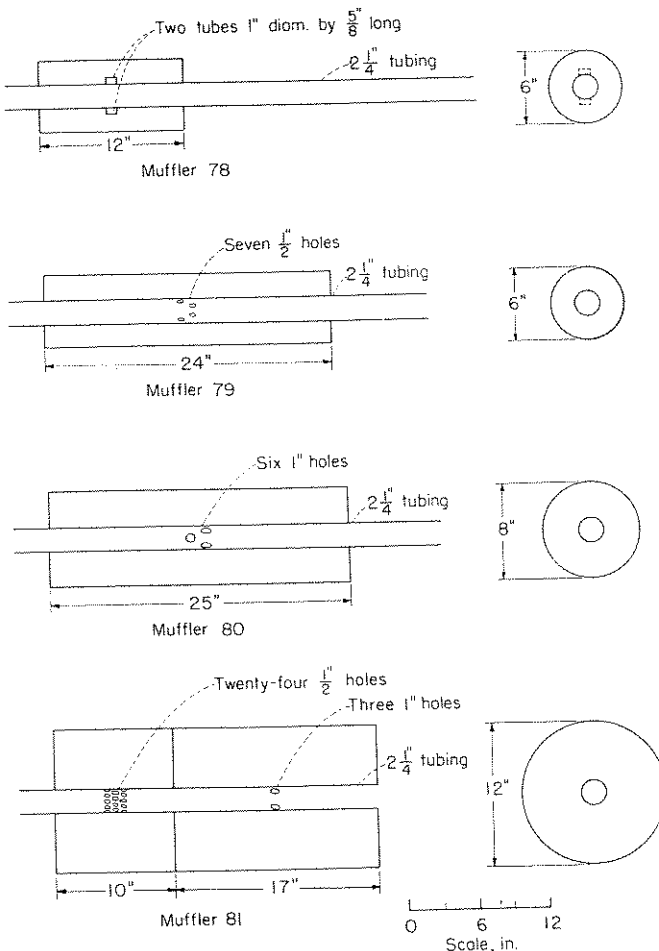


FIGURE 19.—Sketches of muffler-tailpipe combinations tested.

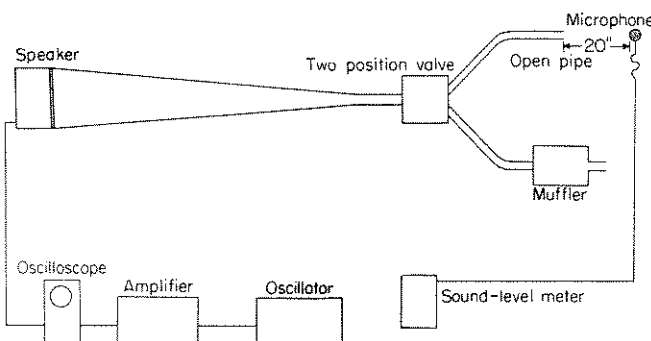


FIGURE 20.—Schematic diagram of the arrangement of apparatus for cold test of mufflers.

## RESULTS

The experimental results obtained from the muffler cold tests and the theoretical attenuation predicted for each muffler are shown in figure 21. The theoretical curves for mufflers 78, 79, and 80, which were computed from equation (D10), show that these mufflers were designed to have chamber resonances (points of maximum attenuation) at approximately 280 cycles per second and tailpipe resonances at about 400, 580, and 580 cycles per second, respectively.

A comparison of the experimental and theoretical data shows good agreement for these three mufflers. For example, the higher frequency cutoff points, which are a function of tailpipe length, are seen to fall very close to the predicted frequencies; furthermore, the measured attenuation

falls near that computed theoretically at all frequencies except those near the computed chamber resonance. The mufflers were not expected to provide the infinite attenuation calculated at the chamber resonant frequency, the calculated infinite values occurred only because the viscous forces were neglected in order to simplify the calculations. With this limitation, it may be concluded that equation (D10) is valid for predicting the attenuation characteristics for muffler-tailpipe combinations under the cold-test conditions.

The double-chamber resonator curve computed for muffler 81 shows two chamber resonant frequencies and no high-frequency tailpipe pass bands. The difference between the curve shapes for the single-chamber and double-chamber mufflers is, of course, due to the changes in the acoustical circuit. The attenuation for muffler 81 was computed by substituting the tailpipe impedance  $iX_t$  from appendix D for the impedance  $Z_6$  in the equations given for a combination of two resonators in appendix C and working out the expression for the attenuation.

For the cold tests, the two largest mufflers (mufflers 80 and 81) were wrapped with several layers of felt. In the absence of the felt wrappings, the maximum attenuation was limited to about 25 to 30 decibels by the radiation from the  $\frac{1}{16}$ -inch-thick outer walls. Reduction of this radiation would be an important factor in the design of a muffler from which a higher attenuation is desired.

## III. APPLICATION TO MUFFLER DESIGN

## VARIABLES DEPENDENT ON OPERATING CONDITIONS

Under the conditions of the investigations discussed in Parts I and II of this report, acoustic theory has been shown to predict the performance of several types of mufflers within a frequency range which is governed by the dimensions of the muffler elements. These investigations were designed to allow the study of several of the dimensional variables involved in exhaust muffling.

In order to isolate the effects of these variables, it was necessary to eliminate certain other variables dependent on operating conditions which could be separately investigated at some future time. The three major variables which have not been discussed are exhaust-gas temperature, exhaust-gas velocity, and exhaust-pipe sound pressure. A discussion of these variables follows.

## TEMPERATURE

The preceding investigations were made at room temperature or at atmospheric temperature and the velocity of sound was about 1,140 feet per second. The higher temperature in the engine exhaust gas will result in a higher sonic velocity. From the data of figure 8 of reference 9 and from temperature measurements made during the engine tests described in Part IV of the present report, the sonic velocity inside the tailpipe is estimated to be about 2,000 feet per second. It is believed that the primary effect of a change in the exhaust-gas temperature is the corresponding change in the velocity of sound. It is necessary in the de-

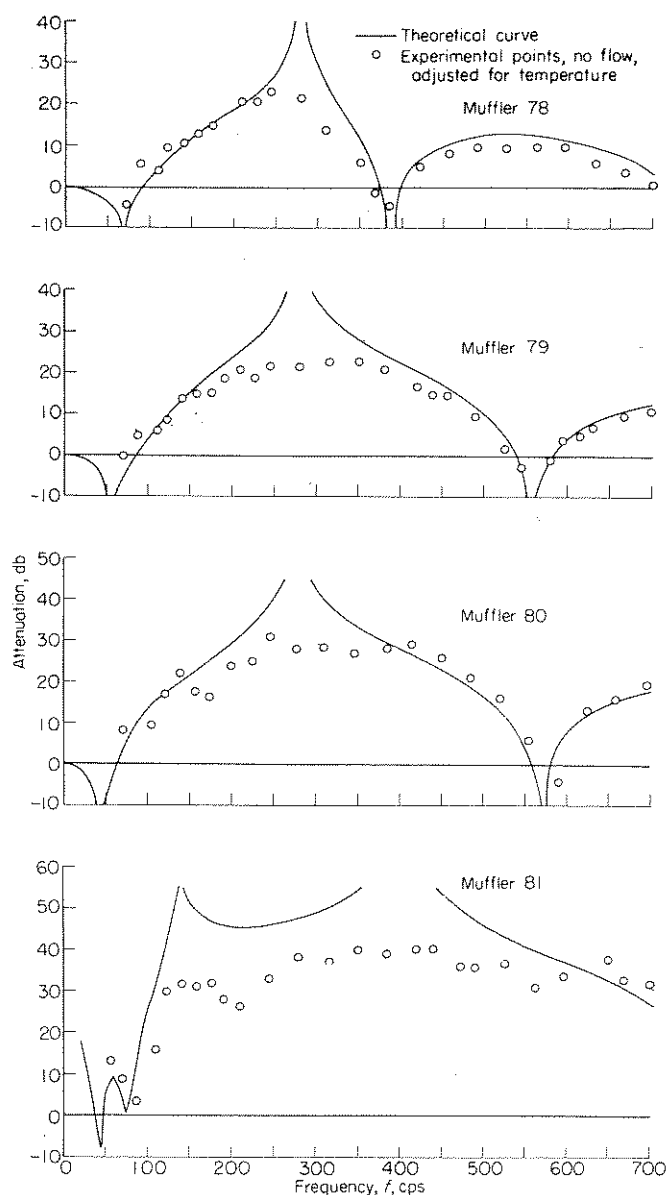


FIGURE 21.—Cold-test data and theoretical curves for mufflers tested.

sign of mufflers to use the actual sonic velocity of the exhaust gas. If the exhaust-gas temperature is known, the approximate velocity of sound may be determined by using the relation which has been found for air  $c=49\sqrt{T}$  feet per second, where  $T$  is the absolute temperature on the Fahrenheit scale.

The calculations that have been presented have included the tacit assumption that the temperature and average density in the muffler chambers are the same as those in the exhaust pipe. If significant differences are found in practice, they can be accounted for by using the most accurate available values for  $\rho$  and  $c$  at each element in calculating the impedance of that element. In this connection, it is interesting to note that the impedance of a resonant chamber is proportional to  $\rho c^2$  (eq. (B5)). But since  $c^2$  is proportional to  $T$  and  $\rho$  is proportional to  $T^{-1}$ , the chamber impedance is independent of  $T$ . The connector impedance is a function of  $T$ , but, unless it is a long tube, the connector will be at the exhaust-gas temperature. Thus, for resonator-type mufflers, a temperature difference between the exhaust pipe and the chamber would be expected to have little effect on the performance of the muffler.

#### EXHAUST-GAS VELOCITY

In an actual engine-exhaust-muffler installation the exhaust gas which transmits the sound is in motion, whereas in the preceding investigations there was no net flow of air. The actual case may be considered to consist of an alternating, or sound, flow superimposed on a steady exhaust-gas flow. A theoretical approach to the problem of determining the effect of the steady flow on the acoustic characteristics of an exhaust system has been made in reference 12. No experimental data, however, are included. The conclusion of the theory is that the velocity effect is a function of  $\sqrt{1-M^2}$ , where  $M$  is the Mach number of the exhaust flow. If the theory is assumed to be essentially correct, the following results are obtained.

Consider first the characteristics of the muffler itself. In the useful range of expansion ratios, the exhaust-gas velocity inside an expansion chamber is much lower than that in the exhaust pipe. Because the permissible engine back pressure limits the Mach number in the exhaust pipe to a value considerably less than 1, the Mach number inside the expansion chamber will be so low that  $M^2$  is negligible when compared with 1. Thus the exhaust velocity will have no appreciable effect on the attenuation of a single expansion chamber. In the case of multiple expansion chambers, however, the exhaust-gas velocity in the connecting tubes may be high enough to alter the muffler characteristics significantly. (See ref. 2 for experimental data.) In the resonant chamber of a resonator-type muffler there is no steady exhaust-gas flow; therefore, the single resonator will not be affected by flow. In the case of multiple resonators, as in multiple expansion chambers, the impedance of the connecting tubes will be affected by the exhaust-gas velocity.

Consider next the tailpipe characteristics. The tailpipe impedance will vary with the flow velocity. This will, of course, affect the attenuation of any practical muffler instal-

lation. According to the theory, the main effect of increased exhaust velocity is to lower the resonant frequencies of the tailpipe and to reduce the attenuation due to the tailpipe at those frequencies for which the tailpipe impedance reaches a maximum. On the whole, these effects are probably relatively small, inasmuch as the tailpipe resonant frequency is reduced by only 9 percent at a Mach number of 0.3, which corresponds to an exhaust velocity of 600 feet per second when  $c$  is 2,000 feet per second.

Note that most of the preceding conclusions regarding the effect of exhaust-gas velocity must be regarded as tentative, because they have been based on an unproved theory. Furthermore, the experimental data of reference 2 tend to cast some doubt on the validity of the theory. This uncertainty shows the need for additional research on the effects of exhaust-gas velocity.

#### INCREASED SOUND PRESSURE

In the derivation of the classical acoustic theory it is assumed that the sound pressures are very small in comparison with the static pressure of the medium (ref. 1). This assumption is made in order to permit the linearization of the differential equation of motion. However, in connection with engine tests previously made at this laboratory (ref. 9) certain nonlinear effects were observed, particularly the buildup of sharp wave fronts in long exhaust pipes as evidenced by the explosive character of the sound from such pipes. The detection of such nonlinear effects indicates that the exhaust sound pressure inside the pipes is high enough so that the classical linearized theory may give results which are somewhat in error. Further study of the behavior of acoustic elements—resonators, orifices, and tubes—in the presence of nonlinear sound fields is required before the effects of very high sound pressures on the performance of an acoustic system will be quantitatively known.

#### RELATIVE MERITS OF MUFFLER TYPES INVESTIGATED

None of the muffler types discussed should have excessive back pressures if the exhaust pipe is the proper size because the exhaust gas is not forced around sharp  $180^\circ$  turns. The expansion chambers will probably have the highest back pressures of the types tested because of the energy losses in the expansion and contraction processes but, at least for the single expansion chambers, this back pressure should be within allowable limits.

In general, single-chamber mufflers are useful where the required frequency range is small; whereas, for high attenuation over a very wide frequency range, two or more different chambers will be required in order to obtain attenuation at the pass frequencies of the individual chambers and the tailpipe.

Reference 7 indicates that, in the case of engine exhausts having large sound pressures, mufflers of the expansion-chamber type must be used, because the attenuation of a resonator is dependent on the existence of small sound pressures. The experiments of reference 9, however, have shown

that resonator mufflers can be quite effective in an engine-exhaust system, even though the theoretical assumption of small sound pressures is violated. (This assumption is actually made also in deriving the equations for the attenuation of expansion-chamber mufflers.) The muffler designer is, therefore, not necessarily restricted to expansion chambers. The answer to the question as to which type, for a given muffler size and a given back pressure, is the more effective depends in part upon the relative magnitudes of the effects of high sound pressure and of exhaust-gas velocity on the two types.

In case the adverse effects of high sound pressures are found to be excessive for resonators, it is suggested that a combination muffler, with the expansion chamber first in order to reduce the sound pressures entering the resonator, may be most effective. (See muffler 67 of ref. 9.)

#### MUFFLER-DESIGN PROCEDURE

On the basis of the theory which has been presented, a muffler-design procedure was developed. Because some of the important variables have not been investigated as yet, the procedure must be judged by the results obtained in practical applications. Modifications of the procedure are to be expected as a result of experience gained in the applications. This procedure begins with the determination of a required attenuation spectrum, which defines the noise reduction that the muffler is expected to produce.

#### REQUIRED ATTENUATION SPECTRUM

The first step in muffler design is to determine, at a known distance from the exhaust pipe, the sound-level spectrum of the engine which is to be quieted. This should be done at several speeds and loads within the operating range or, at the very least, at the maximum and minimum speeds of the normal operating range. In estimating the critical operating conditions likely to be encountered from the standpoint of noise, it is useful to recall that for a particular engine the magnitude of the noise is controlled largely by the engine torque, whereas the frequencies are controlled by the engine speed (refs. 8 and 9).

After the engine-noise spectrum has been determined, an allowable spectrum should be established, consisting of the maximum allowable sound-pressure level as a function of frequency. The fact that other noise sources (such as engine air intake, engine clatter, and the propeller) place a practical limit on the attainable reduction in overall airplane noise will influence the choice of the allowable spectrum. As the desired noise reduction increases, it becomes necessary to treat more of these other noise sources. In particular, it was necessary to treat both the engine exhaust and the propeller to obtain significant noise reduction for the liaison airplane of reference 8.

The difference between the measured and allowable spectra will establish the minimum attenuation which is required at each frequency; this difference will be called the required attenuation spectrum.

#### MUFFLER SELECTION

Compare the required spectrum with the design curves (figs. 22 to 24) and select from these curves a muffler design which will provide somewhat more than the required attenuation throughout the frequency range. (The use of these design curves will be discussed.) In the case of a single expansion chamber or resonator, the tailpipe must be carefully selected. From the required cutoff frequency compute the necessary tailpipe length by using the approximate equations which have been presented (eq. (D6) or (D12)). Next, by use of this tailpipe length, determine the location of the high-frequency pass bands. If the first pass frequency is too low, it will be necessary to choose a larger muffler in order that the tailpipe may be shortened or else to add another chamber which will provide attenuation at the tailpipe pass frequency. If a double expansion chamber or multiple resonator has been selected, the approximate equations or the design curves may be used to determine the cutoff and pass frequencies. Several of the muffler types may be considered in this manner in order to determine which will result in the smallest muffler that will provide the required attenuation in a particular case. It is usually not necessary to carry out detailed attenuation calculations until the final configuration has been closely approached. The detailed calculations will then provide a final check on the theoretical suitability of the selected muffler.

A test of the chosen muffler installation on the engine may show that modifications are required, owing to the influence of factors which have not been investigated as yet (in particular, the high exhaust-pipe sound pressures). Even with the assistance of the information presented in this report, it is likely that a certain amount of trial and error will be necessary in muffler design when the goal is a very highly efficient muffler in terms of attenuation per unit of weight or volume.

#### DESIGN CURVES

Three sets of design curves, showing the attenuation of mufflers terminated with the characteristic pipe impedance  $Z_0$ , are presented in figures 22, 23, and 24; these curves have been calculated from equations (A10), (B10), and (B15), respectively, of the appendixes. Simple examples will be given to indicate how these charts can be used to eliminate the need for detailed attenuation calculations in the preliminary stages of muffler design.

#### SINGLE EXPANSION CHAMBER

Figure 22 shows the attenuation of single expansion chambers in terms of nondimensional parameters. The parameter  $kl_e$  is a combination length and frequency parameter. The other parameter is the expansion ratio  $m$ .

Suppose that a muffler is desired to provide a minimum attenuation of 10 decibels between frequencies of 100 and 300 cycles per second. An expansion ratio of 9 will provide 10 decibels at  $kl_e=0.8$ . At three times this value of  $kl_e$  (i. e.,  $kl_e=2.4$ ), it will also provide about 10 decibels. Thus,  $m=9$

is satisfactory. The length of the muffler is determined by the fact that 100 cycles per second corresponds to  $kl_e = 0.8$ , so that  $0.8 = \frac{2\pi l_e}{c} \times 100$  (let  $c = 2000$  fps, then  $l_e = \frac{2000 \times 0.8}{2\pi \times 100} = 2.54$  ft). If the exhaust-pipe diameter is 2 inches, the expansion-chamber diameter will be  $2\sqrt{9}$  or 6 inches.

If this muffler is too long, another procedure is possible. Let  $m = 25$ ; thus, the diameter is increased to 10 inches. The design curve shows 10-decibel attenuation at  $kl_e = 0.25$ . At a  $kl_e$  of  $\frac{300}{100} \times 0.25 = 0.75$ , the attenuation is more than adequate. The length of this muffler will be  $l_e = \frac{2000 \times 0.25}{2\pi \times 100}$  or 0.795 foot.

#### SINGLE-CHAMBER RESONATOR

Figure 23 shows the attenuation of single-chamber resonators in terms of nondimensional parameters. The attenuation is plotted against  $f/f_r$  which is the ratio between the sound frequency and the resonant frequency of the resonator. Curves are plotted for several values of the attenuation parameter  $\sqrt{c_0 V}/2S$ .

Suppose again that the muffler is desired to provide a minimum attenuation of 10 decibels between  $f = 100$  and 300 cycles per second. In terms of the chart this means that the frequency at which the right leg of the attenuation curve

crosses the 10-decibel line must be three times the frequency at which the left leg crosses the 10-decibel line. The chart shows that this requires a value somewhat higher than 3.16, say approximately 4, for the attenuation parameter. The value of  $f/f_r$  corresponding to 100 cycles per second will be about 0.55

$$f_r = \frac{100}{0.55} = 182 \text{ cps}$$

Therefore,

$$\sqrt{\frac{c_0}{V}} = \frac{2\pi f_r}{c} = \frac{2\pi \times 182}{2000} = 0.57 \text{ ft}^{-1}$$

The exhaust pipe is 2 inches in diameter so that

$$\begin{aligned} \sqrt{c_0 V} &= 2 \times S \times \frac{\sqrt{c_0 V}}{2S} \\ &= 2 \times \left( \frac{\pi}{4} \frac{(2)^2}{(12)^2} \right) \times 4 = 0.174 \text{ ft}^2 \\ c_0 &= 0.57 \times 0.174 = 0.099 \text{ ft} \\ V &= \frac{0.174}{0.57} = 0.305 \text{ ft}^3 \end{aligned}$$

Any combination of length and diameter which will give this volume is permissible, as long as the dimensions are not too large in comparison with the 300-cycle wave length at the exhaust-gas temperature (see experimental results). If a length of 1 foot is selected, the diameter becomes 0.645 foot or 7 1/4 inches.

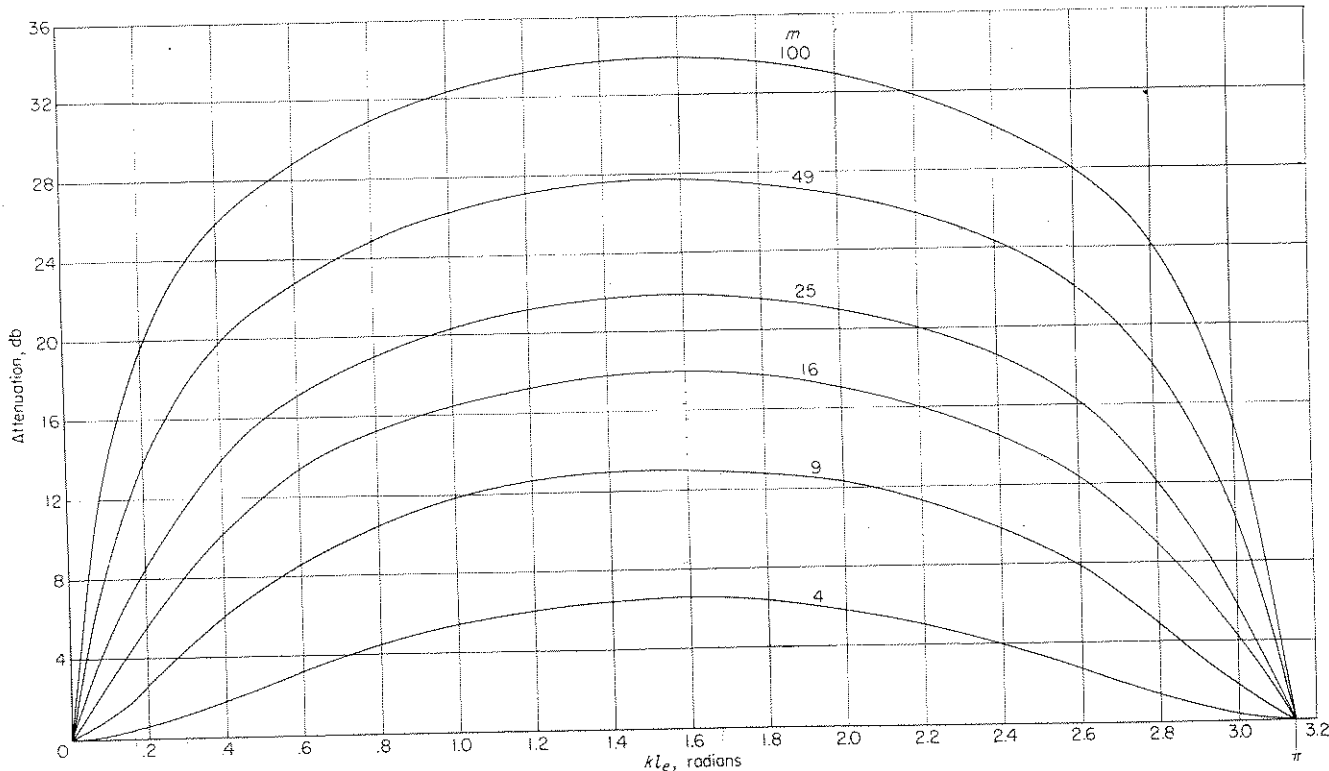


FIGURE 22.—Expansion-chamber design curves.

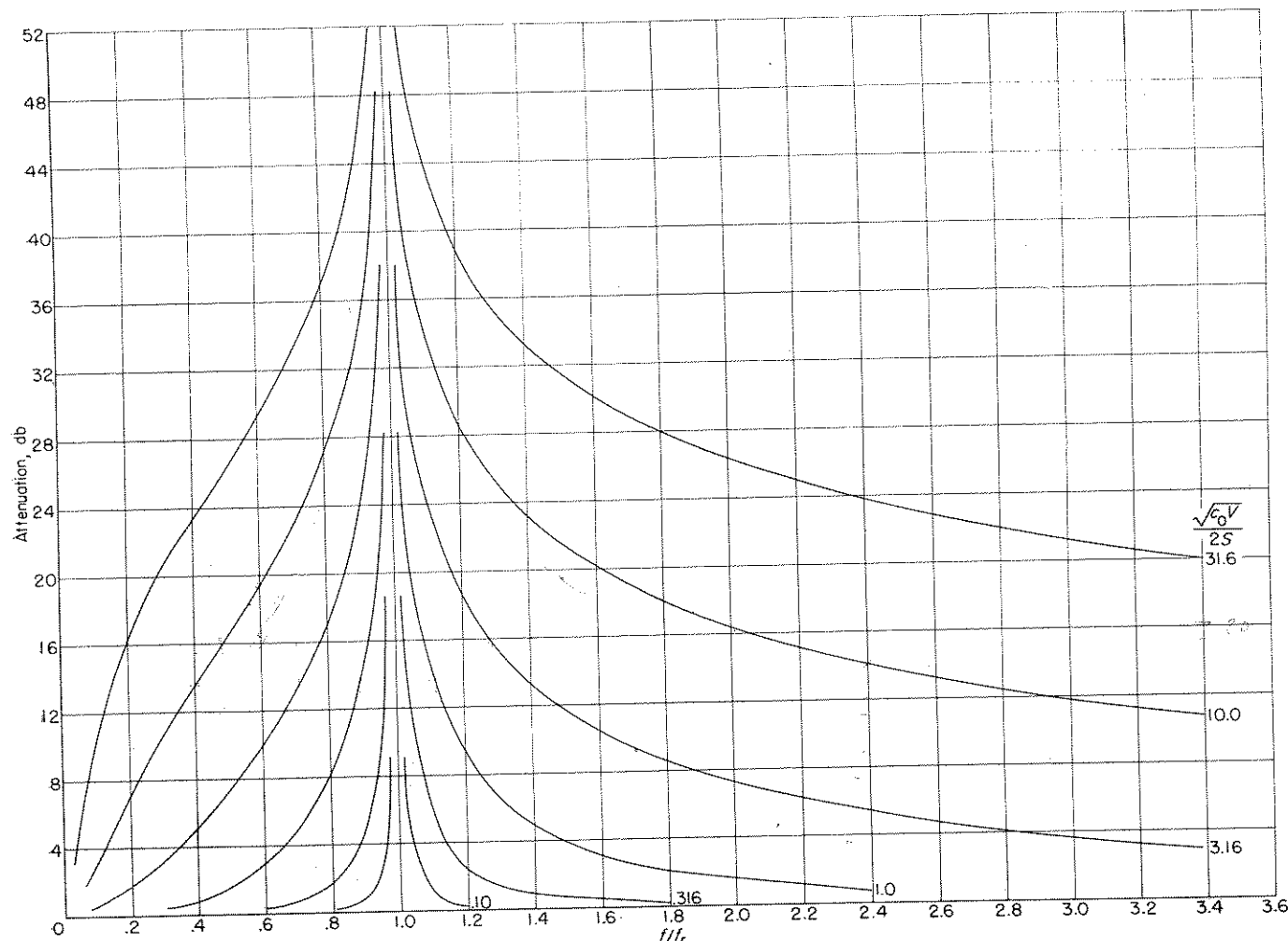


FIGURE 23.—Single-chamber-resonator design curves.

## MULTIPLE-CHAMBER RESONATOR

Figure 24 shows the attenuation per chamber of multiple-chamber resonators in terms of nondimensional parameters. Because three parameters are involved (appendix B), several charts are required to describe fully the possible configurations. Three such charts are presented.

As an example of the use of these charts, assume that for a particular engine spectrum the sound level at the fundamental frequency (100 cycles per second) is to be reduced 13 decibels. The levels at the other frequencies are to be reduced to the point where the speech interference is nowhere greater than at the fundamental frequency. This criterion results in a required attenuation of 13 decibels at 100 cycles per second, 4 decibels at 200 cycles per second, and zero at higher frequencies. The top chart of figure 24 ( $k_r l_1 = \frac{1}{2}$ )

shows that this objective could be met with  $\frac{\sqrt{c_0 V}}{2S} = 1$  for a two-chamber muffler with  $f_r = 100$  cycles per second. By

using these values the muffler dimensions are found as follows:

$$k_r = \frac{2\pi \times 100}{2000} = 0.314 \text{ ft} = \sqrt{\frac{c_0}{V}}$$

$$l_1 = \frac{0.5}{0.314} = 1.59 \text{ ft} = 19 \text{ in.}$$

$$\sqrt{c_0 V} = 2 \times \frac{\pi}{4} \times \frac{(2)^2}{(12)^2} \times 1 = 0.0436 \text{ ft}^2$$

$$c_0 = 0.314 \times 0.0436 = 0.0137 \text{ ft} = 0.164 \text{ in.}$$

$$V = \frac{0.0436}{0.314} = 0.139 \text{ ft}^3$$

In order to obtain this volume with a concentric resonant chamber 19 inches long, a chamber diameter of 4.5 inches is required. The overall length of the two-chamber muffler is 38 inches. The use of a tube connector seems advisable in order to obtain the low  $c_0$  required without creating excessive sound velocities in the connector.

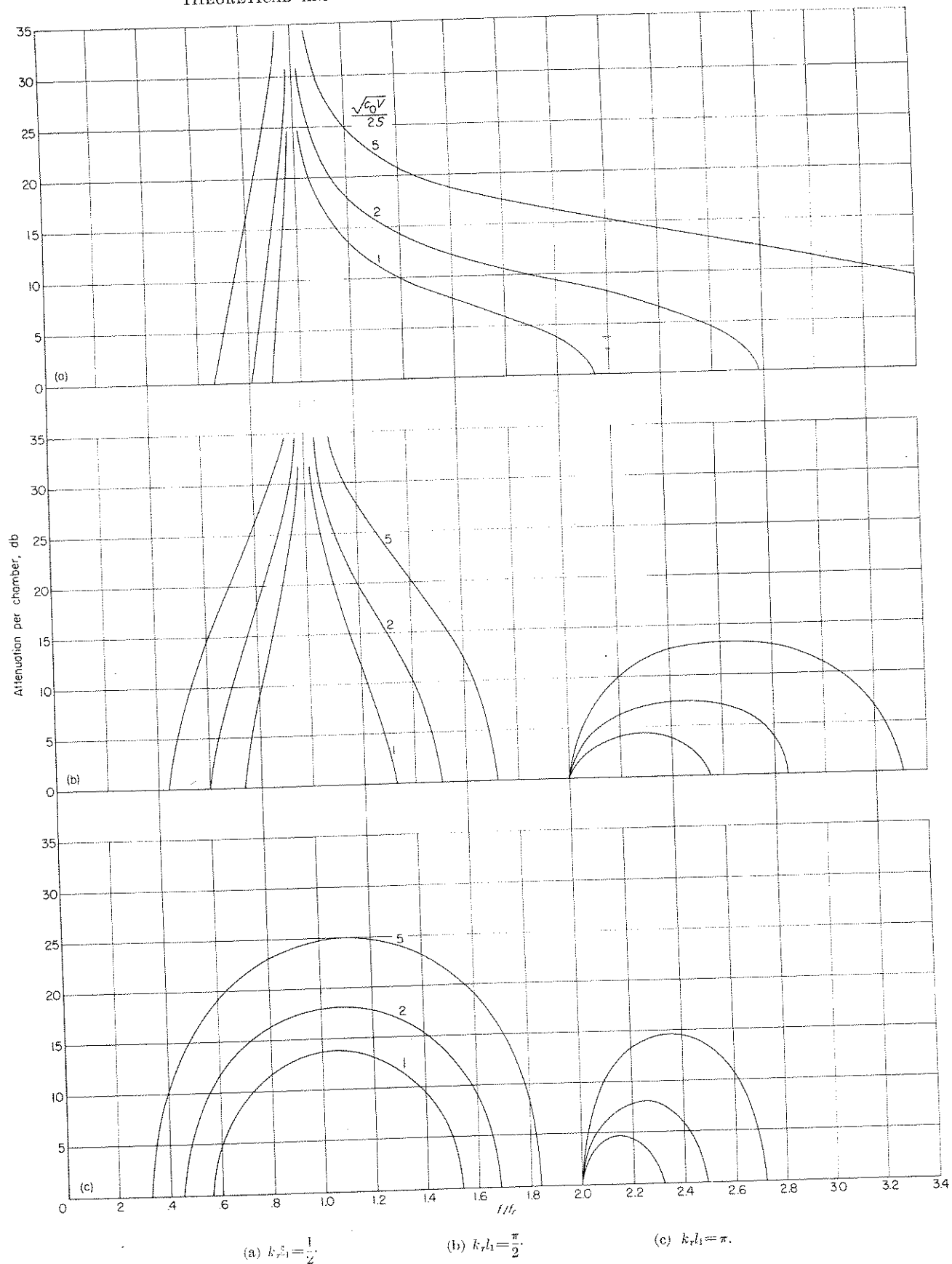


FIGURE 24.—Multiple-chamber-resonator design curves.

#### IV. ENGINE TESTS

In order to study the practicality of the design methods which have been described and, also, to obtain some idea of the size of muffler which is required in practice to provide a significant reduction of engine noise, four mufflers were designed for and tested on an actual aircraft engine. As was stated in the introduction, the engine of a helicopter was used for these tests. The design of the mufflers followed, in general, the design procedure which has been presented.

##### BASIC DATA

The first step in the design procedure is the determination of the engine-exhaust noise spectrum of the unmuffled engine. In the case of the helicopter the spectrum of the exhaust noise alone could not be determined. Instead the overall noise spectrum of the helicopter was measured. This spectrum, which includes an unknown amount of extraneous noise from such sources as the engine air intake, rotor blades, and engine clatter, is presented in figure 25.

Temperature measurements showed the speed of sound in the exhaust pipe to be approximately 2,000 fps.

##### MUFFLERS AND DESIGN

In order to insure that an adequate test range would be covered in the investigation, four resonator-type mufflers were designed and constructed. Three of the mufflers had single resonant chambers, whereas the fourth had two resonant chambers. The double-chamber muffler was designed with the intent to provide enough exhaust-noise attenuation so that the extraneous noise level could be measured. Figure 19 shows schematic drawings of these mufflers.

The mufflers were designed to give successive increases in attenuation and to have the acoustical properties shown in the following table:

Muffler	Chamber resonant frequency, cps	Tailpipe resonant frequency, cps	Attenuation parameter, $\frac{\sqrt{c_0 V}}{2S}$
78	280	400	4.33
79	280	580	6.03
80	280	580	12.00
81	{140, large chamber {400, small chamber}	Undetermined	{9.5, large chamber {16.15, small chamber}

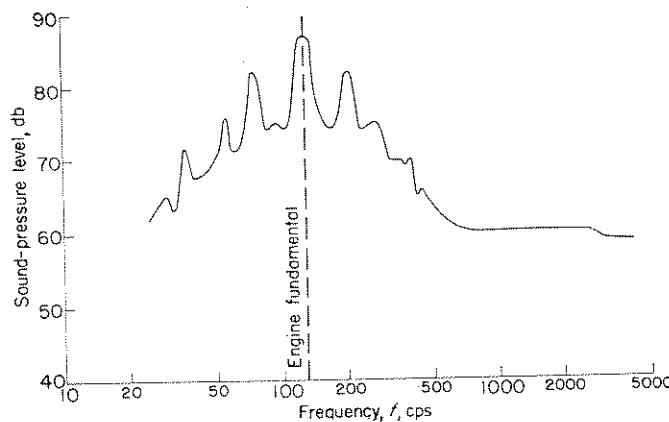


FIGURE 25.—Unmuffled-helicopter-noise frequency analysis.

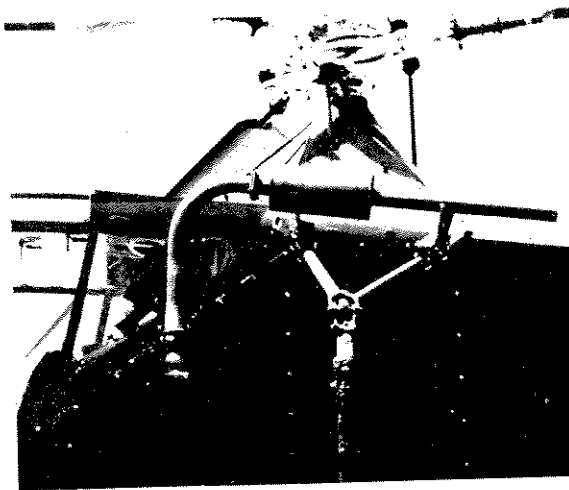
Mufflers 78, 79, 80, and 81 were made from  $\frac{1}{16}$ -inch mild steel and weighed 12, 17, 21, and 32 pounds, respectively. Figure 26 shows the mufflers installed on the test helicopter.

It may be of interest at this point to indicate the method used in the design of these mufflers with a specific example included for muffler 79. The fact that the test helicopter had two exhaust systems, one exhausting three cylinders and the other exhausting four cylinders, did not require the design of different mufflers for the two exhaust pipes. Although the exhaust-pressure pulse from each cylinder contains components at the individual cylinder firing frequency and at harmonics of this frequency, the phase relationships are such that, when the pressure pulses of all seven cylinders are combined in the atmosphere, the components at the cylinder firing frequency and at many of the harmonics are partially canceled. The mufflers must attenuate those frequency components in both exhaust pipes which combine to cause undesirably high noise levels in the atmosphere. Consequently, the mufflers are designed on the basis of the noise in the atmosphere, rather than that inside the individual exhaust pipes, and, as a result, the two mufflers are identical. The seventh harmonic of the cylinder firing frequency is referred to as the engine fundamental frequency. The prominence of this harmonic in the unmuffled engine noise (see fig. 25) is due to the fact that this frequency is the lowest at which the components of all seven cylinders are nearly together in phase.

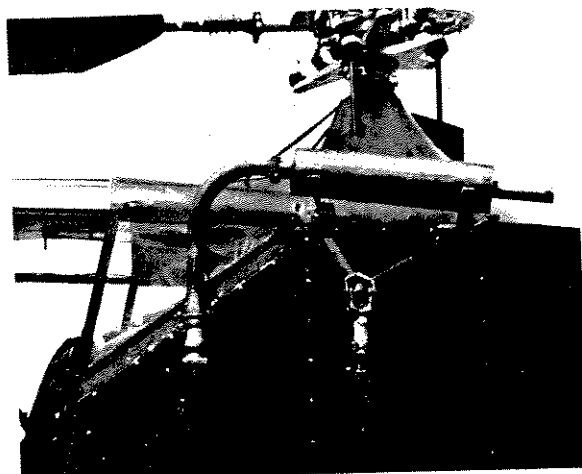
(1) The noise spectrum of the unmuffled helicopter (fig. 25) showed that most of the disturbing noise fell in the frequency range from 70 to 350 cycles per second and that 10 decibels of overall attenuation would reduce the noise to a desired level. The muffler must be made to resonate within this frequency band in order to obtain maximum quieting; thus, 280 cycles per second was chosen for the muffler resonant frequency. In order to provide a 10-decibel reduction from 70 to 350 cycles per second, a muffler having an attenuation parameter  $\frac{\sqrt{c_0 V}}{2S}$  value of approximately 6.0 was selected from the design curves.

(2) A tube for conducting the exhaust gases through the muffler for filtering must be chosen. The engine-exhaust back pressure should be kept small; consequently, a tube used for this purpose must be large enough to keep the back pressure within acceptable limits. The tubing selected for muffler 79 was  $2\frac{1}{4}$  inches, the same size as the existing exhaust ducting on the test helicopter. It should be noted that the attenuation parameter  $\frac{\sqrt{c_0 V}}{2S}$  shows that the internal-tube area governs the muffler size for a given attenuation; for this reason, the tube should be selected as small as practicable.

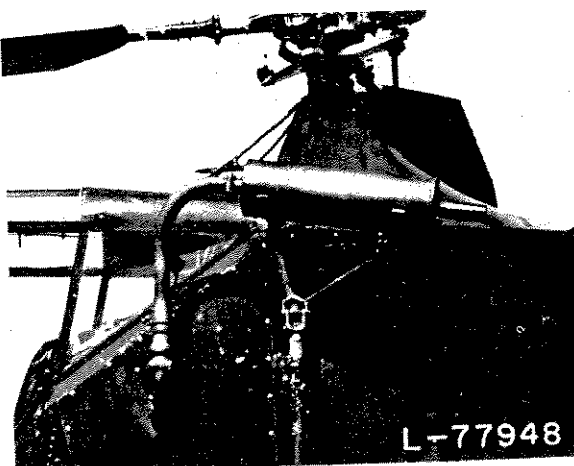
(3) In order to obtain the length for this central tube, a desired tailpipe length is computed and added to the length necessary to conduct the exhaust gases to the conductivity holes. The conductivity holes mark the origin of the tailpipe for single-chamber mufflers. Before the tailpipe length can be computed, however, some specific frequency for tailpipe resonance must be selected. This frequency must fall within a range in which little or no attenuation is needed because, as the tailpipe resonant frequency is neared, the



Muffler 78



Muffler 79



Muffler 80

FIGURE 26.—Muffler installation.

muffler attenuation drops to a negative value over a narrow band. The tailpipe resonant frequency selected for muffler 79 was 580 cycles per second. The effective tailpipe length is computed as follows:

$$l_t = \frac{\lambda}{2} = \frac{c}{2f} = \frac{2000 \times 12}{2 \times 580} = 20.68 \text{ inches}$$

By applying the end correction  $\Delta l_t = 0.61r$  where  $r$  is the tailpipe inside radius, the resulting true tailpipe length is

$$20.68 - 0.61(1.125 - 0.063) = 20.03 \text{ inches}$$

Inasmuch as the tailpipe length also affects the low-frequency cutoff of the muffler, a check is required to see whether this cutoff falls within the desired attenuation band. The cutoff frequency is determined from equation (D12):

$$f_c = \frac{f_r}{\sqrt{1 + \frac{\sqrt{c_0 V}}{2S} k_r l_t}} = \frac{280}{\sqrt{1 + 6 \frac{2\pi 280}{2000} \frac{20.68}{12}}} = 88 \text{ cps}$$

Since the cutoff frequency is within the frequency band in which muffling was desired, a decision must be made as to whether it is beneficial to increase the tailpipe length and thereby lower the high frequency cutoff or to increase the chamber size in order to obtain a small attenuation gain in the low-frequency range. The tailpipe length was not changed, and the resulting loss of low-frequency attenuation was accepted because all available criteria for judging the effects of noise agree that somewhat higher noise levels are tolerable at low frequencies than at higher frequencies.

(4) The conductivity factor  $c_0$  determines the muffler resonant frequency for a given volume. The equation

$$f_r = \frac{c}{2\pi} \sqrt{\frac{c_0}{V}}$$

shows the relationship that exists among the conductivity, volume, and resonant frequency. With the use of this expression and for the values of the parameters chosen, the volume and conductivity for muffler 79 can be determined as follows:

$$f_r = \frac{c}{2\pi} \sqrt{\frac{c_0}{V}} = 280 \text{ cps}$$

Solving for  $\sqrt{\frac{c_0}{V}}$  yields

$$\sqrt{\frac{c_0}{V}} = \frac{280 \times 2\pi}{2000} = 0.880$$

$$\sqrt{\frac{c_0 V}{2S}} = 6$$

and solving for  $\sqrt{c_0 V}$  gives

$$\sqrt{c_0 V} = 6 \times 2 \times \frac{\pi (2.25 - 0.125)^2}{4} = 0.295$$

$$c_0 = \sqrt{\frac{c_0}{V}} \sqrt{c_0 V} = 0.880 \times 0.295 = 0.260 \text{ ft}$$

By substitution

$$V = \frac{0.260}{0.880^2} = 0.336 \text{ cu ft}$$

This volume and a chosen muffler length of 2 feet were used to calculate the muffler diameter, 5.9 inches. For the sake of construction simplicity, the diameter was chosen to be 6.0 inches. This diameter change required small adjustments to be made in the values of volume and conductivity; the new values calculated were 0.338 cubic foot and 0.261 foot for volume and conductivity, respectively.

(5) The required muffler conductivity was obtained by drilling several  $\frac{1}{2}$ -inch holes in the central tube of the muffler. In determining the number of holes required, a value of  $\frac{\pi}{2}$  was used for the constant  $\beta$  in the conductivity equation. The calculation follows:

$$\begin{aligned} n &= \frac{c_0 \text{ chosen for muffler 79}}{c_0 \text{ per } \frac{1}{2}\text{-inch hole}} \\ &= \frac{0.261}{\pi \left( \frac{1}{4} \frac{1}{12} \right)^2} = 7.27 \text{ or 7 holes} \\ &= \frac{1}{16} \frac{1}{12} + \frac{\pi}{2} \frac{1}{4} \frac{1}{12} \end{aligned}$$

Experience has shown that there are some effects on the conductivity caused by the close spacing of holes which often require the number of holes to be changed in order to obtain the desired conductivity  $c_0$ , or resonant frequency. The actual conductivity  $c_0$  can be determined by experimental tests.

(6) After all dimensions for the muffler have been deter-

mined, the theoretical attenuation characteristics of the resonator should be computed and analyzed with the use of equation (D10). This equation may also be written in the following form:

$$\begin{aligned} \text{Attenuation} &= 10 \log_{10} \left( \frac{p_1}{p_t} \right)^2 \\ &= 10 \log_{10} \left[ 1 + \frac{c}{S} \frac{1}{2\pi f} \frac{c^2}{c_0} \sin \left( \frac{4\pi f}{c} \right) l_t + \right. \\ &\quad \left. \left( \frac{c}{S} \right)^2 \left( \frac{1}{2\pi f} \frac{c^2}{c_0} \right)^2 \sin^2 \left( \frac{2\pi f}{c} \right) l_t \right] \end{aligned}$$

If the predicted attenuation does not conform to the desired conditions, small changes in the originally selected design values may be made to achieve the desired results.

#### APPARATUS

The test helicopter (fig. 27) was used as the muffler test bed in this investigation. The tail rotor was removed for the tests to prevent its noise from interfering with the sound measurements. The noise emanating at the main rotor fundamental frequency (13 cps) was known to be of little significance in these tests. However, a possibility that the higher harmonics of the rotor might interfere with the exhaust noise measurements was recognized.

The helicopter was powered by a R-550-1, 180-horsepower, 7-cylinder engine having twin exhaust stacks. One stack exhausted three cylinders and the other, four. Figure 28 shows a diagrammatic sketch of the field-test setup and surrounding terrain.



FIGURE 27.—Muffler 79 installed on helicopter with tail rotor removed.

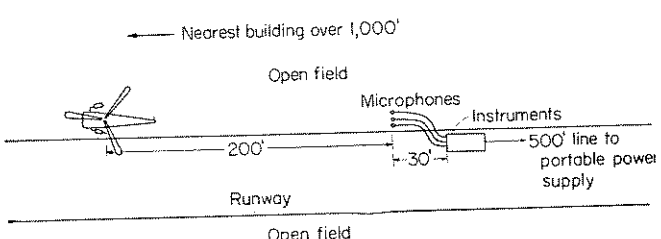


FIGURE 28.—Engine-test arrangement.

The sound measuring equipment used in the field tests consisted of a General Radio Company type 759-B sound-level meter, a General Radio Company type 760-A sound-level analyzer, and a Western Electric type 700-A sound-level meter and filter set. Both the frequency analysis and the overall sound pressure level were recorded on a twin recorder. This equipment gave an overall measuring accuracy of about 2 decibels when operating under field conditions. The response of the equipment was found to drop rapidly for frequencies below 40 cycles per second. A water-cooled crystal pressure pickup was utilized to obtain a time history of the pressure variation inside the exhaust pipe ahead of the muffler. Indications of the exhaust-gas temperatures were obtained through use of chromel-alumel thermocouples and a Lewis potentiometer.

### TESTS

The field tests were conducted before sunrise on the Langley landing field. The ambient field noise level was approximately 62 decibels at the start of the field tests. Changes that may have occurred in the ambient field noise after the helicopter engine was started could not be determined. The muffler field test included the investigation of the four mufflers of different size on the modified helicopter to determine the attenuation characteristics of the mufflers at an engine speed of approximately 2,200 revolutions per minute. In order to determine more fully the conditions under which the mufflers were operating, internal exhaust-gas sound pressures and temperatures were measured during one of the test runs.

As a further check on the practicality of the muffler design, the helicopter was flown with the first three mufflers attached. The pilot, who had considerable flying experience with the test helicopter, reported no noticeable change in performance.

### RESULTS AND DISCUSSION

The results of these muffler tests, which are discussed in the following sections, show the effectiveness of the muffler in reducing the exhaust noises along with the merits and shortcomings of the theoretical equation under investigation (eq. (D10)). The muffler experimental results are presented in the form of tables and curves.

#### MUFFLER-ENGINE TESTS

The muffler-engine-test results are shown in figure 29 and table V. These data describe the manner in which the amplitude of the exhaust noise varies with frequency.

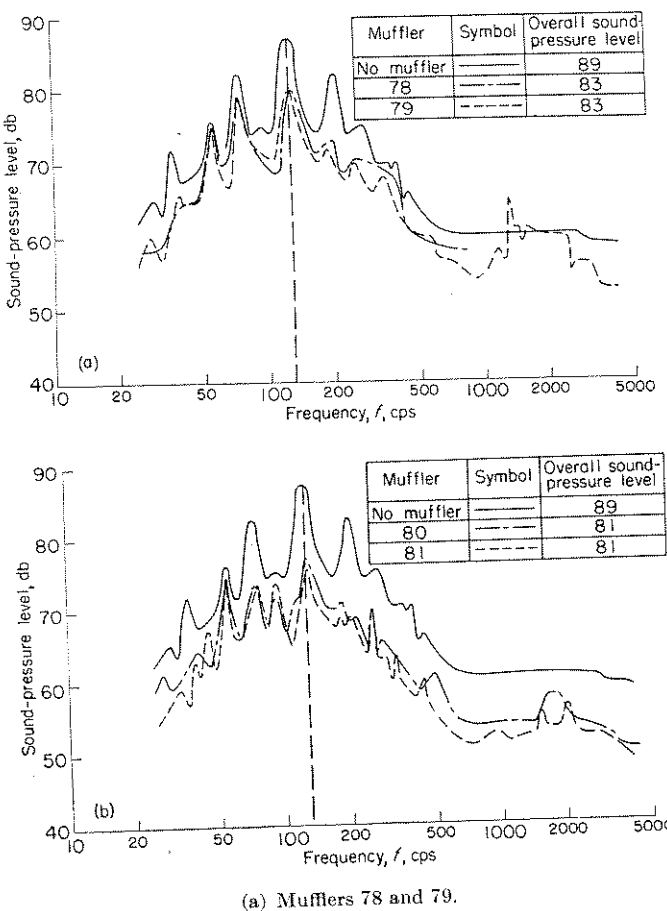


FIGURE 29.—Comparison of recorded frequency analyses of helicopter noise with and without mufflers.

Figure 29 (a) shows the unmuffled-exhaust noise spectrum in addition to the noise spectrums for both mufflers 78 and 79. Similarly, the spectrums for mufflers 80 and 81 are shown in figure 29 (b).

**Frequency analysis.**—The curve describing the envelope for the unmuffled-exhaust noise frequencies shows that the fundamental firing frequency (noted by the dashed line) is by far the largest noise-producing harmonic and, thus, is the frequency which should be given the greatest attenuation. The peaks occurring at 75 and 205 cycles per second are the next largest sound-producing frequencies of the engine noise. These two peaks, along with the fundamental peak mentioned previously, define the frequency band where most of the annoying noise is found to exist and, consequently, the range which should be given the greatest attention. When the noise spectrum from each of the four mufflers is compared with that of the unmuffled engine, it becomes obvious that considerable muffling was obtained in the 75 to 205 cycles per second frequency band. In general, the curves are seen to have the same characteristic shape.

Suppose now that a comparison is made between the cold tests and the engine tests. (See figs. 21 and 29.) Figure 21 shows that mufflers 78, 79, and 80 should have yielded their

TABLE V.—BAND-PASS ANALYSIS OF HELICOPTER NOISE AT 200 FEET

Muffler	Overall sound level, db	Sound pressure level, db, from—									
		0 to 50 cps	50 to 100 cps	75 to 150 cps	100 to 200 cps	150 to 300 cps	200 to 400 cps	300 to 600 cps	400 to 800 cps	600 to 1,200 cps	
78	85	72	80	81	81	77	75	70	60	54	
79	85	70	79	82	81	76	73	69	60	58	
80	83	70	78	80	79	74	72	67	60	57	
81	83	70	78	80	78	73	72	67	59	58	
No muffler	91	74	84	88	87	83	81	71	61	58	

greatest attenuation at 280 cycles per second and no attenuation in one lower and one higher frequency cutoff band. A point-by-point comparison between the data of these two figures showed that the helicopter noise spectrum was not reduced by the amount predicted for the muffler in the cold test. For instance, the cold-test data for muffler 79 showed about 11 decibels of attenuation was obtained at 128 cycles per second; the engine test, however, showed that 7 decibels of attenuation was realized when the muffler was tested on the helicopter. Similarly, at 200 cycles per second, approximately 20 decibels of attenuation may have been expected but only 11 decibels were measured during the engine test. After inspecting the data for all mufflers tested it was concluded that, although effective muffling was received, no muffler reduced the helicopter noise by the amounts predicted from the muffler cold tests.

**Band-pass analysis.**—In order to provide a rough check on the frequency-analyses data, certain band-pass analyses were made. These band-pass data (table V) give sound pressure levels with overlapping octaves for frequency bands, ranging from 0 to 1,200 cycles per second. Before further discussion of these data, it should be pointed out that the meter used in taking these measurements was of a different type from that used for the frequency analysis. A constant 2-decibel calibration difference was found to exist between the two meters used. For identical sound signals, the meter used to record the band-pass analysis always read 2 decibels more than the meter used to record the frequency spectrum.

Good agreement between these data was found in the frequency range of 75 to 400 cycles per second. This range is most important in the present study because most of the annoying noise falls within these limits. The band-pass analysis generally is not as useful for analyzing the data as the frequency spectrums; nevertheless, it can be used profitably to check other data and to find regions of large sound energies.

**Tailpipe characteristics.**—The theoretical data previously discussed (fig. 21) showed that certain pass bands occurred at frequencies both above and below the muffler resonant frequency. For muffler 78, these bands are from 0 to 93 cycles per second and from 375 to 400 cycles per second. Although the theoretical data showed no attenuation should have been obtained in the frequency range from 0 to 93 cycles per second, the frequency analysis of figure 29 (a) indicates that some effective quieting was received. Some muffling also was obtained in the predicted high-frequency pass band. In this band, however, the attenuation is very small, ranging from  $\frac{1}{2}$  to 2 decibels. The marked decrease in attenuation in the frequency range from 375 to 400 cycles

per second is sufficient to indicate that the tailpipe resonance must have occurred in this frequency band; this result agrees with the theory. The cold tests also showed this attenuation decrease. It may therefore be concluded that the theoretical expression is valid for predicting the tailpipe resonance of the muffler under engine test conditions and that some slight attenuation may be realized during such resonances. Further evidence of these tailpipe resonances may be found by checking the data for mufflers 79 and 80.

**Internal sound pressures of the exhaust system.**—As stated previously, the test engine had two separate exhaust manifolds, one exhausting three cylinders and the other, four. A schematic drawing showing this arrangement appears in figure 30. Sound-pressure data, as signaled by a crystal pickup gage placed in the left exhaust manifold, are presented in figure 31. The curve of figure 31 (a) describes one cycle of this sound variation. The curve of figure 31 (b), having 4 humps, shows the exhaust-pressure variation for the 4-cylinder exhaust. This curve was not obtained directly from recorded data but was synthesized with the aid of the measured 3-cylinder exhaust curve.

Close examination of the plot showing the 3-cylinder exhaust pressure reveals that the sound pressure in the system did not go as high when the second consecutive exhaust valve opened as when the first valve opened. An examination of the exhaust system reveals that the first cylinder exhaust valve remains open for a considerable time after the second cylinder valve opens; thus, the volume of the system is increased. This increased volume allows, in effect, an additional expansion of the exhausting gases and provides a damping of the peak sound pressures.

The maximum peak exhaust pressure measured is shown to be approximately 7 pounds per square inch. This value corresponds to a sound-pressure level of 189 decibels. This pressure is far greater than both the pressure assumed in theory and the sound pressure used for the cold tests. The peak pressures measured entering the mufflers attached to the cold-test setup were of the order of 141 decibels or 0.028 pound per square inch. In order to reduce large peak sound pulses, collector rings may be employed. The pressure records of figure 31, for example, indicate that, if a complete circular collector ring had been installed on the engine, the magnitude of the pressure peaks might have been reduced by over 50 percent. In addition, only one muffler would have been required.

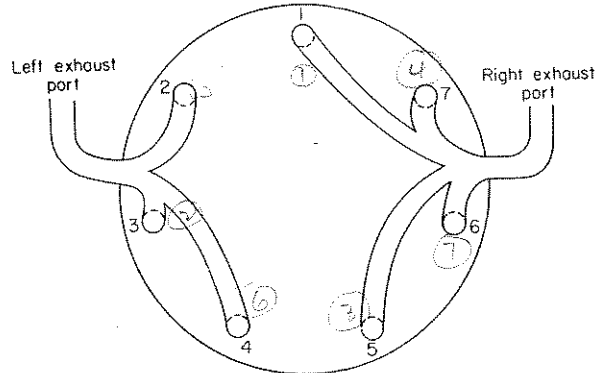
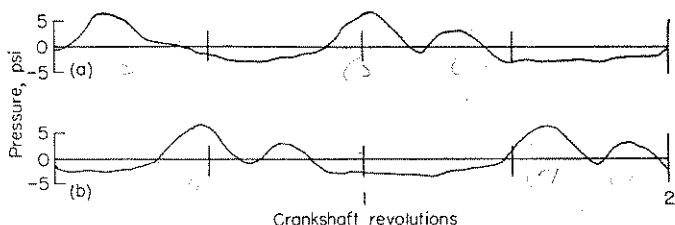


FIGURE 30.—Schematic drawing of helicopter-engine-exhaust system.  
Firing order: 1, 3, 5, 7, 2, 4, 6.



(a) Variation of sound pressure measured in the 3-cylinder exhaust of the test helicopter.  
 (b) Variation of sound pressure in the 4-cylinder exhaust of the test helicopter as estimated from 3-cylinder data.

FIGURE 31.—Exhaust-pipe sound pressure.

#### POSSIBLE REASONS FOR DISCREPANCIES BETWEEN COLD TESTS AND ENGINE TESTS

Some reasons may be given to account for the discrepancies that exist between the attenuations obtained from the cold tests and those obtained from the engine tests. These reasons include (1) the large differences in operating conditions, and (2) the prevailing extraneous noises of the engine tests.

**Differences in operating conditions.**—In the section entitled "Variables Dependent on Operating Conditions" in Part III, the possible effects of three variables were discussed. The effect of temperature was taken into account in the design of the engine mufflers by using the speed of sound in the hot exhaust gas. The exhaust-gas velocity was not taken into account, but it is doubtful whether this factor could have caused a loss of attenuation, inasmuch as the available evidence indicates that the exhaust-gas velocity either causes an increase in attenuation or has little influence on attenuation. The exhaust-gas velocity for this engine is estimated to be about 500 feet per second. The cold-test experiments were conducted with peak sound pressures of the order of 141 decibels (0.028 psi); whereas, the peak sound pressures from the engine entering the mufflers were about 189 decibels (7.0 psi). This sound-pressure increase of 250 times in the muffler system raises the sound pressure to a point where it is no longer small with respect to the static (atmospheric) pressure. An original assumption made in the development of the theoretical equation was that the sound pressure would be small in comparison with the static pressure. It is obvious that this assumption was not satisfied during the engine tests, and this fact may be responsible for some loss of attenuation.

**Extraneous noise.**—Another factor which may account for some of the discrepancies between data is extraneous noise. The influence of this factor on the exhaust noise spectrum presented is difficult to determine. No pure extraneous noise spectrum could be obtained whereby a quantitative point-by-point comparison could be made. The extraneous noise, as discussed herein, is made up of all noises which originate from sources other than the exhaust gas. These noises include engine air intake, engine blower, engine clatter, vibrating fuselage, main rotor, and distant aircraft. The combination of these noises, when integrated with those from the exhaust gases, yields all the curves described in figure 29. If the exhaust-gas noise is the most pronounced noise in a system and if it is reduced continuously, some

point will be passed where the exhaust and extraneous noises will be equal. At this point the extraneous noise will be equally as important as the exhaust in determining the noise spectrum. Thus, the spectrum will stop defining the shape of exhaust noise in detail and begin to show some characteristics of the extraneous noises. A reduction of the exhaust noise well below that of the extraneous noise will leave a spectrum containing principally extraneous noise. With this fact in mind, the large, two-chamber muffler (81) was designed to attenuate the exhaust noise so much that the extraneous noise spectrum could be approximately determined. The spectrum for muffler 81 (fig. 29 (b)) has practically the same shape as that for muffler 80. This observation indicates that muffler 80 must have reduced the exhaust noise to a point where the extraneous noise became prevalent and that muffler 81 could have only further reduced the exhaust noise; consequently, only slightly more overall noise reduction was provided. Overall sound-pressure measurements showed the same sound energy (81 decibels) was present at the microphones when both mufflers 80 and 81 were installed. Thus, the exact attenuation provided by the mufflers could not be determined because of the extraneous noise level. It is of interest to note here that, as the extraneous noise level is approached, the mufflers must reduce the exhaust noise in greater increments to reduce the overall noise level by equal amounts. For instance, if the extraneous noise is 85 decibels and the exhaust noise is 100 decibels, the overall noise will be 100.1 decibels. If a muffler reduces the exhaust noise by 12 decibels, the overall noise will be reduced by 10.4 decibels to 89.7 decibels. If the exhaust noise is reduced another 12 decibels (to 76 decibels), the overall noise level is reduced by only 4.2 decibels to 85.5 decibels. This explanation shows very clearly that the amount of overall noise reduction which can be gained by the use of a given muffler is dependent upon the relative intensities of the extraneous and exhaust noises. It may be concluded, therefore, that a muffler used to attenuate a noise level which considerably exceeds that of the extraneous noise can provide much more overall noise reduction than if it were working in a noise range close to the extraneous noise.

#### SIGNIFICANCE OF MEASURED NOISE REDUCTION

In order that the significance of the noise reductions obtained may be interpreted, some comparisons and comments are made on the basis of the information contained in reference 13 regarding the sound levels of aircraft traffic. For those familiar with the noise of various types of airplanes on takeoff, figure 27 of this reference provides a meaningful comparison. The noise of the unmuffled 180-horsepower helicopter has about the same intensity level as that of the 150-horsepower Stinson Voyager or the 165-horsepower Beech Bonanza. The smallest muffler tested on the helicopter reduced the intensity to about that of the quietest airplane of figure 27 of reference 13, a 65-horsepower Piper Cub. These comparisons are made at takeoff power at a distance of 200 feet. The three airplanes mentioned were all equipped with standard production mufflers.

As a further indication of the significance of the sound levels measured in this investigation, a comparison in terms

of relative loudness is made. Relative loudness is defined herein, as in reference 13, as the perceived loudness of sound heard by the average ear relative to the loudness of the normal conversational voice at a 3-foot distance. The variation in perceived loudness with the loudness level (in phons or decibels) is taken from the American Standards Association Standard Z24.2-1942. Relative loudnesses of the five configurations of this investigation, based on the overall sound levels given in table V, are approximately 5.3 for the unmuffled helicopter, 2.9 with mufflers 1 and 2, and 2.5 with mufflers 3 and 4, all at a distance of 200 feet at takeoff power. Thus, muffler 78, for example, reduces the loudness of the noise as perceived by the average ear by about 45 percent. This example gives an indication of the magnitude of the noise reduction obtained although, of course, the human mind takes into account other factors besides loudness in judging the annoyance due to a particular noise. On the basis of the data in reference 13, the distances at which the helicopter noise would have the same loudness as the reference conversational voice are estimated at about 1,800 feet for the unmuffled helicopter, 800 feet with mufflers 78 and 79, and 630 feet with mufflers 80 and 81. It is evident from this discussion that the mufflers produced a very significant reduction in the noise of the helicopter.

#### CONCLUDING REMARKS

Attenuation curves have been calculated for a large number of mufflers, all of which are designed to permit the exhaust gas to flow through the mufflers without turning. Comparison of the calculated curves with experimental data has shown that it is possible, by means of the acoustic theory, to predict the attenuation in still air at room temperature of mufflers of the size required for aircraft engines. There are, however, certain limits to the muffler size and the frequency range within which these equations are applicable. These limits include:

- (a) For expansion chambers, the acoustic wave length must be greater than about 0.82 times the chamber diameter.
- (b) For resonators, if the connector is longer than about one-fifth of the wave length at the desired resonant frequency, the wave nature of the sound flow in the connector must be taken into account.
- (c) For resonators, if the acoustic path length from the connector to the closed end of the chamber is of the order

of one-eighth wave length or more, the wave nature of the flow in the chamber must be accounted for.

The conductivity was predicted with reasonable accuracy for connectors composed of a small number of holes or tubes. Where large numbers of holes in close proximity were used, the conductivity was not accurately predictable. In such cases, the designer must rely on an experimental determination of the conductivity through measurement of the resonant frequency.

Methods have been found which, in theory, will eliminate pass bands in three specific cases. The pass bands that can be eliminated are:

- (a) The odd-numbered upper pass bands of a double-expansion-chamber muffler.
- (b) The first upper pass band of a multiple-resonator muffler.
- (c) The first upper tailpipe pass band of a single-resonator muffler.

A method has been presented which permits the effect of the tailpipe to be included in the muffler calculations. Specific equations have been developed for the attenuation with tailpipes of single expansion chamber and single-chamber-resonator mufflers. Experimental verification of the equation for the single-chamber resonator was obtained under cold-test conditions.

Four resonator-type mufflers have been tested on a helicopter engine. Even the smallest of these mufflers reduced the overall noise by a significant amount. Because this overall noise included a considerable amount of extraneous noise, an accurate determination of the exhaust-noise reduction was not possible. The experimental results seem to indicate, however, that the exhaust-noise reduction may have been considerably less than that which was obtained in the cold tests of these same mufflers. The theory is handicapped severely by the fact that the sound pressures inside the exhaust pipe were found to be much larger than those assumed in the basic theory. In order to isolate the effects of large sound pressures and exhaust-gas flow velocities on the attenuating properties of mufflers, further tests are necessary in which extraneous noises are held to a low level.

LANGLEY AERONAUTICAL LABORATORY,  
NATIONAL ADVISORY COMMITTEE FOR AERONAUTICS,  
LANGLEY FIELD, VA., October 6, 1952.

## APPENDIX A

### ATTENUATION OF EXPANSION-CHAMBER MUFFLERS

#### ASSUMPTIONS AND GENERAL METHOD

In the derivation of the equations for the attenuation of expansion-chamber mufflers, the following conditions are assumed:

- (1) The sound pressures are small compared with the absolute value of the average pressure in the system.
- (2) The tailpipe is terminated in its characteristic impedance (no reflected waves in the tailpipe).
- (3) The muffler walls neither conduct nor transmit sound energy.
- (4) Only plane pressure waves need be considered.
- (5) Viscosity effects may be neglected.

By definition, the attenuation in decibels due to a combination of acoustic elements placed in a tube is

$$10 \log_{10} \left( \frac{\text{Average incident sound power}}{\text{Average transmitted sound power}} \right) \quad (\text{A1})$$

In the manner of reference 1 (p. 72), let the displacements and particle velocities of the incident and reflected waves at an arbitrary point  $x$  be written as

$$\left. \begin{aligned} \xi_i &= A e^{i(\omega t - kx)} & \dot{\xi}_i &= i\omega A e^{i(\omega t - kx)} \\ \xi_{re} &= B e^{i(\omega t + kx)} & \dot{\xi}_{re} &= i\omega B e^{i(\omega t + kx)} \end{aligned} \right\} \quad (\text{A2})$$

where the positive  $x$ -direction is taken as the direction of propagation of the incident wave and the constants  $A$  and  $B$  are, in general, complex numbers. For plane waves the acoustic pressure  $p$  is equal to  $\mp \rho c^2 \frac{\partial \xi}{\partial x}$ , where  $\rho$  is the average density of the gas. The incident and reflected pressures can therefore be written as

$$\left. \begin{aligned} p_i &= i\omega \rho c A e^{i(\omega t - kx)} \\ p_{re} &= i\omega \rho c B e^{i(\omega t + kx)} \end{aligned} \right\} \quad (\text{A3})$$

The average sound power in the incident wave is

$$\frac{\omega}{2\pi} \int_0^{2\pi/\omega} p_i \dot{\xi}_i S dt$$

where, since this is a calculation of actual power, only the real parts of  $p_i$  and  $\dot{\xi}_i$  can be considered. After the integra-

tion is performed, the average sound power is obtained as

$$\frac{1}{2} \rho c \omega^2 S |A|^2$$

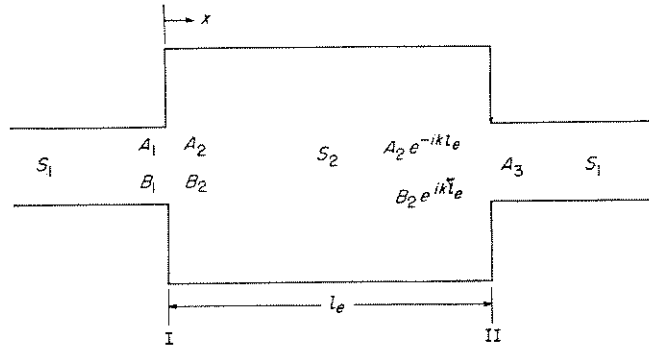
If the attenuation between two points located at cross sections of equal area is desired, the formula is

$$\text{Attenuation} = 10 \log_{10} \left| \frac{A_1}{A_2} \right|^2 \quad (\text{A4})$$

provided there are no reflected waves at the point 2.

#### SINGLE EXPANSION CHAMBER

A schematic diagram of a single expansion chamber is shown below:



The origin of  $x$  is taken at junction I. If constant factors are omitted, the equations for continuity of pressure and flow volume at junction I can be written, with the assistance of equations (A2) and (A3), as

$$A_1 + B_1 = A_2 + B_2 \quad (\text{A5})$$

$$S_1 (A_1 - B_1) = S_2 (A_2 - B_2)$$

or

$$A_1 - B_1 = m (A_2 - B_2) \quad (\text{A6})$$

Similarly, at junction II, the expressions are

$$A_2 e^{-ikl_e} + B_2 e^{ikl_e} = A_3 \quad (\text{A7})$$

$$m (A_2 e^{-ikl_e} - B_2 e^{ikl_e}) = A_3 \quad (\text{A8})$$

If, now, equations (A5), (A6), (A7), and (A8) are solved simultaneously for the ratio  $A_1/A_3$ , the result is

$$\left. \begin{aligned} \frac{A_1}{A_3} &= \cos kl_e + i \frac{1}{2} \left( m + \frac{1}{m} \right) \sin kl_e \\ \left| \frac{A_1}{A_3} \right| &= \sqrt{1 + \frac{1}{4} \left( m - \frac{1}{m} \right)^2 \sin^2 kl_e} \end{aligned} \right\} \quad (A9)$$

and the attenuation (see eq. (A4)) is

$$\text{Attenuation} = 10 \log_{10} \left[ 1 + \frac{1}{4} \left( m - \frac{1}{m} \right)^2 \sin^2 kl_e \right] \quad (A10)$$

The design curves of figure 22 were obtained by plotting this equation against  $kl_e$ .

If the equations are solved for  $B_1/A_3$ , the result is

$$\frac{B_1}{A_3} = -i \frac{1}{2} \left( m - \frac{1}{m} \right) \sin kl_e \quad (A11)$$

When measurements are taken in the manner described in the section entitled "Methods and Tests" in Part I, the maximum pressure measurable in the exhaust pipe to the left of junction I will be proportional to

$$\left| \frac{A_1}{A_3} \right| + \left| \frac{B_1}{A_3} \right|$$

and will be found at the station  $x$  at which the incident and reflected waves are in phase with each other. The maximum measured attenuation will thus be given by

$$10 \log_{10} \left( \left| \frac{A_1}{A_3} \right| + \left| \frac{B_1}{A_3} \right| \right)^2 \quad (A12)$$

Substitution of equations (A9) and (A11) into equation (A12) results in

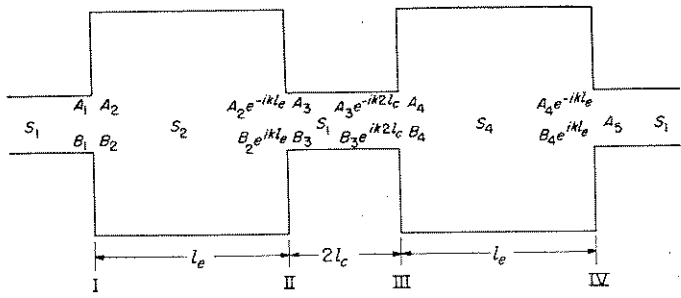
$$\text{Maximum measured attenuation} = 10 \log_{10} \left[ 1 + \frac{1}{2} \left( m - \frac{1}{m} \right)^2 \sin^2 kl_e + \left( m - \frac{1}{m} \right) \sin kl_e \sqrt{1 + \frac{1}{4} \left( m - \frac{1}{m} \right)^2 \sin^2 kl_e} \right] \quad (A13)$$

The upper curve of figure 8 was computed from this equation.

#### DOUBLE EXPANSION CHAMBER WITH EXTERNAL CONNECTING TUBE

A schematic diagram of a double-expansion-chamber muffler with the connecting tube external to the chambers is

shown below, with the symbols to be used also included:



The effective length of the connecting tube  $2l_c$  is equal to the physical length plus an end correction. If the same basic method is used as for the single expansion chamber, the equations of continuity of pressure and flow at the four indicated junctions are:

At junction I

$$A_1 + B_1 = A_2 + B_2$$

$$A_1 - B_1 = m(A_2 - B_2)$$

At junction II

$$A_2 e^{-ikl_e} + B_2 e^{ikl_e} = A_3 + B_3$$

$$m(A_2 e^{-ikl_e} - B_2 e^{ikl_e}) = A_3 - B_3$$

At junction III

$$A_3 e^{-ik2l_e} + B_3 e^{ik2l_e} = A_4 + B_4$$

$$m(A_3 e^{-ik2l_e} - B_3 e^{ik2l_e}) = A_4 - B_4$$

At junction IV

$$A_4 e^{-ikl_e} + B_4 e^{ikl_e} = A_5$$

$$m(A_4 e^{-ikl_e} - B_4 e^{ikl_e}) = A_5$$

The simultaneous solution of these equations results in

$$\begin{aligned} \frac{A_1}{A_5} &= \frac{1}{16m^2} [(m+1)^4 e^{2ik(l_e + l_c)} - (m^2-1)^2 e^{-2ik(l_e + l_c)} - \\ &\quad 2(m^2-1)^2 e^{2ikl_e} + 2(m^2-1)^2 e^{-2ikl_e} - \\ &\quad (m^2-1)^2 e^{2ik(l_e - l_c)} + (m-1)^4 e^{-2ik(l_e - l_c)}] \end{aligned}$$

This equation can be written, in terms of trigonometric functions, as

$$\frac{A_1}{A_5} = \frac{1}{16m^2} \{ [4m(m+1)^2 \cos 2k(l_e + l_c) - 4m(m-1)^2 \cos 2k(l_e - l_c)] + i[2(m^2+1)(m+1)^2 \sin 2k(l_e + l_c) - 2(m^2+1)(m-1)^2 \sin 2k(l_e - l_c)] \} \quad (A14)$$

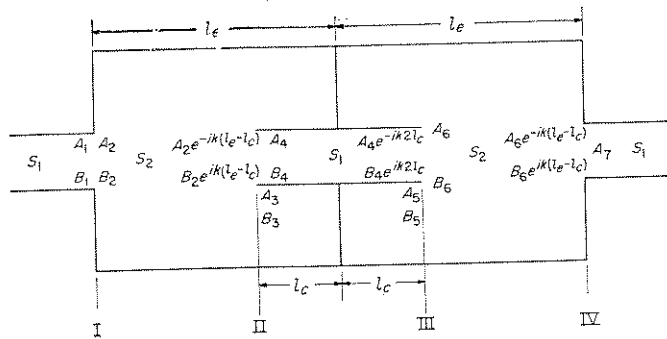
The attenuation is

$$\text{Attenuation} = 10 \log_{10} \left\{ \left[ R \left( \frac{A_1}{A_5} \right) \right]^2 + \left[ I \left( \frac{A_1}{A_5} \right) \right]^2 \right\} \quad (A15)$$

where R and I are used to denote the real and imaginary parts, respectively.

#### DOUBLE EXPANSION CHAMBER WITH INTERNAL CONNECTING TUBE

A schematic diagram of a double-expansion-chamber muffler with the connecting tube internal to the expansion chambers is shown below, with the symbols to be used also indicated:



The basic equations of continuity of pressure and flow at the four indicated junctions are:

At junction I

$$A_1 + B_1 = A_2 + B_2$$

$$A_1 - B_1 = m(A_2 - B_2)$$

At junction II

$$A_2e^{-ik(l_e - l_c)} + B_2e^{ik(l_e - l_c)} = A_3 + B_3 = A_4 + B_4$$

$$m(A_2e^{-ik(l_e - l_c)} - B_2e^{ik(l_e - l_c)}) = A_4 - B_4 + (m-1)(A_3 - B_3)$$

At junction III

$$A_4e^{-2ikl_c} + B_4e^{2ikl_c} = A_5 + B_5 = A_6 + B_6$$

$$A_4e^{-2ikl_c} - B_4e^{2ikl_c} + (m-1)(A_5 - B_5) = m(A_6 - B_6)$$

At junction IV

$$A_6e^{-ik(l_e - l_c)} + B_6e^{ik(l_e - l_c)} = A_7$$

$$m(A_6e^{-ik(l_e - l_c)} - B_6e^{ik(l_e - l_c)}) = A_7$$

In addition, because of the total reflection from the bulkhead separating the two chambers,

$$B_3 = A_3e^{-2ikl_c}$$

$$B_5 = A_5e^{2ikl_c}$$

The simultaneous solution of these equations results in

$$\frac{A_1}{A_7} = \cos 2kl_e - (m-1) \sin 2kl_e \tan kl_e + \frac{i}{2} \left\{ \left( m + \frac{1}{m} \right) \sin 2kl_e + (m-1) \tan kl_e \left[ \left( m + \frac{1}{m} \right) \cos 2kl_e - \left( m - \frac{1}{m} \right) \right] \right\} \quad (A16)$$

The attenuation is

$$\text{Attenuation} = 10 \log_{10} \left\{ \left[ R \left( \frac{A_1}{A_7} \right) \right]^2 + \left[ I \left( \frac{A_1}{A_7} \right) \right]^2 \right\} \quad (A17)$$

#### CUTOFF FREQUENCY

In the design of double-expansion-chamber mufflers, it is important to be able to predict the low-frequency limit of the first effective attenuation region. This frequency is called the cutoff frequency  $f_c$ . It may, of course, be found from a plot of equation (A17) but a more rapid method of estimating  $f_c$  is desirable for use in the preliminary design of a muffler. The semiempirical equation

$$f_c \approx \frac{c}{2\pi} \frac{1}{\sqrt{ml_e l_c + \frac{l_e}{3}(l_e - l_c)}} \quad (A18)$$

has been found quite satisfactory for this purpose within the range of variables covered in this investigation (see table II).

## APPENDIX B

### ATTENUATION OF RESONATOR MUFFLERS

#### SINGLE RESONATORS

In the derivation of the equation for the attenuation due to a single resonator in a side branch, assumptions (1), (2), and (3) of appendix A are required. Assumptions (4) and (5) are modified as follows:

(4) Only plane pressure waves are propagated in the exhaust pipe and the tailpipe.

(5) The influence of the viscosity of the fluid may be neglected everywhere except in the tubes or orifices which form the connector between the exhaust pipe and the volume chamber of the resonator.

The following two additional assumptions are necessary:

(6) The boundary-layer thickness is small compared to the diameter of the tube or orifice in which viscosity effects are considered.

(7) The dimensions of the resonator are small relative to the wave length of the sound considered.

Consider the effect of a side branch of impedance  $Z_b = R_b + iX_b$  opening into a tube in which plane sound waves are propagated. At the point where the branch joins the tube, the conditions of continuity of pressure and sound current give

$$p_i + p_{re} = p_b = p_{tr} \quad (B1)$$

$$I_i - I_{re} = I_b + I_{tr} \quad (B2)$$

where subscripts  $i$  and  $re$  refer to the incident and reflected waves ahead of the branch,  $b$  refers to the branch, and  $tr$  refers to the transmitted wave behind the branch. For a plane wave  $p = Z_0 I$ , where  $Z_0$  is the characteristic impedance of the tube. If the currents are written in terms of pressure and impedance, equation (B2) becomes

$$\frac{1}{Z_0} (p_i - p_{re}) = p_{tr} \left( \frac{1}{Z_b} + \frac{1}{Z_0} \right) \quad (B3)$$

If, now, equations (B1) and (B3) are solved simultaneously for the ratio  $p_i/p_{tr}$ , the result is

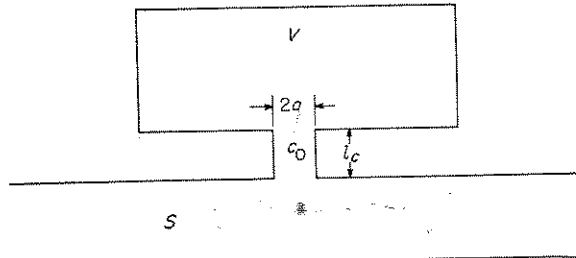
$$\frac{p_i}{p_{tr}} = 1 + \frac{Z_0}{2Z_b} = 1 + \frac{Z_0}{2(R_b + iX_b)}$$

Hence the attenuation is

$$\text{Attenuation} = 10 \log_{10} \left| \frac{p_i}{p_{tr}} \right|^2 = 10 \log_{10} \frac{\left( R_b + \frac{Z_0}{2} \right)^2 + X_b^2}{R_b^2 + X_b^2} \quad (B4)$$

A schematic diagram of a single-resonator muffler is shown

below with the symbols that are used indicated:



On the basis of the listed assumptions, the impedances of the various components are (ref. 1, p. 118)

$$\text{Volume-chamber impedance} = -i \frac{\rho c^2}{\omega V} \quad (B5)$$

$$\text{Connector impedance} = \frac{l_c}{\pi a^3} \sqrt{2\mu\rho\omega} + i \left( \frac{\omega\rho}{c_0} + \frac{l_c}{\pi a^3} \sqrt{2\mu\rho\omega} \right) \quad (B6)$$

where  $c_0$  is the conductivity and  $l_c$  is the effective length of the connector. Since, in the resonator side branch, the volume chamber and the connector are in series

$$R_b = \frac{l_c}{\pi a^3} \sqrt{2\mu\rho\omega} \quad (B7)$$

$$X_b = \frac{\omega\rho}{c_0} - \frac{\rho c^2}{\omega V} + \frac{l_c}{\pi a^3} \sqrt{2\mu\rho\omega} \quad (B8)$$

These values, when substituted into equation (B4), give the attenuation of a single-resonator muffler.

In many cases it is possible to neglect the effect of viscosity without introducing excessive error, except at the resonant frequency. If  $\mu=0$ , equation (B4) simplifies to

$$\text{Attenuation} = 10 \log_{10} \left( 1 + \frac{Z_0^2}{4X_b^2} \right) \quad (B9)$$

By inserting the value of  $X_b$  and making use of the fact that  $f_r = \frac{c}{2\pi} \sqrt{\frac{c_0}{V}}$  it is possible to bring equation (B9) into the form

$$\text{Attenuation} = 10 \log_{10} \left[ 1 + \left( \frac{\sqrt{c_0 V}}{2S} \frac{f}{f_r} \right)^2 \right] \quad (B10)$$

The design curves of figure 23 have been obtained from this equation. Since viscosity has been neglected, the predicted attenuation rises to infinity at the resonant frequency  $\frac{f}{f_r} = 1$ .

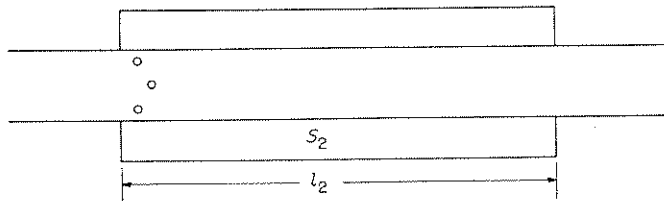
If the effective length of the connector  $l_c$  is not sufficiently short compared to the sound-wave length, assumption (7) of appendix B is violated and the wave nature of the flow in the connector must be considered. Muffler 28 is an example of this case. For a connector of length  $l_c$  and area  $S_c$  terminated by a volume  $V$ , the branch reactance (with viscosity omitted) is

$$X_b = \frac{\rho c}{S_c} \left( \frac{\tan kl_c - \frac{S_c}{kV}}{\frac{S_c}{kV} \tan kl_c + 1} \right) \quad (B11)$$

This expression can be obtained from equation 5.30, page 125, reference 1 by substituting the volume-chamber impedance  $-\frac{i\rho c^2}{\omega V}$  for the impedance which is symbolized by  $Z_b$  in the reference. Having obtained the branch reactance, the attenuation, with viscosity neglected, is calculated from equation (B9). The attenuation of muffler 28 was calculated in this manner. Strictly speaking, an end correction is required at both ends of the connector in determining the effective connector length  $l_c$  when equation (B11) is used. This correction will reach a maximum of about 0.8 times the connector radius, at each end of the connector, if the connector radius is much smaller than that of the exhaust pipe and the volume chamber.

If the resonant chamber is itself long, the resonance becomes a length-controlled phenomenon instead of a volume-controlled one and the attenuation can be determined by assuming plane-wave motion in both the connector and the chamber.

In case the connector is short and the chamber is long, as in the following sketch, another approach may be used:



Again, the problem is to determine the branch impedance. For a closed chamber the branch impedance is (again with viscosity omitted)

$$Z_b = i \left( \frac{\rho \omega}{c_0} - \frac{\rho c}{S_2} \cot kl_2 \right) \quad (B12)$$

The attenuation is therefore

$$10 \log_{10} \left[ 1 + \frac{1}{4} \left( \frac{m}{\frac{kS_2}{c_0} - \cot kl_2} \right)^2 \right] \quad (B13)$$

For a muffler in which the connector is located at the center of the resonant chamber, rather than at the end, the effective chamber length is one-half the actual chamber length  $l_2$

and the effective expansion ratio is twice the physical expansion ratio  $m$ . These effective values should be used in equation (B12) or (B13). Because of the typical attenuation characteristics of resonators of this type (eq. (B13)), they are called "quarter-wave" resonators.

#### MULTIPLE RESONATORS

The attenuation of  $M$  identical chambers of an infinite filter composed of branch resonators is given by (see ref. 8)

$$\text{Attenuation} = -8.69M \cosh^{-1} \left| \cos kl_1 + i \frac{Z_0}{2Z_b} \sin kl_1 \right| \quad (B14)$$

where

$$\frac{Z_0}{2Z_b} = \frac{\rho c}{2S} \frac{1}{i \left( \frac{2\pi f \rho}{c_0} - \frac{\rho c^2}{2\pi f V} \right)}$$

By use of the substitution  $\sqrt{\frac{c_0}{V}} = \frac{2\pi f_r}{c}$ , this equation may also be written as

$$\frac{Z_0}{2Z_b} = -i \frac{\sqrt{c_0 V}}{\frac{f}{f_r} - \frac{f_r}{f}}$$

Substituting this expression in equation (B14) and making use of the fact that  $k_r = \frac{2\pi f_r}{c}$  gives

$$\text{Attenuation} = -8.69M$$

$$\cosh^{-1} \left| \cos \left( k_r l_1 \frac{f}{f_r} \right) + i \frac{\sqrt{c_0 V}}{\frac{f}{f_r} - \frac{f_r}{f}} \sin \left( k_r l_1 \frac{f}{f_r} \right) \right| \quad (B15)$$

where the inverse hyperbolic cosine is taken with a negative sign. Thus at a given frequency the attenuation, per chamber, of a multiple-resonator muffler is a function of three basic parameters:  $\sqrt{c_0 V}/2S$ ,  $k_r l_1$ , and  $\sqrt{c_0 V}$  (since  $f_r$  is controlled by  $\sqrt{c_0 V}$ ). The design curves of figure 24 were calculated from equation (B15).

In reference 1 the cutoff frequency is given as

$$f_c = \frac{c}{\pi} \sqrt{\frac{S}{l_1 V} \left( \frac{1}{1 + \frac{4S}{l_1 c_0}} \right)} \quad (B16)$$

In terms of the resonant frequency equation (B16) can be written in the form

$$f_c = \frac{f_r}{\sqrt{1 + \frac{c_0 l_1}{4S}}} \quad (B17)$$

These equations for  $f_c$  are, in reality, approximations since lumped impedances were assumed in the derivation (see ref. 1). The approximation should be valid within the range of variables where  $\tan k_r l_1$  can be taken as  $k_r l_1$  within the permissible limits of accuracy.

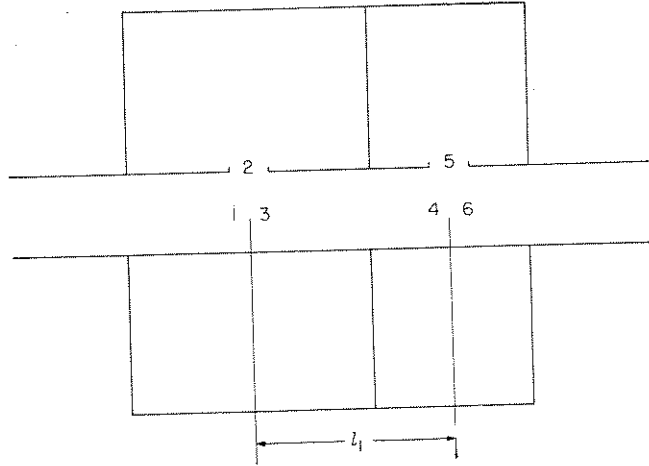
In the case of mufflers with long chambers the expression for  $Z_b$  given by equation (B12) can be used in equation (B14). Instances where this substitution has been made are pointed out in the text and in the figures.

## APPENDIX C

### COMBINATIONS

#### TWO RESONATORS TUNED AT DIFFERENT FREQUENCIES

A schematic diagram of a muffler composed of two resonators tuned at different frequencies is shown below with the subscripts that will be used to indicate various locations also shown:



The assumptions made are the same as for the single resonators. At station 1 let

$$Z_1 = \frac{p_1}{I_1} = \frac{i\omega\rho c(A_1 + B_1)e^{i\omega t}}{i\omega S(A_1 - B_1)e^{i\omega t}} = Z_0 \frac{A_1 + B_1}{A_1 - B_1}$$

From this relationship

$$\frac{B_1}{A_1} = \frac{Z_1 - Z_0}{Z_1 + Z_0} \quad (C1)$$

where  $Z_1$  is the impedance of the first branch and the circuit to the right of this branch in parallel. Similarly

$$\frac{B_3}{A_3} = \frac{Z_3 - Z_0}{Z_3 + Z_0} \quad (C2)$$

working out the expression for

$$\text{Attenuation} = 10 \log_{10} \left| \frac{A_1}{A_6} \right|^2 \quad (C7)$$

If the branch impedances have no resistive components, the result obtained is

$$\frac{A_1}{A_6} = \frac{1}{2} \frac{[R_3 X_2^2 + Z_0 R_3^2 + Z_0 (X_2 + X_3)^2] + i[R_3^2 X_2 + X_2 X_3 (X_2 + X_3)]}{[R_3 X_2^2 \cos kl_1 + Z_0 X_2 R_3 \sin kl_1] + i[R_3^2 X_2 + X_2 X_3 (X_2 + X_3) \cos kl_1 - Z_0 X_2 (X_2 + X_3) \sin kl_1]} \quad (C8)$$

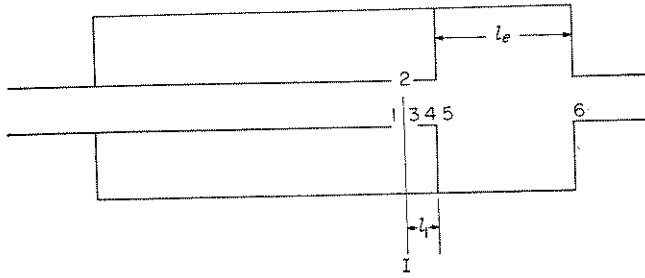
where

$$\left. \begin{aligned} R_3 &= \frac{Z_0 X_5^2 (Z_0^2 + X_5^2)}{[(Z_0^2 + X_5^2) \cos kl_1 - Z_0 X_5 \sin kl_1]^2 + X_5^4 \sin^2 kl_1} \\ X_3 &= \frac{Z_0^2 X_5 (Z_0^2 + X_5^2) \cos 2kl_1 + \frac{1}{2} (Z_0^5 + Z_0^3 X_5^2) \sin 2kl_1}{[(Z_0^2 + X_5^2) \cos kl_1 - Z_0 X_5 \sin kl_1]^2 + X_5^4 \sin^2 kl_1} \end{aligned} \right\} \quad (C9)$$

These equations were used to calculate the attenuation of muffler 73 (see fig. 16). It has been found necessary to include the length  $l_1$ , even though it may be much less than the sound wave length under consideration.

#### A RESONATOR AND AN EXPANSION CHAMBER

A schematic diagram of a muffler composed of a resonator in combination with an expansion chamber is shown below:



The boundary conditions to be satisfied at station 1 are

$$A_1 + B_1 = A_2 + B_2 = A_3 + B_3 \quad (C10)$$

$$S_1(A_1 - B_1) = S_2(A_2 - B_2) + S_1(A_3 - B_3) \quad (C11)$$

From equations (C10) and (C11)

$$A_1 = \frac{1}{2} \frac{S_2}{S_1} (A_2 - B_2) + A_3 \quad (C12)$$

For the side branch

$$Z_2 = \frac{p_2}{I_2} = \frac{i\omega\rho c (A_2 + B_2) e^{i\omega t}}{i\omega S_2 (A_2 - B_2) e^{i\omega t}} = \frac{\rho c}{S_2} \frac{A_2 + B_2}{A_2 - B_2}$$

from which

$$A_2 - B_2 = \frac{\rho c}{S_2 Z_2} (A_2 + B_2) = \frac{\rho c}{S_2 Z_2} (A_3 + B_3) \quad (C13)$$

If equation (C13) is substituted into equation (C12), the result is

$$A_1 = \frac{S_2}{2S_1} \frac{\rho c}{S_2 Z_2} (A_3 + B_3) + A_3$$

Since  $A_3 = A_4 e^{ikl_1}$ ,  $B_3 = B_4 e^{-ikl_1}$ , and  $\frac{\rho c}{S_1} = Z_0$ , the preceding equation can also be written as

$$A_1 = \left( 1 + \frac{Z_0}{2Z_2} \right) A_4 e^{ikl_1} + \frac{Z_0}{2Z_2} B_4 e^{-ikl_1} \quad (C14)$$

Let the subscripts 1 and 3 of equations (A9) and (A11) be replaced by 4 and 6, respectively. Then the ratios  $A_4/A_6$  and  $B_4/A_6$  can be written as

$$\frac{A_4}{A_6} = \cos kl_e + i \frac{1}{2} \left( m + \frac{1}{m} \right) \sin kl_e \quad (C15)$$

$$\frac{B_4}{A_6} = -i \frac{1}{2} \left( m - \frac{1}{m} \right) \sin kl_e \quad (C16)$$

By using equations (C14), (C15), and (C16), the ratio  $A_1/A_6$  can be written as

$$\begin{aligned} \frac{A_1}{A_6} &= \left( 1 + \frac{Z_0}{2iX_b} \right) \left[ \cos kl_e + i \frac{1}{2} \left( m + \frac{1}{m} \right) \sin kl_e \right] e^{ikl_1} + \\ &\quad \frac{Z_0}{2iX_b} \left[ -i \frac{1}{2} \left( m - \frac{1}{m} \right) \sin kl_e \right] e^{-ikl_1} \\ &= \left\{ \left( 1 - i \frac{Z_0}{2X_b} \right) \left[ \cos kl_e + i \frac{1}{2} \left( m + \frac{1}{m} \right) \sin kl_e \right] - \right. \\ &\quad \left. \frac{Z_0}{4X_b} \left( m - \frac{1}{m} \right) \sin kl_e e^{-2ikl_1} \right\} e^{ikl_1} \\ &= \left\{ \cos kl_e + \frac{Z_0}{4X_b} \left( m + \frac{1}{m} \right) \sin kl_e - \right. \\ &\quad \left. \frac{Z_0}{4X_b} \left( m - \frac{1}{m} \right) \cos 2kl_1 \sin kl_e + i \left[ \frac{1}{2} \left( m + \frac{1}{m} \right) \sin kl_e - \right. \right. \\ &\quad \left. \left. \frac{Z_0}{2X_b} \cos kl_e + \frac{Z_0}{4X_b} \left( m - \frac{1}{m} \right) \sin 2kl_1 \sin kl_e \right] \right\} e^{ikl_1} \end{aligned} \quad (C17)$$

The attenuation is given by

$$\begin{aligned} \text{Attenuation} &= 10 \log_{10} \left| \frac{A_1}{A_6} \right|^2 \\ &= 10 \log_{10} \left\{ \left[ \cos kl_e + \frac{Z_0}{4X_b} \left( m + \frac{1}{m} \right) \sin kl_e - \right. \right. \\ &\quad \left. \left. \frac{Z_0}{4X_b} \left( m - \frac{1}{m} \right) \cos 2kl_1 \sin kl_e \right]^2 + \right. \\ &\quad \left. \left[ \frac{1}{2} \left( m + \frac{1}{m} \right) \sin kl_e - \frac{Z_0}{2X_b} \cos kl_e + \right. \right. \\ &\quad \left. \left. \frac{Z_0}{4X_b} \left( m - \frac{1}{m} \right) \sin 2kl_1 \sin kl_e \right]^2 \right\} \end{aligned} \quad (C18)$$

## APPENDIX D

### ATTENUATION OF MUFFLERS WITH FINITE TAILPIPES

#### SINGLE EXPANSION CHAMBER

Consider a muffler composed of an expansion chamber with expansion ratio  $m$  terminated with a tailpipe of effective length  $l_t$ . At the upstream end of the muffler,

$$A_1 + B_1 = A_2 + B_2 \quad (D1)$$

$$A_1 - B_1 = m(A_2 - B_2) \quad (D2)$$

At the downstream end, assuming total reflection from the end of the tailpipe

$$A_2 e^{-ikl_e} + B_2 e^{ikl_e} = A_3 + B_3 = A_3 (1 - e^{-i2kl_t}) \quad (D3)$$

$$m(A_2 e^{-ikl_e} - B_2 e^{ikl_e}) = A_3 (1 + e^{-i2kl_t}) \quad (D4)$$

These four equations, when solved simultaneously for  $A_1/A_3$ , give

$$\frac{A_1}{A_3} = \frac{1}{4m} \{ [4m \cos kl_e - 2(m^2 - 1) \sin 2kl_t \sin kl_e] + i [2(m^2 + 1) \sin kl_e - 2(m^2 - 1) \cos 2kl_t \sin kl_e] \}$$

The attenuation is  $10 \log_{10} \left| \frac{A_1}{A_3} \right|^2$  where

$$\left| \frac{A_1}{A_3} \right|^2 = 1 + \frac{(m^2 - 1)^2}{2m^2} \sin^2 kl_e - \frac{m^2 - 1}{2m} \sin 2kl_t \sin 2kl_e - \frac{m^4 - 1}{2m^2} \cos 2kl_t \sin^2 kl_e \quad (D5)$$

The approximate cutoff frequency is found by setting the preceding expression equal to zero and solving for  $k$ , with the approximations that

$$\sin kl_e = kl_e$$

$$\sin 2kl_e = 2kl_e$$

$$\sin 2kl_t = 2kl_t$$

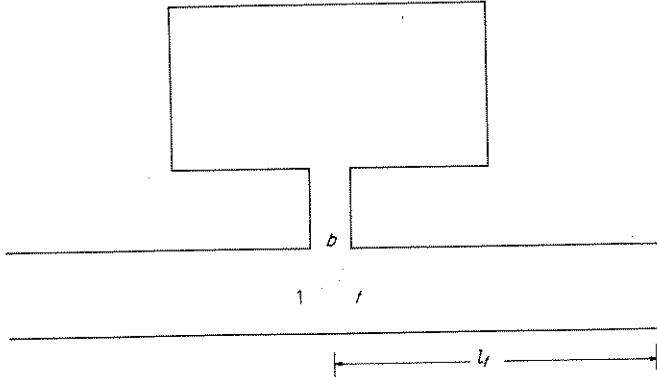
$$\cos kl_t = 1$$

The result is

$$f_c \approx \frac{c}{2\pi} \sqrt{\frac{4 + \frac{2l_e}{ml_t}}{\left(m + \frac{1}{m}\right)l_e l_t}} \quad (D6)$$

#### SINGLE RESONATOR

A schematic diagram of a single-resonator muffler with a finite tailpipe is shown below:



The method of appendix C gives

$$\frac{A_1}{A_t} = \frac{Z_t}{Z_1} \frac{Z_1 + Z_0}{Z_t + Z_0}$$

If now the substitution

$$Z_1 = \frac{Z_b Z_t}{Z_b + Z_t}$$

is made, the result is

$$\frac{A_1}{A_t} = 1 + \frac{Z_0/Z_t}{\frac{Z_0}{Z_t} + 1} \quad (D7)$$

If the correct values for  $Z_0/Z_b$  and  $Z_0/Z_t$  are inserted in this equation, the attenuation may be calculated from equation (A4). As an example, the attenuation equation will be developed for the case where  $Z_b$  is a pure reactance and total reflection is assumed at the open end of the tailpipe. In this case

$$\frac{A_1}{A_t} = 1 + \frac{Z_0/iX_b}{\frac{Z_0}{iX_t} + 1} \quad (D8)$$

Upon reduction this gives

$$\left| \frac{A_1}{A_t} \right|^2 = 1 + \frac{2(Z_0/X_b)(Z_0/X_t)}{(Z_0/X_t)^2 + 1} + \frac{(Z_0/X_b)^2}{(Z_0/X_t)^2 + 1} \quad (D9)$$

Finally, for the single-branch resonator with a tailpipe substitute

$$\frac{Z_0}{X_t} = \cot kl_t$$

where  $l_t$  includes the end correction mentioned in Part II of this report under the heading "Theory." Substitute also

$$kl_t = k_r l_t \frac{f}{f_r}$$

and

$$\frac{Z_0}{X_b} = \frac{\sqrt{c_0 V}}{S \left( \frac{f}{f_r} - \frac{f_r}{f} \right)}$$

with the result

$$\text{Attenuation} = 10 \log_{10} \left[ 1 + \frac{\sqrt{c_0 V}}{S} \frac{\sin 2k_r l_t \frac{f}{f_r}}{\left( \frac{f}{f_r} - \frac{f_r}{f} \right)} + \frac{c_0 V}{S^2} \frac{\sin^2 k_r l_t \frac{f}{f_r}}{\left( \frac{f}{f_r} - \frac{f_r}{f} \right)^2} \right] \quad (\text{D10})$$

Note that in equation (D10) the parameters which determine the attenuation characteristics are  $\sqrt{c_0 V}/S$ ,  $k_r l_t$ , and  $f_r$  (or  $\sqrt{c_0 V}$ ).

The pass frequencies can be found by setting the sum of the second and third terms of equation (D10) equal to zero, with the result

$$\tan kl_t = -2S \left( \frac{k}{c_0} - \frac{1}{kV} \right) \quad (\text{D11})$$

The attenuation will be zero for any value of  $k$  which satisfies this equation. For the cutoff frequency this equation can be simplified by the use of the approximation

$$\tan kl_t = kl_t$$

with the result

$$f_c = \frac{f_r}{\sqrt{1 + \frac{\sqrt{c_0 V}}{2S} k_r l_t}} = \frac{f_r}{\sqrt{1 + \frac{c_0 l_t}{2S}}} \quad (\text{D12})$$

Use of this equation gives a value of approximately 88 cycles per second for the cutoff frequency of the muffler of figure 18 (a). The more exact calculation gives  $f_c = 85$  cycles per second. Note the similarity in form between equation (D12) and equation (B17).

#### REFERENCES

1. Stewart, George Walter, and Lindsay, Robert Bruce: *Acoustics*. D. Van Nostrand Co., Inc., 1930.
2. Davis, A. H. (With Appendix by N. Fleming): *Further Model Experiments Concerning the Acoustical Features of Exhaust Silencers*. Rep. No. N.108, British N.P.L. (Rep. No. 1421, A.R.C.), Feb. 1935.
3. Davis, A. H., and Fleming, N.: *The Attenuation Characteristics of Some Aero-Engine Exhaust Silencers*. Rep. No. N.125, British N.P.L. (Rep. No. 2249, A.R.C.), Feb. 1936.
4. Morley, A. W.: *Progress in Experiments in Aero-Engine Exhaust Silencing*. R. & M. No. 1760, British A.R.C., 1937.
5. Martin, Herbert: *Muffling Without Power Loss in the Four-Stroke-Cycle Engine*. Translation No. 328, Materiel Div., Army Air Corps, Aug. 3, 1938.
6. Buschmann, H.: *Noise in Motor Vehicles*. R.T.P. Translation No. 2584, British Ministry of Aircraft Production.
7. Martin, H., Schmidt, U., and Willms, W.: *The Present Stage of Development of Exhaust Silencers*. R.T.P. T.I.B. Translation No. 2596, British Ministry of Aircraft Production. (From MTZ, No. 12, 1940).
8. Czarnecki, K. R., and Davis, Don D., Jr.: *Dynamometer-Stand Investigation of the Muffler Used in the Demonstration of Light-Airplane Noise Reduction*. NACA TN 1688, 1948.
9. Davis, Don D., Jr., and Czarnecki, K. R.: *Dynamometer-Stand Investigation of a Group of Mufflers*. NACA TN 1838, 1949.
10. Chu, Lan Jen: *Electromagnetic Waves in Elliptic Hollow Pipes of Metal*. Jour. Appl. Phys., vol. 9, no. 9, Sept. 1938, pp. 583-591.
11. Levine, Harold, and Schwinger, Julian: *On the Radiation of Sound From an Unflanged Circular Pipe*. Phys. Rev., vol. 73, no. 4, Second ser., Feb. 15, 1948, pp. 383-406.
12. Trimmer, John D.: *Sound Waves in a Moving Medium*. Jour. Acous. Soc. Am., vol. 9, no. 2, Oct. 1937, pp. 162-164.
13. Field, R. L., Edwards, T. M., Kangas, Pell, and Pigman, G. L.: *Measurement of Sound Levels Associated With Aircraft, Highway and Railroad Traffic*. Tech. Dev. Rep. 68, CAA, U. S. Dept. Commerce, July 1947.